수의학박사학위논문

Helicobacter 감염에 의한 위염에서 위 점막 수지상세포의 역할

The roles of gastric mucosal dendritic cell in *Helicobacter*-induced gastritis

2019 년 8 월

서울대학교 대학원

수의학과 수의병리학 전공

고 두 민

ABSTRACT

The roles of gastric mucosal dendritic cell in *Helicobacter*-induced gastritis

(Supervisor: Dae-Yong Kim, D.V.M., Ph.D.)

Du-Min Go

Department of Veterinary Pathology, College of Veterinary Medicine, Graduate School, Seoul National University

Dendritic cells (DCs) are known to be important immune-regulator in all organs, but DCs within the stomach remain poorly characterized. DCs have been reported to play a role in regulating host immune responses to *Helicobacter* infection, but the precise role of gastric DCs in gastritis remains unclear. Here, gastric DCs were finely characterized and their roles in *Helicobacter*-induced gastritis were investigated. Gastric tissues from DC-deficient mouse models and control mice with *Helicobacter* infection were comparatively analyzed using histopathology, flow cytometry, immunohistochemistry or immunofluorescence, quantitative real-time PCR and luminex immunoassays. Programmed death ligand 1 (PD-L1)–deficient mouse models were also used to confirm the T cell regulation

mechanism of gastric DCs. The clinical aspects were confirmed by conducting multiplexed immunohistochemistry on paraffin-embedded gastric tissue microarrays of patients with gastritis. Gastric DCs were composed of $CD103^{+}CD11b^{-}$, $CD103^{-}CD11b^{+}$, and $CD103^{-}CD11b^{-}$ subsets, and all subsets expanded during *Helicobacter* infection. *Helicobacter*-infected classical DC-deficient mice showed severe gastritis and T cell accumulation compared to control mice. However, the degree of infiltration of regulatory T cells was not different between the two groups. Gastric DCs expressed considerably higher level of PD-L1 than other immune cells and co-localized with T cells in mouse and human stomach. Blockade of PD-L1 exacerbated gastritis with severe T cell accumulation during *Helicobacter* infection. This study indicate that gastric classical DCs attenuate *Helicobacter*-induced gastritis by regulating T cell recruitment through PD-L1 expression and that considering the possibility of inflammatory side-effects on the stomach would be important when treating cancer patients with PD-L1 inhibitors.

Keywords: dendritic cell, gastritis, *Helicobacter*, programmed death ligand 1 (PD-L1), programmed death 1 (PD-1), T cell

Student Number: 2012-21535

CONTENTS

ABBREVIATIONS

Ab: antibodies

ATPase: adenosine triphosphatase

BM: bone marrow

cDCs: classical dendritic cells

CDP: common-DC progenitors

CMoP: common-monocyte progenitors

CTLA-4: cytotoxic T lymphocyte–associated antigen 4

DCs: dendritic cells

DN: double-negative

DT: diphtheria toxin

DTR: diphtheria toxin receptor

FACS: flow cytometry

Flt3: fms-like tyrosine kinase 3

Flt3L: fms-like tyrosine kinase 3 ligand

H&E: hematoxylin and eosin

HBSS: Hank's balanced salt solution

H. felis: *Helicobacter felis*

H. pylori: *Helicobacter pylori*

IFN-γ: interferon gamma

IHC: immunohistochemistry

IL: interleukin

IRAEs: immune-related adverse events

IRF: interferon regulatory factor

KO: knockout

M-CSF: macrophage-colony stimulating factor

MDP: macrophage-DCs progenitors

MHC: major histocompatibility complex

moDCs: monocyte-derived DCs

PD-1: programmed death 1

pDCs: plasmacytoid DCs

PD-L1: programmed death ligand 1

PD-L2: programmed death ligand 2

qRT-PCR: quantitative real-time PCR

SPEM: spasmolytic polypeptide-expressing metaplasia

SS1: Sydney strain 1

TCR: T-cell antigen receptor

Th: helper T cell

TLR: toll-like receptor

TGF: transforming growth factor

TIP DCs: tumor necrosis factor-inducible nitric oxide synthase-producing DCs

TNF: tumor necrosis factor

Tregs: regulatory T cells

WT: wild type

LITERATURE REVIEW

Introduction

Dendritic cells (DCs) were initially discovered during the preparation of adherent mononuclear cells from mouse spleens (Liu and Nussenzweig 2010). DCs were recognized as novel cell populations with a characteristic morphology and movement, and functional differentiation from other cells, including macrophages in the mouse peripheral lymphoid organs (Steinman and Cohn 1973; Steinman and Cohn 1974). The "dendritic cell" was named by Ralph Steinman in 1973 due to the distinct morphological features (Steinman and Cohn 1973); however, DCs were "accessory" cells with a small number in organs, and thus the biological significance of DCs was viewed skeptically (Mildner and Jung 2014). Steinman and his colleagues showed that DCs are representative antigen-presenting cells that initiate antigen-specific cellular immune responses, presenting invaluable evidence (Banchereau and Steinman 1998; Mildner and Jung 2014). Immunology had focused only on antigens and lymphocytes for some time, and DCs provided insights into immune responses that were not adequately explained by only these two factors (Banchereau and Steinman 1998).

Since this discovery, various aspects of DCs, such as functions, development, subsets, and migration, have been extensively studied. These studies have been carried out *in vitro* mainly by purifying DCs from mouse spleens or by differentiating mouse bone marrow (BM) cells or human monocytes into DCs using the granulocyte-macrophage colony-stimulating factor or the fms-like tyrosine kinase 3 ligand (Flt3L) (Liu and Nussenzweig 2010). However, DCs are a heterogeneous population composed of several subsets and share certain surface

markers with immune cells belonging to the mononuclear phagocyte system such as macrophages and monocytes, making it difficult to only identify pure DCs (Worbs, Hammerschmidt et al. 2017). In addition, several DC-deficient mouse models have been used to identify the role of DCs in infectious, autoimmune, and metabolic diseases and tumors, but DCs can exhibit various aspects depending on the type of disease or the target organs where the lesion occurs. Thus, detailed DCs characterization is important in the study of DCs.

Initiation of T cell immunity

DCs are superior to other immune cells in capturing and processing antigens and presenting treated antigen to T cells via the T-cell antigen receptor (TCR) (Nussenzweig, Steinman et al. 1980). DCs are indispensable for the stimulation of T cells that cannot directly recognize antigens (Banchereau and Steinman 1998). DCs present endogenous and exogenous antigens to T cells through the major histocompatibility complex (MHC) I and the MHC II, respectively. In addition, DCs induce cytotoxic $CD8^+$ T cell immunity by presenting exogenous antigens to T cells through MHC I, which is called cross-presentation. Cross-presentation is crucial for immunity against viruses and intracellular bacteria (Rock 2003). The binding of MHC-peptide complexes on DCs and T cells induces distinct outcomes depending on the context of antigens, signals provided by B7 family members on DCs and instructing cytokines (Mildner and Jung 2014). In relation to pathogens or danger-associated molecular patterns, DCs and T cells can recognize the contexts of antigens. In the crosstalk between T cells and DCs, pro-inflammatory T cell responses or T cell tolerance is induced depending on the co-stimulatory or co-

inhibitory signals transmitted by DCs or the maturation state of DCs (Mildner and Jung 2014). Thus, DCs play a central role in controlling T cell immunity.

Development and function of DC subsets

DCs are classified into classical DCs (cDCs), monocyte-derived DCs (moDCs), and plasmacytoid DCs (pDCs). They share origins initially in the BM and are divided into common-DC progenitors (CDP) and common monocyte progenitors (CMoP) according to Flt3L and the macrophage-colony stimulating factor (M-CSF) signaling in macrophage-DCs progenitors (MDP). Subsequently, cDCs and pDCs are differentiated by fms-like tyrosine kinase 3 (Flt3)-Flt3L signaling from CDP, and monocytes and their descendants are differentiated from CMoP. cDCs arise from pre-DCs differentiated from CDP in the BM, and the differentiated pre-DCs migrate through the blood and are distributed in the peripheral organs. pDCs are differentiated from CDP in BM and migrated to peripheral organs, and moDCs are differentiated from monocytes in peripheral organs (Fig. 1) (Liu and Nussenzweig 2010).

cDCs are classified into at least two subsets according to the expression of CD8α and CD103 or CD11b surface markers. First, $CD8\alpha^+$ cDCs are present in lymphoid tissues including the spleen, lymph node and BM. $CD103^+$ cDCs are considered to be the same population as $CD8\alpha^+$ cDCs present in non-lymphoid tissues (del Rio, Rodriguez-Barbosa et al. 2007; Edelson, KC et al. 2010). $CD8\alpha^+$ cDCs and $CD103^+$ cDCs are the most well-characterized cDCs subsets based on their phenotypic and gene expression characteristics (Mildner and Jung 2014). These $CD8\alpha^+$ and $CD103^+$ cDCs are referred to as the cDC1, and cDC1 is known

to be functionally specific for cross-presentation (den Haan, Lehar et al. 2000; Bedoui, Whitney et al. 2009). Interferon regulatory factor (IRF) 8, Id2, BATF3, and NFIL3 have been reported as transcription factors involved in the development of cDC1 lineage (Mildner and Jung 2014). Among them, IRF8 is presumed to be the master regulator of cDC1 lineage (Seillet, Jackson et al. 2013). $CD11b^+$ cDCs are referred to as cDC2 and are known as heterogeneous populations, unlike $CD8\alpha^+$ and $CD103^+$ cDCs. Due to the complexity of this heterogeneity, the characterization of $CD11b^+$ cDCs is relatively unclear. RelB, NOTCH2, RBP-J, IRF2, and IRF4 have been known to regulate $CD11b^+$ cDCs development (Mildner and Jung 2014). Of these, IRF4 has also been implicated in the function and migration of $CD11b^+$ cDCs (Mildner and Jung 2014). Compared to $CD8\alpha^+$ and $CD103^+$ cDCs, $CD11b^+$ cDCs are ineffective for cross-presentation but have been reported to be more effective for the induction of $CD4^+$ T cell immunity (Lewis, Caton et al. 2011).

moDCs also exist in the steady state, but are referred to as "inflammatory DCs" because they rapidly aggregate into inflammatory sites (Goudot, Coillard et al. 2017; Segura and Amigorena 2013). In addition, tumor necrosis factor (TNF)-inducible nitric oxide synthase-producing DCs (TIP DCs) present in pathogen-associated inflammation have been considered typical moDCs, but recent studies have suggested that TIP DCs correspond to activated effector monocytes rather than to DCs (Mildner, Yona et al. 2013). moDCs are difficult to distinguish from $CD11b^+$ cDCs because they share surface markers such as CD11c, MHC II, and CD11b, with cDCs and can migrate to draining lymph nodes similarly to cDCs to induce adaptive immune responses (Liu and Nussenzweig 2010; Chow, Sutherland et al.

2017). Detailed studies that explore distinguishing between them would be helpful in understanding heterogeneous CD11b^{+} cDCs.

pDCs are BM-derived DCs subsets that are rarely found in peripheral blood and peripheral organs. Like cDCs, pDCs development is dependent on Flt3-Flt3L signaling, and activated pDCs are known to play a role in naive CD4^{+} T cell priming in lymph nodes (Kingston, Schmid et al. 2009; Sapoznikov, Fischer et al. 2007). However, they are best known as a population that produces type I interferon in response to viral infections, and thus the role of pDCs in innate and adaptive immune responses to viral infections has been the subject of many studies (Colonna, Trinchieri et al. 2004; Yun, Lee et al. 2016). In addition, the roles of pDCs in peripheral and central immune tolerance have been reported in association with regulatory T cells (Tregs) induction (Yun, Lee et al. 2016).

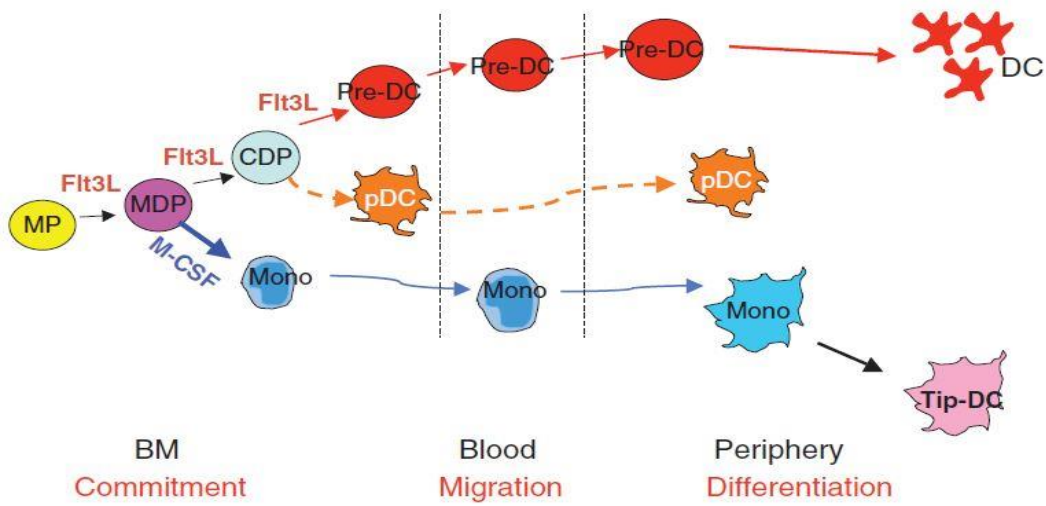

Fig 1. Dendritic cell and monocyte origin and development (Liu and Nussenzweig 2010)

DCs-mediated immune tolerance

Although DCs induce effective immune response to antigens, they also play an important role in maintaining immune tolerance. DCs maintain immune tolerance by inducing apoptosis of autoreactive thymocytes and promoting Treg differentiation by presenting self-antigens in the thymus (central tolerance). In addition, DCs induce anergy, apoptosis of T cells in peripheral organs, and promote immune tolerance by promoting Treg response (peripheral tolerance) (Audiger, Rahman et al. 2017). Thus, DCs contribute to the balance between immunity and tolerance, which is influenced both by various DC factors and by local environmental factors that modulate the tolerogenic functions of the DCs.

Signal transduction through contact between T cells and DCs is an important process that determines immunogenic or tolerogenic pathways. The mature state of DCs has a significant influence on this signal transmission. Mature DCs, sensing pathogens by pattern recognition receptor such as toll-like receptors (TLR) (immunogenic maturation), highly express co-stimulatory molecules such as CD80, CD86, and CD40, which enhances the efficiency of TCR signaling and promotes effector T cell responses. However, immune tolerance is induced when these signals are transmitted to Tregs (Yamazaki, Iyoda et al. 2003; Salomon, Lenschow et al. 2000). On the other hand, DCs matured by self-antigens in steady states (homeostatic maturation) and immature DCs expressing low co-stimulatory molecules induce immune tolerance (Ardouin, Luche et al. 2016). In addition, DCs can induce tolerance by expressing co-inhibitory molecules, canceling stimulatory signals that are transmitted to T cells, and delivering inhibitory signals. Among these co-inhibitory molecules, programmed death ligand 1 (PD-L1) and

programmed death ligand 2 (PD-L2) are well known, and they transmit signals through the programmed death 1 (PD-1) expressed in T cells. In addition, the CD86 and CD80 expressed by DCs can induce T cell tolerance by binding to the cytotoxic T lymphocyte–associated antigen 4 (CTLA-4) expressed in T cells (Probst, McCoy et al. 2005).

Specific local environmental factors can also influence the immune tolerance role of DCs. DCs present at specific anatomical locations, such as the intestine which is continuously exposed to microflora and food antigens, or the skin, are known to be suitable for promoting immune tolerance (Audiger, Rahman et al. 2017). Furthermore, in inflammatory conditions, inflammation-related signals such as TLR2, TNF-α, and prostaglandin receptors, and Tregs regulate DCs to perform immunoregulatory roles (Popov, Driesen et al. 2008; Darrasse-Jèze, Deroubaix et al. 2009).

The here-described significance of DCs in maintaining immune tolerance has been demonstrated to some extent by the phenotype of DC-deficient mouse models, and tolerogenic DCs are attracting attention as a potential solution for conditions requiring immune tolerance such as autoimmune diseases (Audiger, Rahman et al. 2017). Thus, studies have been carried out on murine tolerogenic DC subsets and their human equivalents (Robbins, Walzer et al. 2008; Guilliams, Dutertre et al. 2016).

Function of DCs in *Helicobacter* infection

It is known that TLR2 and TLR4 play an important role for DCs to recognize *Helicobacter pylori* (*H. pylori*) and produce cytokines (Rad, Ballhorn et al. 2009).

Furthermore, recent studies have shown that $CD11b^+$ gastric DC directly recognize and engulf *H. pylori* in the stomach (Arnold, Zhang et al. 2017).

Helicobacter-recognizing DCs express maturation markers such as CD80 and CD86, and produce pro-inflammatory cytokines such as interleukin (IL)-6, IL-12, and IL-23, and activate co-cultured autologous $CD4^+$ T cells to secrete interferon gamma (IFN-γ) or IL-17 (Hafsi, Voland et al. 2004; Khamri, Walker et al. 2010). Contrary to these pro-inflammatory roles, DCs also play an immune tolerance role by inducing Tregs or producing anti-inflammatory cytokines such as IL-10 and transforming growth factor (TGF)-β (Rizzuti, Ang et al. 2015; Zhang, Liu et al. 2010). These *in vitro* studies were performed using human moDCs or mouse BM-derived DCs. As described above, DCs have a dual role against *Helicobacter*.

In vivo studies to confirm the function of DCs in *Helicobacter* infection have been performed using the CD11c-diphtheria toxin receptor (DTR) which can ablate DCs. This study demonstrated the tolerogenic role of DCs against *H. pylori* (Hitzler, Oertli et al. 2011; Oertli, Sundquist et al. 2012), but other $CD11c^+$ cells in addition to DCs could also be affected in CD11c-DTR mice (Probst, Tschannen et al. 2005; Bennett and Clausen 2007). Therefore, *in vivo* studies using mouse models that ablate DCs only will help identify the role of gastric DCs in *Helicobacter* infection.

Mouse model of *Helicobacter* infection

In the 1980s, Pelayo Correa suggested chronic gastritis as a gastric cancer precursor based on clinical and epidemiological observations, proposing sequential events leading to the development of gastric adenocarcinoma (Correa 1983; Correa 1984). Chronic-active gastritis induced by unknown factors progressed to

multifocal atrophic gastritis with loss of parietal cells and chief cells, and intestinal metaplasia (Sakagami, Dixon et al. 1996). Afterwards, the finding that *H. pylori* was the cause of chronic-active gastritis provided a missing link in the Correa pathway (Sakagami, Dixon et al. 1996).

The only available animal models of *H. pylori* infection were germ-free piglets and non-human primates, and the limited host range of *H. pylori* has restricted the study of the pathogenesis of the disease (Lee, Fox et al. 1990). Although these animal models provided important information, the need for a small animal model was raised because it was unmanageable, expensive, and only available to a few investigators (Lee, O'Rourke et al. 1997). However, early attempts to colonize *H. pylori* on rodents were unsuccessful (Ehlers, Warrelmann et al. 1988; Cantorna and Balish 1990). On the other hand, *Helicobacter felis* (*H. felis*) isolated from stomach of cat was more closely related to *H. pylori* than any other bacteria based on 16s ribosomal RNA sequencing and showed gastric trophism with stable colonization in mouse stomach (Lee, Fox et al. 1990). *H. felis* caused lesions similar to human gastric lesions following *H. pylori* infection in some mouse strains including C57BL/6 (Lee, Fox et al. 1990). In particular, C57BL/6 mice showed chronic-active gastritis, gastric atrophy, metaplasia as well as dysplasia and gastric cancer after 12-15 months of infection (Fox et al. 2002).

Meanwhile, *H. pylori* isolated from the stomach of patients at the gastroenterology clinic in Sydney, Australia, was subsequently colonized stably in the stomach of mice through long-term adaptation, which was named the Sydney strain 1 (SS1) (Lee, O'Rourke et al. 1997). *H. pylori* SS1 induced gastric pathology

similar to that of *H. pylori*-infected patients in mice, but could not induce gastric cancer (Duckworth, Burkitt et al. 2015).

Objective

DCs are the central immune cells that regulate innate and adaptive immunity in a wide range of pathophysiological conditions. DCs modulate the appropriate immune response in various organs while promoting immunity against pathogens and maintaining immune tolerance. Based on these important roles, many studies have been conducted on the overall characterization of DCs.

However, gastric DCs are relatively unknown compared to the DCs of other organs. In particular, the importance of gastric DCs has been emphasized in controlling immunity against *H. pylori* infection, which is closely related to chronic gastritis and gastric cancer in humans. However, *in vivo* studies to clarify the role of gastric DCs in *Helicobacter* infection are rarely reported.

In the present study, I tried to characterize gastric DCs. Gastric DCs were examined closely *in vivo* in both steady state and *Helicobacter*-induced gastritis. Furthermore, I tried to identify the major role of gastric DCs in *Helicobacter* infection, and the mechanisms of the role by using genetically engineered mouse models.

CHAPTER I.

Gastric classical dendritic cells attenuate *Helicobacter*-induced gastric inflammation via controlling T cell immunity

Abstract

Approximately 50% of the human population is infected by *H. pylori*. However, the host's immune system cannot eradicate colonized *H. pylori* in the gastric mucosa, causing chronic gastritis. *H. pylori*-induced chronic gastritis may progress to severe gastropathy such as peptic ulcer and gastric cancer. DCs have been reported to play an important role in regulating the host immune responses to *Helicobacter* infection, but the precise role of DCs in the stomach remains unclear. To investigate the roles of gastric DCs in *Helicobacter*-induced gastritis, DC-deficient mice were infected with *H. felis* and then gastric tissues were analyzed by histopathology, flow cytometry, immunohistochemistry, quantitative real-time PCR and magnetic luminex immunoassays. It was found that gastric DCs were composed of $CD103^{+}CD11b^{-}$, $CD103^{-}CD11b^{+}$, and $CD103^{-}CD11b^{-}$ subsets, and all these subsets expanded during *H. felis* infection. *H. felis*-infected Flt3 knockout (KO) and Zbtb46-DTR mice, not BDCA2-DTR mice, showed severe gastric lesions with prominent T cell infiltration compared to control group mice. This study indicate that gastric cDCs play an important role in suppressing T cell responses during *Helicobacter* infection.

Introduction

H. pylori is a gram negative bacterium that can colonize and survive in the human gastric mucosa. Approximately 50% of the human population is colonized by *H. pylori*, and about 15% of them develop severe lesions such as severe chronic gastritis, peptic ulcer, gastric adenocarcinoma and lymphoma (Kronsteiner, Bassaganya-Riera et al. 2014). *H. pylori*-induced gastropathy is influenced by various factors such as host, bacterial pathogen, and environment-related factors, and host's immune system against *H. pylori* has been reported to be closely related to lesion development (Kusters, van Vliet et al. 2006).

Various components and products of *H. pylori* and signals from mucosal epithelial cells in contact with *H. pylori* cause infiltration of innate immune cells such as DCs, macrophages, monocytes and neutrophils. Among these innate immune cells, DCs have been shown to play an important role in the host T cell immune response to *H. pylori* (Shiu and Blanchard 2013).

DCs are representative antigen-presenting cells with an exceptional ability to modulate the overall immune response to invasive pathogens (Steinman 2012). These properties of DCs imply the importance of DCs in the immune responses of the gastrointestinal tract, which is constantly exposed to various pathogens. To determine the role of DCs in *H. pylori* infection, many previous studies have focused on the direct response of DCs to *H. pylori* by incubating human moDCs or mouse BM-derived DCs with live *H. pylori* or *H. pylori*-related proteins *in vitro*. DCs have been shown to recognize *H. pylori* via pattern recognition receptor such as Toll-like receptors (Rad, Ballhorn et al. 2009), and *H. pylori*-stimulated DCs secrete pro-inflammatory cytokines such as IL-6, IL-12 and IL-23 and activate co-

cultured autologous $CD4^+$ T cells to secrete IFN-γ or IL-17 (Hafsi, Voland et al. 2004; Khamri, Walker et al. 2010). In contrast to these pro-inflammatory roles, *H. pylori*-stimulated DCs also play an immune tolerance role by inducing Tregs or producing anti-inflammatory cytokines such as IL-10 and TGF-β (Zhang, Liu et al. 2010; Rizzuti, Ang et al. 2015). As described above, since DCs might have dual roles against *H. pylori*, *in vivo* studies are highly required to determine the effects of DCs on *Helicobacter*-infected individuals. Several previous *in vivo* studies used the CD11c-DTR mice in which DCs can be ablated and confirmed the tolerogenic role of DCs in *H. pylori* infection (Hitzler, Oertli et al. 2011; Oertli, Sundquist et al. 2012). However, as macrophages can also be ablated in CD11c-DTR mice, elucidating the function of gastric DCs in *H. pylori*-induced gastritis is difficult (Bennett and Clausen 2007). Meanwhile, one study demonstrated that gastric $CD11b^+$ DCs engulf *H. pylori* in gastric mucosa (Arnold, Zhang et al. 2017). However, the exact immunological roles of gastric DCs in *Helicobacter*-induced gastritis are largely unknown.

Many studies on human and animal models of *H. pylori* infection have suggested that $CD4^+$ T cell responses such as helper T cell (Th) 1, Th17, and Tregs are predominantly controlled by gastric DCs (Bimczok, Clements et al. 2010; Zhang, Liu et al. 2010). However, these $CD4^+$ T cell-mediated immune responses were not effective in eradicating the colonized *H. pylori* in the gastric mucosa, rather causing gastritis to become chronic, which is a risk factor for the development of peptic ulcer or gastric cancer (Peek, Fiske et al. 2010). Furthermore, $CD8^+$ T cell infiltration has been shown to be increased in patients with *H. pylori* infection, and IFN-γ production in response to *H. pylori* infection is greater in $CD8^+$ T cells than

in $CD4^+$ T cells (Bamford, Fan et al. 1998; Quiding-Järbrink, Lundin et al. 2001). T cell-mediated IFN-γ improved *Helicobacter* clearance but contributed to the development of severe gastric lesions (Sayi, Kohler et al. 2009). Therefore, $CD8^+$ T cell infiltration appear to be closely related to the severity of gastritis and *Helicobacter* clearance, and recent human clinical studies have emphasized the potential relevance of $CD8^+$ T cells in the immune response to *H. pylori* (Kronsteiner, Bassaganya-Riera et al. 2014).

Here gastric DCs were characterized and immune regulatory effect of gastric DCs on T cells in *Helicobacter*-induced gastritis was identified by examining the immune responses of *Helicobacter*-infected DC-deficient mice, including Flt3 KO mice, BDCA2-DTR mice, and Zbtb46-DTR mice. Gastric DCs consist of three subsets: $CD103^+CD11b^-$ –, $CD103^-CD11b^+$ –, and $CD103^-CD11b^-$ – DCs. These DC subsets were gradually increased during *Helicobacter* infection. Flt3 KO mice showed more severe gastritis with profound infiltration of $CD8^+$ T cells and lower bacterial load. Moreover, cDC-ablation increased T cell accumulation in the gastric mucosa. These findings indicate that gastric cDCs have a significant impact on the T cell immune responses to *Helicobacter* infection.

Materials and Methods

Mice

Flt3 KO, Zbtb46-DTR, CD11c-EYFP, and BDCA2-DTR mice with C57BL/6J background were individually housed in the animal facility of Seoul National University or Hanyang University and provided a normal mouse diet and water *ad libitum*. Male C57BL/6J wildtype (WT) mice were purchased from the Japan SLC Inc. (Hamamatsu, Shizuoka, Japan) through the Central Lab. Animal Inc. (Seoul, Korea). All mice experiments were approved by the Animal Care and Use Committees of Seoul National University or Hanyang University (certification number: SNU-140320-2-9, HY-IACUC-18-0048).

Bone marrow transplantation

BM cells from Flt3 KO, Zbtb46-DTR, or BDCA2-DTR mice were injected intravenously into lethally irradiated (500 rad twice, 3 hours interval) WT C57BL/6 mice. BM transplanted mice were fed water containing 7.6% Baytril (Bayer Korea, Seoul, Korea) for 2 weeks and monitored about, 6 weeks, until the transplanted BM is effectively reconstructed.

Helicobacter culture and Infection

H. felis (ATCC 49179) was cultured in sterile-filtered brucella broth (Becton Dickinson, Sparks, MD, USA) containing 10% FBS. Mouse-adapted *H. pylori* SS1 was cultured on brain heart infusion agar plates (Becton Dickinson) containing 10% sheep blood and *H. pylori* Selective Supplement (Thermo Fisher Scientific,

Rockford, IL, USA). The brucella broth and brain heart infusion agar plates were maintained under microaerobic conditions produced using the GasPak™ EZ Campy Container System (Becton Dickinson) at 37°C. The brucella broth was maintained at 150 rpm shaking. After 24 hour fasting, 8-week-old mice were orally administered 0.2 ml suspension containing 2×10^8 *H. felis* or 1×10^9 colony-forming unit/ml *H. pylori* 4 times every other day.

Diphtheria toxin injection

The cDCs and pDCs were depleted by intraperitoneally administering diphtheria toxin (DT; Calbiochem, San Diego, CA, USA) to Zbtb46-DTR BM transplanted mice and BDCA2-DTR BM transplanted mice, respectively. 500 ng DT was injected 2 days before *H. felis* infection. During the infection period, Zbtb46-DTR BM transplanted mice were treated with 100 ng DT every 2 days, and BDCA2-DTR BM transplanted mice were treated with 200 ng DT every 3 days. The control group was treated with PBS instead of DT with the same schedule.

Necropsy and Tissue preparation

At 2, 4, and 8 weeks after *H. felis* infection, each group of mice was sacrificed together with the non-infected control group, and stomach, gastric lymph node, and spleen were removed. The stomach was incised along the greater curvature and spread on a filter paper. After cutting the lesser curvature, half of the stomach was used for flow cytometry (FACS) and *H. felis* quantification. The lesser curvature portion of the other half was fixed in 10% neutral buffered formalin for histopathologic examinations, and the remaining was stored in a -70°C deep freezer

for subsequent analysis. At 18 months after *H. pylori* infection, the *H. pylori*-infected groups were treated in the same manner as above.

Histopathologic Examinations

Gastric tissues fixed in 10% neutral buffered formalin were cut into two strips. After standard tissue processing, gastric tissues were embedded in paraffin wax. Paraffin sections were stained with haematoxylin and eosin (H&E) and Alcian Blue (pH 2.5) stain kit (Vector Laboratories, Burlingame, CA, USA) and performed immunohistochemistry (IHC) for H^+/K^+-adenosine triphosphatase (ATPase) to assess histopathological changes. The degree of gastritis and pathological mucosal changes were assessed on the basis of previously established updated Sydney classification (Chen, van der Hulst et al. 1999; Sayi, Kohler et al. 2009). In the sections stained with Alcian Blue, the amount of mucin in the gastric mucosa was measured using mean intensity in Image J software (National Institutes of Health, Bethesda, MD, USA). In the sections with IHC for H^+/K^+-ATPase, the number of positive cells was manually counted. The mucosa of two different areas was examined per slide at ×100 magnification, and the same anatomic areas were selected for each sample.

Single-Cell Preparations and Flow Cytometric Analysis

Gastric single cells were prepared to investigate the type of inflammatory cells that infiltrate into the stomach during *Helicobacter* infection. The gastric tissues were incubated in Hank's balanced salt solution (HBSS) containing 2 mM EDTA (Cosmo Genetech, Seoul, Korea), 2% FBS, and 1 mM DL-Dithiothreitol (Sigma-

Aldrich, St. Louis, MO, USA) for 15 min at 37°C with shaking. Then, the gastric tissue was finely trimmed and grinded using gentleMACS^{TM} Dissociator (Miltenyi Biotec, Bergisch Gladbach, Germany) and incubated in HBSS containing 100 U/ml collagenase D (Roche, Mannheim, Germany), 10% FBS, and 10 mM HEPES for 30 min at 37°C with shaking. After incubation, the gastric tissue was grinded once more using the gentleMACS^{TM} Dissociator, filtered through a 70 μm cell strainer, and centrifuged to collect the separated single cells. Finally, the single cells were prepared by combining the cells collected from the suspension and from the gastric tissue. The gastric lymph node and spleen were incubated with 400 U/ml collagenase D at 37°C for 20 min to obtain separated single cells. The prepared single cells were primarily stained with Zombie Aqua (BioLegend, San Diego, CA, USA) to discriminate dead cells as per manufacturer's protocol. Zombie aqua stained cells were then processed for Fc receptor block by using TruStain FcX antibody (anti-CD16/32, clone 93, BioLegend), to avoid non-specific binding. After the Fc receptors block, cells were incubated with a mixture of fluorochrome-labelled antibodies at 4°C for 30 min. To stain transcription factors (Foxp3, IRF4, IRF8 and Zbtb46), cells were fixed and permeabilized with Foxp3/Transcription Factor Staining Buffer Set (Thermo Fisher Scientific), as per manufacturer's protocol, and then stained with antibody against each transcription factor. After washing briefly with RPMI 1640 medium with 10% FBS, cells were analyzed using BD LSRFortessa (BD Biosciences, San Jose, CA, USA) and FlowJo software (version 9.9 and 10.4; developed by FlowJo, LLC).

Antibodies for flow cytometry

The antibodies used for FACS are listed in Table 1.

Table 1. List of antibodies

Antibody	Clone	Catalog No.	Source
CD103	2E7	11-1031-81	eBioscience
Foxp3	FJK-16s	17-5773-82	eBioscience
IRF8	V3GYWCH	17-9852	eBioscience
Siglec-H	eBio440c	48-0333-80	eBioscience
CD4	GK1.5	553730	BD Bioscience
Zbtb46	U4-1374	565832	BD Bioscience
Siglec-F	E50-2440	562681	BD Bioscience
CD11b	M1/70	101206, 101216, 101212, 101226	BioLegend
CD64	X54-5/7.1	139304, 149320	BioLegend
MHC II	M5/114.15.2	107621, 107628	BioLegend
Ly6C	HK1.4	128006	BioLegend
CD45	30-F11	103130	BioLegend
CD11c	N418	117318	BioLegend
NK1.1	PK136	108714	BioLegend
CD8α	53-6.7	100762	BioLegend
F4/80	BM8	123146	BioLegend
IRF4	IRF4.3E4	646408	BioLegend
PDCA-1	927	127015	BioLegend
CD19	6D5	115527	BioLegend
B220	RA3-6B2	103223	BioLegend
CD3	17A2	100228	BioLegend

Ly6G	1A8	127641	BioLegend
XCR1	ZET	148220	BioLegend
Rat IgG2α, κ Isotype	RTK2758	400507, 400511, 400526, 400542, 400549	BioLegend

Immunohistochemistry and Immunofluorescence

After paraffin-embedded sections were dewaxed and hydrated, antigen retrieval was performed using citrate buffer (pH 6.0; Sigma-Aldrich). Next, the sections were incubated with 0.3% hydrogen peroxide solution for 30 min to block endogenous peroxidase activity. The ImmPRESS Peroxidase Polymer kit (Vector Laboratories) was used according to manufacturer's protocol. Briefly, paraffin-embedded sections were blocked with 2.5% normal horse serum or 2.5% normal goat serum for 1 hour and then incubated with the following primary antibodies at 4°C overnight or at 20°C for 2 hours: rabbit anti-CD3 (1:200; Dako, Glostrup, Denmark), rabbit anti-CD11c (1:400; Cell Signaling Technology, Danver, MA, USA), and mouse anti-ATPase (1:4000; MBL, Woburn, MA, USA). The paraffin-embedded sections were washed with PBS and then incubated with appropriate horseradish peroxidase-conjugated secondary antibody (Vector Laboratories) for 1 hour. ImmPACT DAB substrate (Vector Laboratories) was used for chromogenic detection. The sections were counterstained with hematoxylin. In anti-ATPase IHC, Mouse on Mouse ImmPRESS Peroxidase Polymer Kit (Vector Laboratories) was used to block endogenous mouse immunoglobulin.

For frozen sections of CD11c-EYFP mice, the sections were counterstained with DAPI and mounted using mounting medium (Vector Laboratories). The

images were obtained using confocal fluorescence microscope (Eclipse TE200; Nikon, Japan).

H. felis Quantification

Total DNA was extracted from the gastric tissues (corpus and antrum) by using QIAamp DNA mini kit (Qiagen, Hilden, Germany) and used to identify *H. felis* DNA. Quantitative real-time PCR (qRT-PCR) was performed using specific primers for *H. felis* flagellar filament B (Fla-B), Rotor-Gene SYBR Green PCR kit, and Rotor-Gene Q (Qiagen). The amplified target DNA was analyzed using Rotor-Gene Q series software. The *H. felis* Fla-B primer–F: 5′-TTC GAT TGG TCC TAC AGG CTC AGA-3′ and R: 5′-TTC TTG TTG ATG ACA TTG ACC AAC GCA-3′– was used (El-Zaatari, Kao et al. 2013). Next, the Warthin-Starry Stain Kit (Abcam) was used to identify the location of *H. felis* and to assess the extent of colonization in the stomach. Colonized *H. felis* were counted manually from two sections of each gastric tissue.

Quatitative Reverse Transcription-PCR

Total RNA from gastric tissues was extracted using Hybrid-R RNA purification kit (GeneAll, Seoul, Korea). The cDNA was synthesized from 0.1 μg of RNA by using QuantiTect Reverse Transcription kit (Qiagen). qRT-PCR was performed using specific primers, Rotor-Gene SYBR Green PCR kit, and Rotor-Gene Q (Qiagen). The amplified target cDNA was analyzed using Rotor-Gene Q series software against the housekeeping gene GAPDH. The specific primer pairs were F: 5′-TGC ACC ACC AAC TGC TTA G-3′ and R: 5′-GGA TGC AGG GAT

GAT GTT C-3′ for mouse GAPDH; F: 5′-AGC GGC TGA CTG AAC TCA GAT TGT AG-3′ and R: 5′-GTC ACA GTT TTC AGC TGT ATA GGG-3′ for mouse IFN-γ; F: 5′-GCT CCA AGA CCA AGG TGT CT-3′ and R: 5′-CTA GGT CCT GGA GTC CAG CA-3′ for mouse IL-10; and F: 5′-CTT CAA TAC GTC AGA CAT TCG GG-3′ and R: 5′-GTA ACG CCA GGA ATT GTT GCT A-3′ for mouse TGF-β. Primers for mouse Granzyme A (cat. QT01551690) and perforin (cat. QT00282002) were purchased from Qiagen QuantiTect Primer Assay (Qiagen).

Magnetic Luminex immunoassay

For protein extraction, gastric tissues of *H. felis*-infected and non-infected WT and Flt3 KO mice were lysed using Cell Lysis Buffer 2 (R&D systems, Minneapolis, MN, USA). Chemokine and cytokine protein concentrations were measured using Mouse Premixed Multi-Analyte Kit (cat. LXSAMSM; R&D systems,) according to the manufacturer protocol.

Statistical Analysis

All data are shown as means ± standard errors. Statistical analysis was performed using GraphPad Prism 7.00 (GraphPad Software, San Diego, CA, USA). Two groups were compared using Mann-Whitney *U* test or unpaired *t*-test with two-tailed distributions. When three or more groups were included, the results were analyzed using Kruskal-Wallis test or ordinary one-way ANOVA followed by Mann-Whitney *U* test or unpaired *t*-test with two-tailed distributions. Meanwhile, Pearson's correlation coefficient was used to determine statistical dependence of *H.*

felis clearance and immune cell population. Two-tailed *P* values less than 0.05 were considered significant.

Results

Gastric DCs have three distinct subpopulations

To characterize gastric DCs, $CD45^+$ leukocytes were gated out from live cells and neutrophils ($Ly6G^+CD11b^+$), eosinophils (Siglec F^+CD11b^+), and macrophages ($CD64^+CD11b^+$) were sequentially excluded from the $CD45^+$ cells. Next, gastric DCs were defined as $CD64^-CD11c^+$MHC II^+ cells and their levels of CD103 and CD11b expression were further analyzed (Fig 1A). Under normal condition, the gastric $CD64^-CD11c^+$MHC II^+ cells occupied about 0.24% of the total live single cells and were composed of three subsets including $CD103^+CD11b^-$ (17.9%), $CD103^-CD11b^+$ (45.3%), and $CD103^-CD11b^-$ (double-negative, DN; 32.1%) populations (Fig 1A and 2A).

To confirm that these subsets are DCs, the level of surface marker expression of each subset was measured by FACS analysis. The expression of Zbtb46, which is expressed specifically in human and murine cDCs (Reizis 2012; Satpathy, KC et al. 2012), was higher in all subsets, especially in the $CD103^+$ subset, than in the isotype control. The expression of IRF4 and IRF8 was significantly higher in the $CD11b^+$ and $CD103^+$ subsets than in the isotype control. The DN subset also showed higher levels of IRF4 and IRF8 than those in the isotype control. The transcription factors IRF4 and IRF8 regulate $CD11b^+$ and $CD103^+$ cDC development, respectively (Mildner and Jung 2014). Among the known transcription factors involved in $CD103^+$ cDC development, IRF8 appears to be the most important factor (Seillet, Jackson et al. 2013). The expression of XCR1, a potential marker for human and mouse $CD103^+$ DCs (Bachem, Güttler et al. 2010),

was higher in all DC subsets than in the isotype control and was more prominent in the $CD103^+$ subset (Fig 1B).

To further confirm that the $CD64^-CD11c^+MHC\ II^+$ cells are DCs, the stomachs of Flt3 KO mice deficient in peripheral DCs were examined. Flt3 is an important regulator of DC homeostasis at the periphery, and only cDCs and pDCs are deficient in peripheral lymphoid organs of Flt3 KO mice (Waskow, Liu et al. 2008). Further, as the non-lymphoid tissues of Flt3 KO mice, the aorta have fewer cDCs and pDCs (Choi, Cheong et al. 2011; Yun, Lee et al. 2016). The number of $CD64^-CD11c^+MHC\ II^+$ cells and $CD103^+$, $CD11b^+$, and DN subsets was markedly lower in the stomach of Flt3 KO mice than in that of WT mice (Fig 1C). To confirm the location of DCs in the normal mouse stomach, immunostaining of CD11c was performed and the gastric tissues of normal CD11c-EYFP mice were observed by confocal microscopy. The $CD11c^+$ cells were very few and were mainly located in the superficial layer of the mucosal lamina propria and were well observed around the limiting ridge (Fig 1D).

A

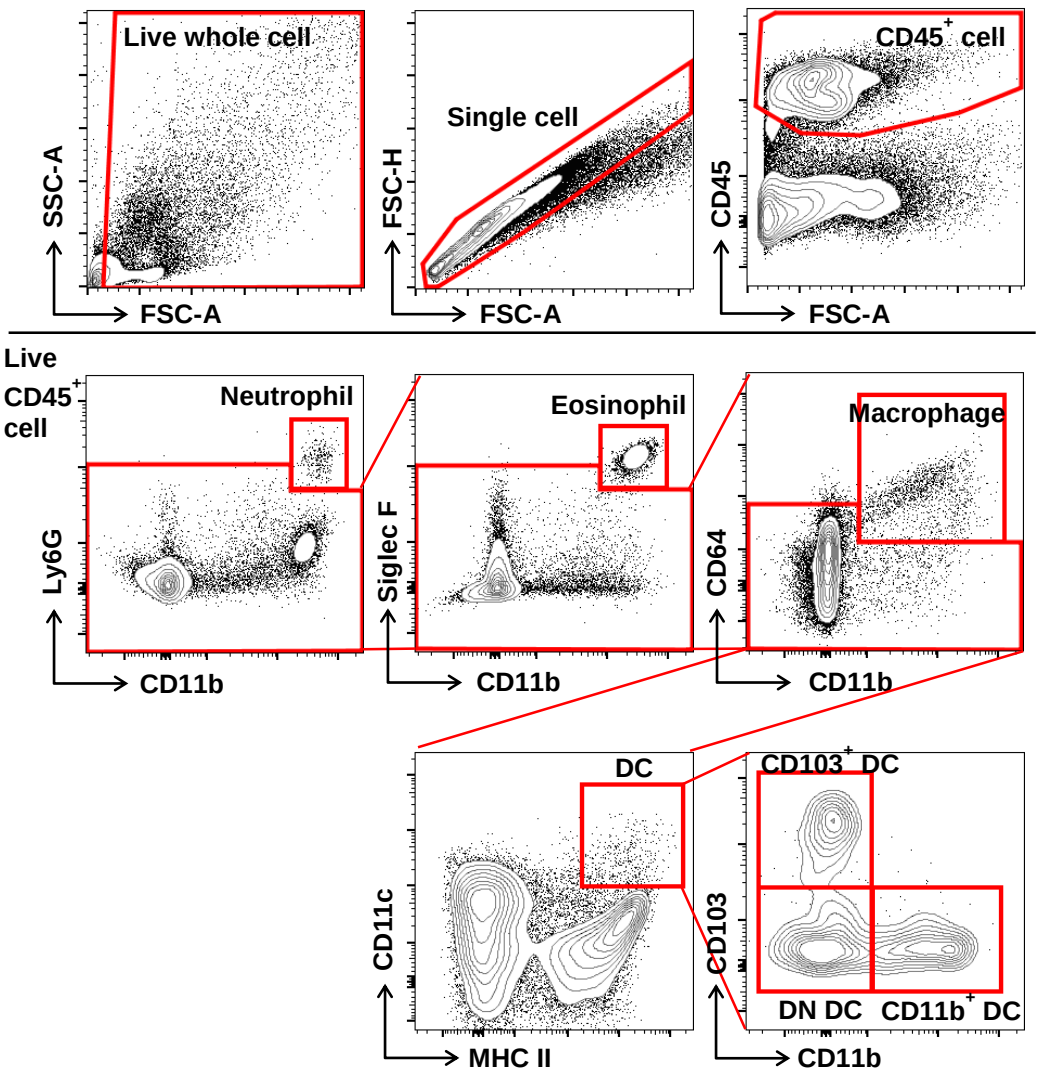
Live whole cell
SSC-A
FSC-A
Single cell
FSC-H
FSC-A
CD45+ cell
CD45
FSC-A
Live
CD45+
cell
Neutrophil
Ly6G
CD11b
Eosinophil
Siglec F
CD11b
Macrophage
CD64
CD11b
DC
CD11c
MHC II
CD103+ DC
CD103
DN DC
CD11b+ DC
CD11b

B

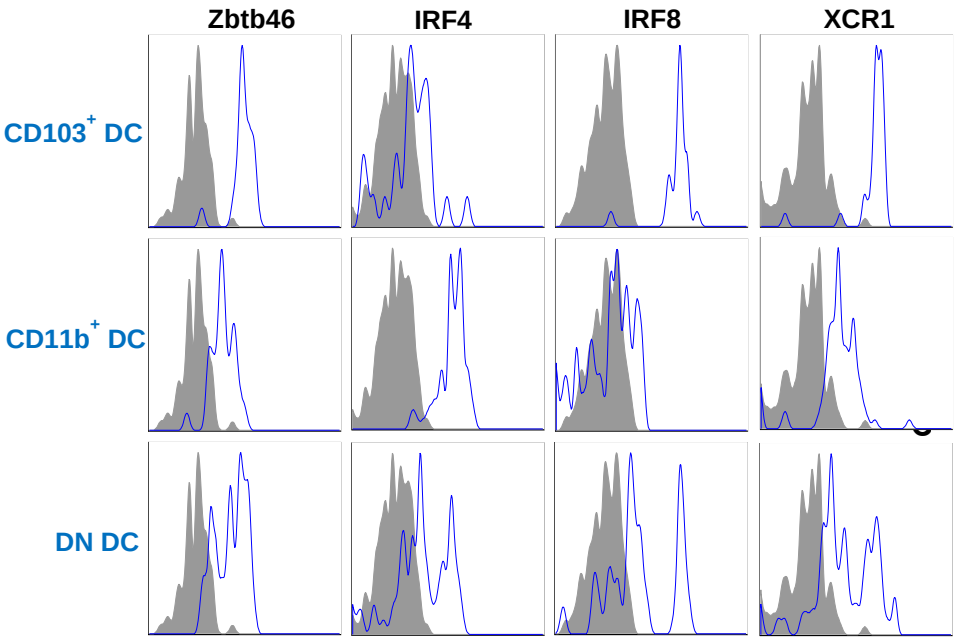
Zbtb46
IRF4
IRF8
XCR1
CD103+ DC
CD11b+ DC
DN DC

C

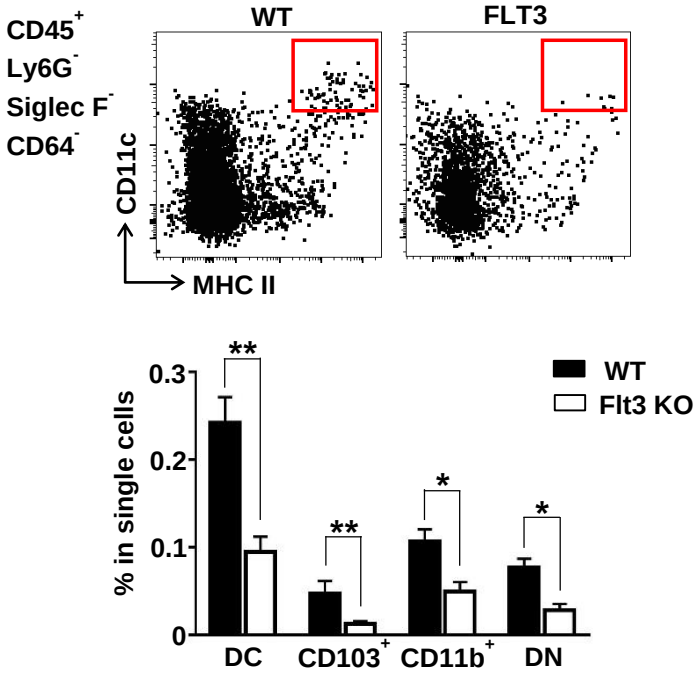
CD45+
Ly6G-
Siglec F-
CD64-
WT
FLT3
CD11c
MHC II
**
**
*
*
0.3
0.2
0.1
0
% in single cells
WT
Flt3 KO
DC
CD103+
CD11b+
DN

D

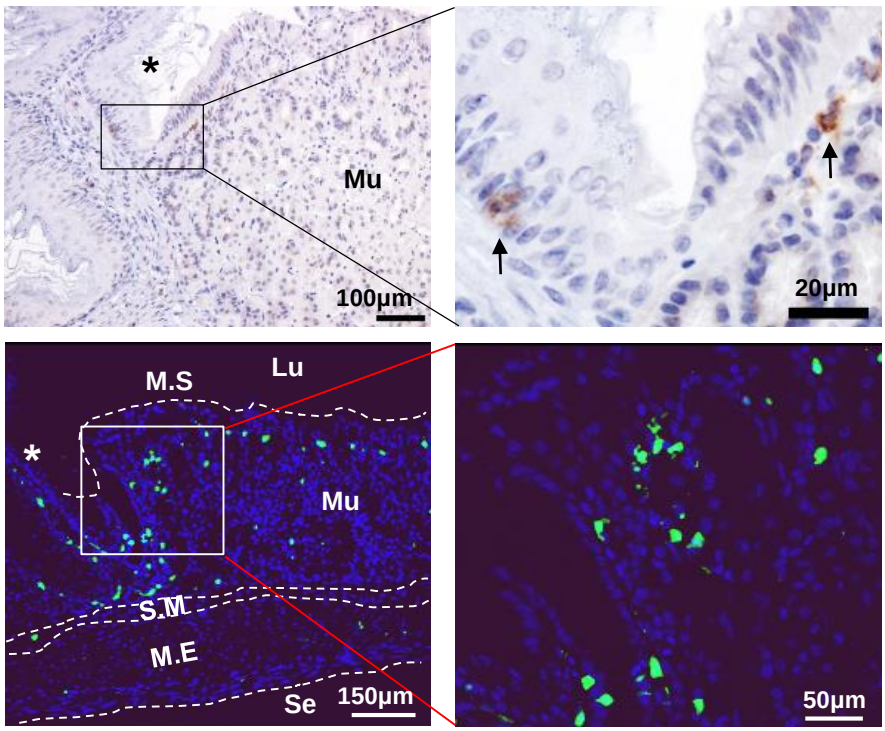

Fig 1. Characterization of gastric DCs. (A) Gating strategy to identify DCs and DC subsets from isolated cells of entire glandular stomach. (B) Distinctive marker expression of DC subsets. $CD103^{+}$ DCs are $IRF8^{+}XCR^{high}$, $CD11b^{+}$ DCs are $IRF4^{+}XCR^{low}$, and $CD103^{-}CD11b^{-}$ DCs show mixed expression profile of these markers. Note that all DC subsets express Zbtb46. (C) The percentage of DCs and DC subsets in the live single cells of the stomach in the normal Flt3 KO and WT mice. Representative FACS plots (left panel). Gastric DCs and all DC subsets are deficient in Flt3 KO mice (n=9) compared to WT mice (n=11). (*$P < 0.01$ and **$P < 0.001$) (D) Localization of gastric $CD11c^{+}$ DCs (arrows) under the steady state. Top panel: Representative images of CD11c IHC (DAB). Bottom panel: Representative images of normal CD11c-EYFP mouse stomach. The asterisk indicates a limiting ridge that is the boundary of the glandular and nonglandular stomach. (Lu: lumen, M.S: mucosal surface, Mu: mucosa, S.M: submucosa, M.E: muscularis externa, and Se: serosa)

Helicobacter infection increased the number of DCs in the stomach

To investigate the role of DCs in gastritis, changes of gastric DCs in *H. felis*-infected WT mice were examined by sequential autopsy at 2, 4, and 8 weeks after infection. FACS analysis showed that, with an increase in the duration of *H. felis* infection, the infiltration of leukocytes and DCs into the stomach increased. During 2 to 8 weeks of *H. felis* infection, infiltration of $CD45^+$ leukocytes and $CD64^-$ $CD11c^+$MHC II^+ DCs into the stomach was more apparent than that under steady state, approximately 1.8 to 2.8 fold and 2.1 to 4.2 fold, respectively, based on the ratio of single cells. Furthermore, the $CD103^+$ and DN subsets increased markedly at 2, 4, and 8 weeks after *H. felis* infection, and the $CD11b^+$ subset increased significantly at 4 and 8 weeks after *H. felis* infection (Fig 2A). To observe the changes in the distribution and number of DCs in the stomach, immunostaining of CD11c was performed. $CD11c^+$ cells were mainly located in the inflamed submucosa and mucosal laminar propria right above the muscularis mucosa, and a few were distributed throughout the mucosal lamina propria. The number of $CD11c^+$ cells infiltrating the stomach gradually increased during *H. felis* infection (Fig 2B).

A

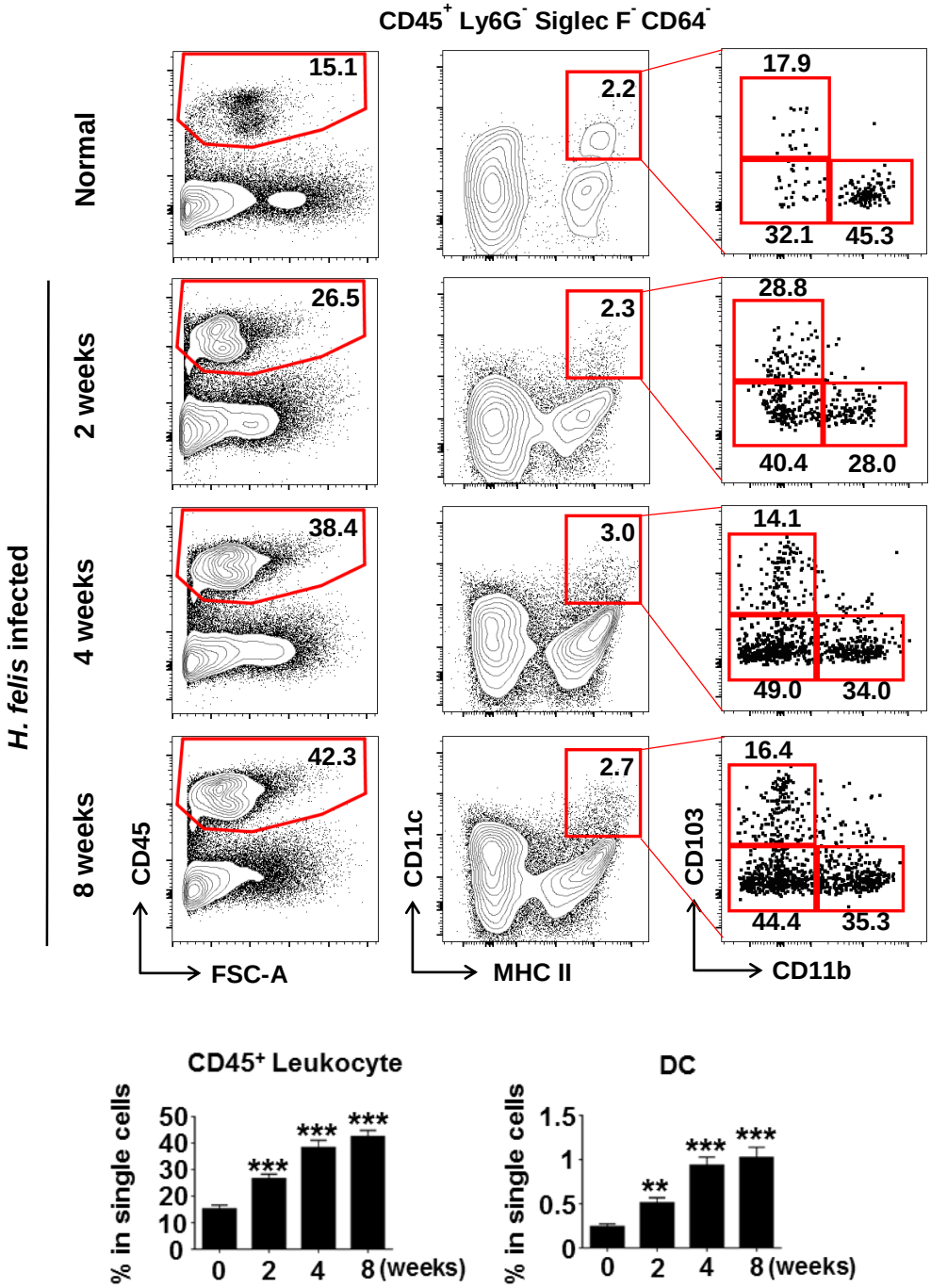
CD45+ Ly6G- Siglec F- CD64-
Normal
2 weeks
4 weeks
8 weeks
H. felis infected
15.1
2.2
17.9
32.1
45.3
26.5
2.3
28.8
40.4
28.0
38.4
3.0
14.1
49.0
34.0
42.3
2.7
16.4
44.4
35.3
CD45
FSC-A
CD11c
MHC II
CD103
CD11b
CD45+ Leukocyte
% in single cells
50
40
30
20
10
0
***
***
***
0
2
4
8 (weeks)
DC
% in single cells
1.5
1
0.5
0
**
***
***
0
2
4
8 (weeks)

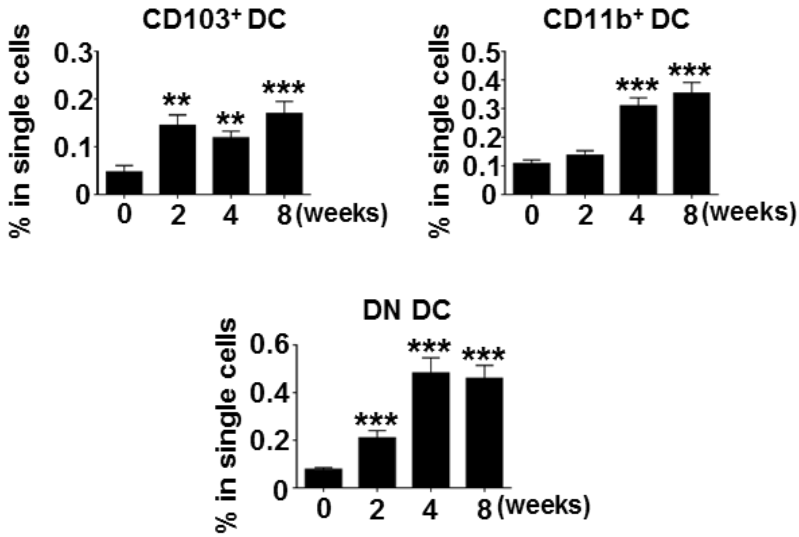
CD103+ DC
% in single cells
0.3
0.2
0.1
0
**
**
***
0
2
4
8 (weeks)
CD11b+ DC
% in single cells
0.5
0.4
0.3
0.2
0.1
0
***
***
0
2
4
8 (weeks)
DN DC
% in single cells
0.6
0.4
0.2
0
***
***
***
0
2
4
8 (weeks)

B

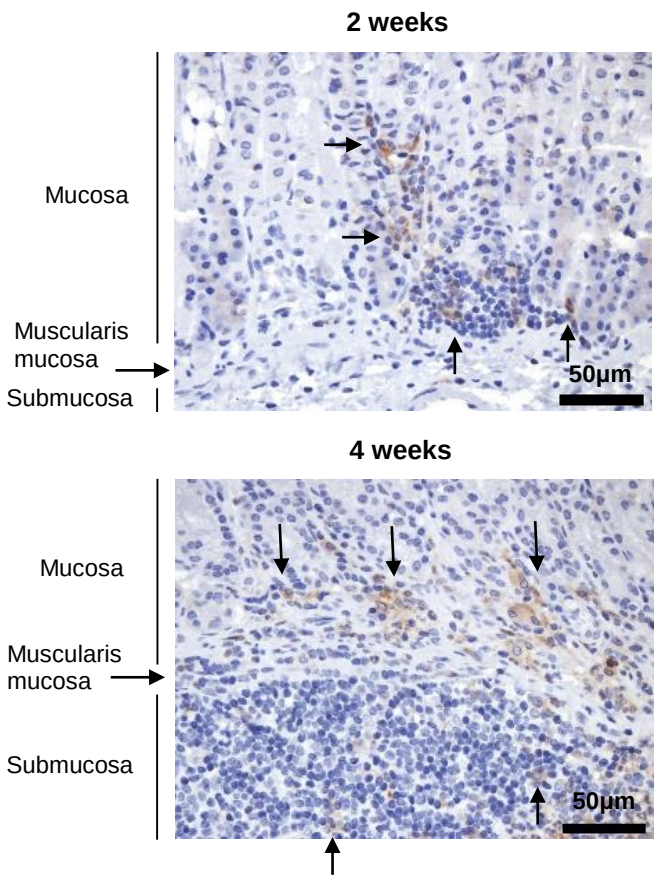
2 weeks
Mucosa
Muscularis mucosa
Submucosa
50μm
4 weeks
Mucosa
Muscularis mucosa
Submucosa
50μm

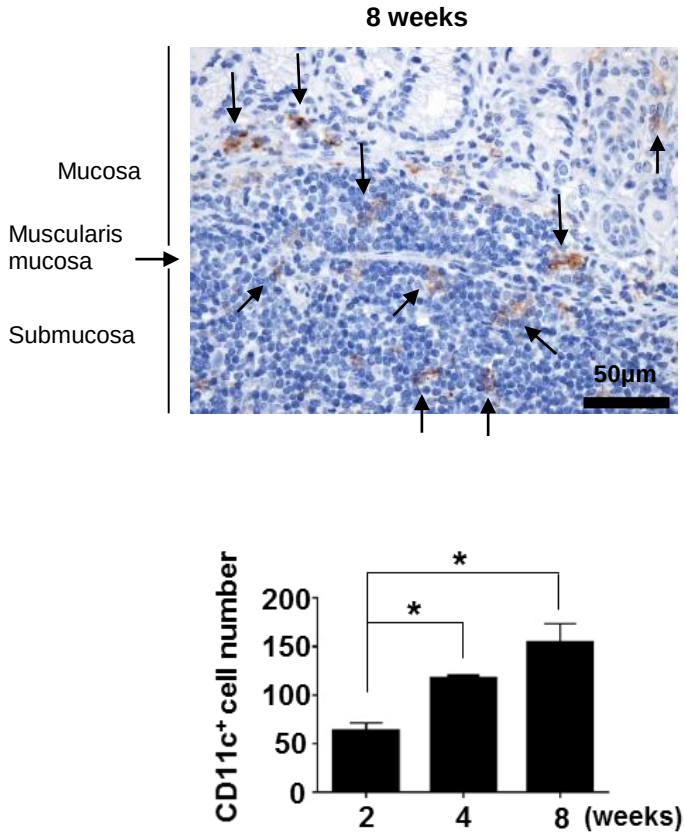

Fig 2. Numerical increase and location of gastric DCs during *H. felis* infection. (A) The percentage of leukocytes, DCs, and DC subsets in the live single cells of the stomach in the WT mice with *H. felis* infection. Top panel: Representative FACS plots. Bottom panel: Asterisks at 2, 4, and 8 weeks after *H. felis* infection (n=13-14 for each group) signify significant increase compared to that in normal WT mice (n=11). (B) Localization of $CD11c^+$ DCs (arrows) in *H. felis* infected WT mouse stomach. Top: CD11c IHC (DAB). Bottom: Manual cell count number of $CD11c^+$ DCs in 2 paraffin sections (n=5 for each group) (*$P < 0.01$, **$P < 0.001$, and ***$P < 0.0001$) Weeks: duration of infection

Flt3 KO mice have more severe gastric inflammation with less Helicobacter colonization

To determine the role of DCs in *Helicobacter*-induced gastritis, whether the immune responses differed between *H. felis*-infected Flt3 KO and WT mice was investigated. First, the severity of gastritis between the two groups was compared at 2, 4, and 8 weeks after *H. felis* infection. Histologically, inflammation occurred mainly in the corpus. In the WT mice, infiltration of neutrophils into the submucosa was mainly observed after 2 weeks of infection, and infiltration of lymphocytes and plasma cells as well was noted at 4 weeks and the most prominently at 8 weeks after infection. These inflammatory cells mostly infiltrated into the submucosa, and, as the severity of gastritis increased, they infiltrated into the mucosal lamina propria. In addition, lymphoid follicles were occasionally present in the submucosa or mucosa. In contrast, in Flt3 KO mice, infiltration of not only neutrophils but also many lymphocytes and plasma cells was noted at 2 weeks and continued to increase gradually until 8 weeks. The infiltration of inflammatory cells was mainly observed in the submucosa, but often diffusely expanded to the entire mucosal lamina propria. Therefore, gastritis was more marked in Flt3 KO mice than in WT mice (Fig 3A). In the corpus mucosa of mice in which inflammation had spread to the mucosa, varying numbers of parietal cells were lost and replaced by foveolar cell and mucous neck cell hyperplasia. In addition, some mature chief cells transdifferentiated to the metaplastic mucous-secreting cells, which appears to be a process of spasmolytic polypeptide-expressing metaplasia (SPEM) (Weis, Sousa et al. 2013). The degree of loss of parietal cells was confirmed by IHC for H^+/K^+ ATPase and the degree of mucous neck cell hyperplasia and transdifferentiation of

chief cells was confirmed by Alcian blue staining (Fig 3B). The mucosal changes were more prominent in Flt3 KO mice, which have more severe gastritis, than in WT mice (Fig 3C). Furthermore, in *H. pylori* infection, gastritis tended to be more severe in Flt3 KO mice than in WT mice. According to the updated Sydney classification, inflammation scores were 2 ± 1 in Flt3 KO mice and 1 or 2 in WT mice (Fig 3D).

Many previous studies have shown a strong positive correlation between the degree of inflammation and clearance of infectious agents. The clearance of *Helicobacter* in the stomach has been reported to be dependent on $CD4^+$ T cell-mediated IFN-γ (Sayi, Kohler et al. 2009). Therefore, the degree of *H. felis* colonization in each group was measured. *H. felis* was mainly present in the gastric pits and mucus layer throughout the glandular part (Fig 3E). The degree of *H. felis* colonization increased during 8 weeks of infection. Bacterial load was lower in Flt3 KO mice than in WT mice, and this difference was the most noticeable after 8 weeks of infection (Fig 3F and 3G).

A

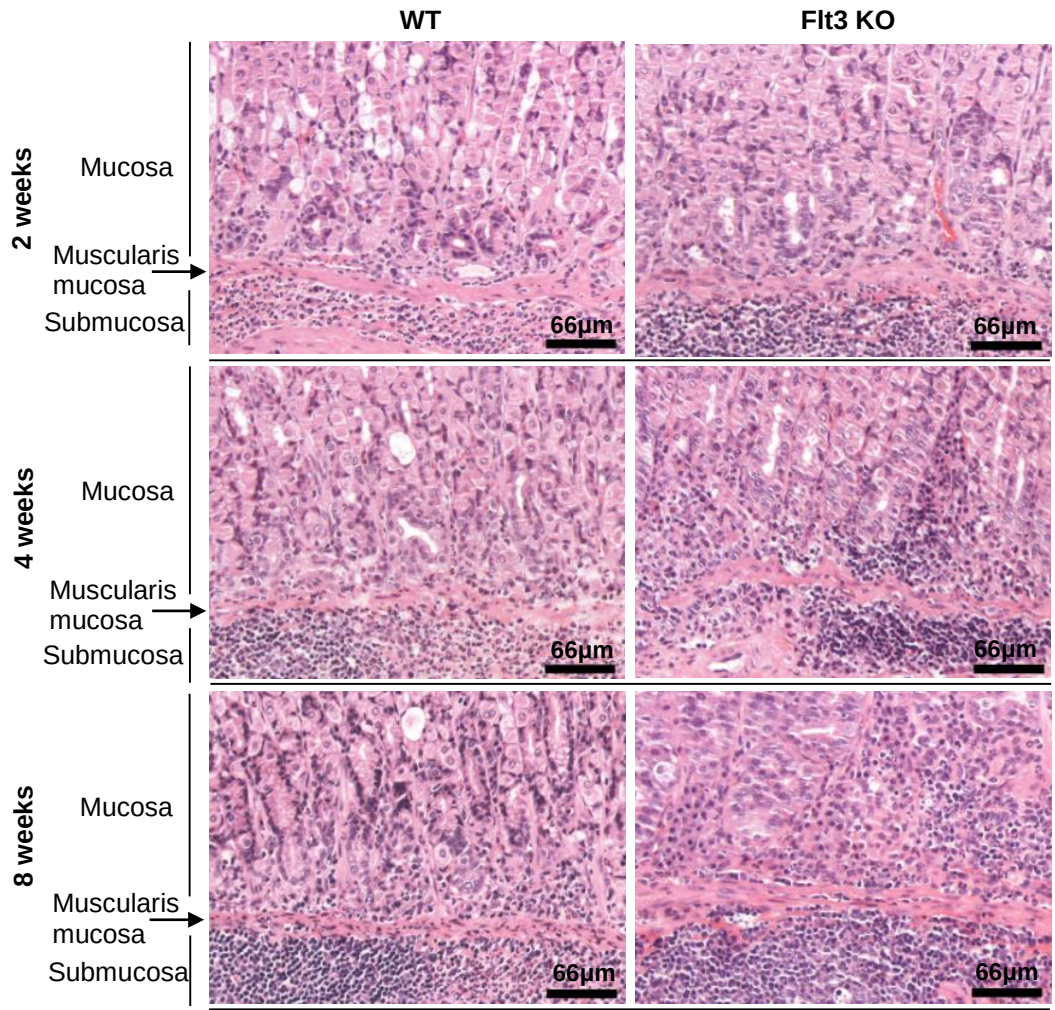
WT
Flt3 KO
2 weeks
Mucosa
Muscularis mucosa
Submucosa
66μm
4 weeks
Mucosa
Muscularis mucosa
Submucosa
66μm
8 weeks
Mucosa
Muscularis mucosa
Submucosa
66μm

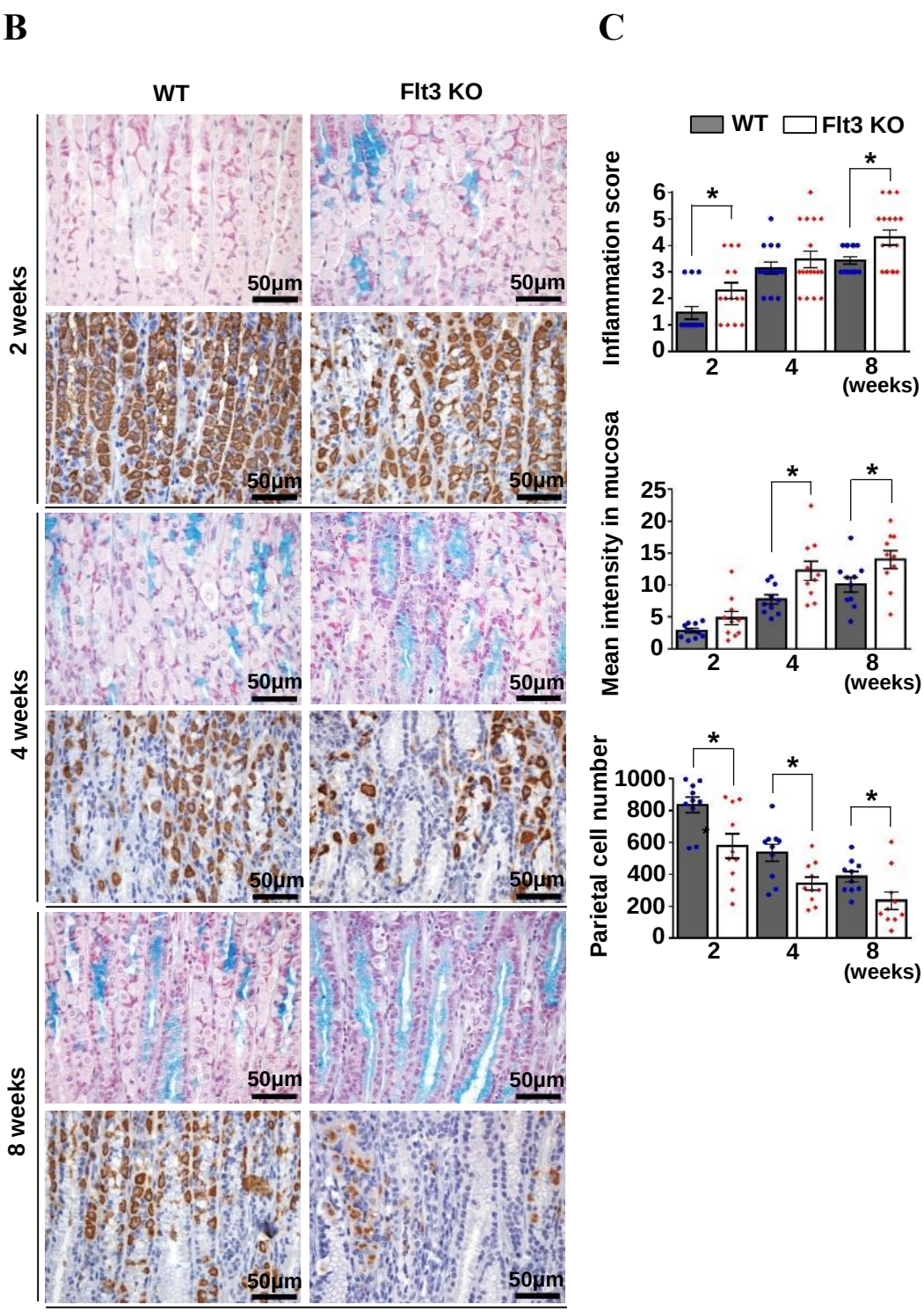
B
C
WT
Flt3 KO
2 weeks
4 weeks
8 weeks
50μm
WT
Flt3 KO
Inflammation score
Mean intensity in mucosa
Parietal cell number
(weeks)
*

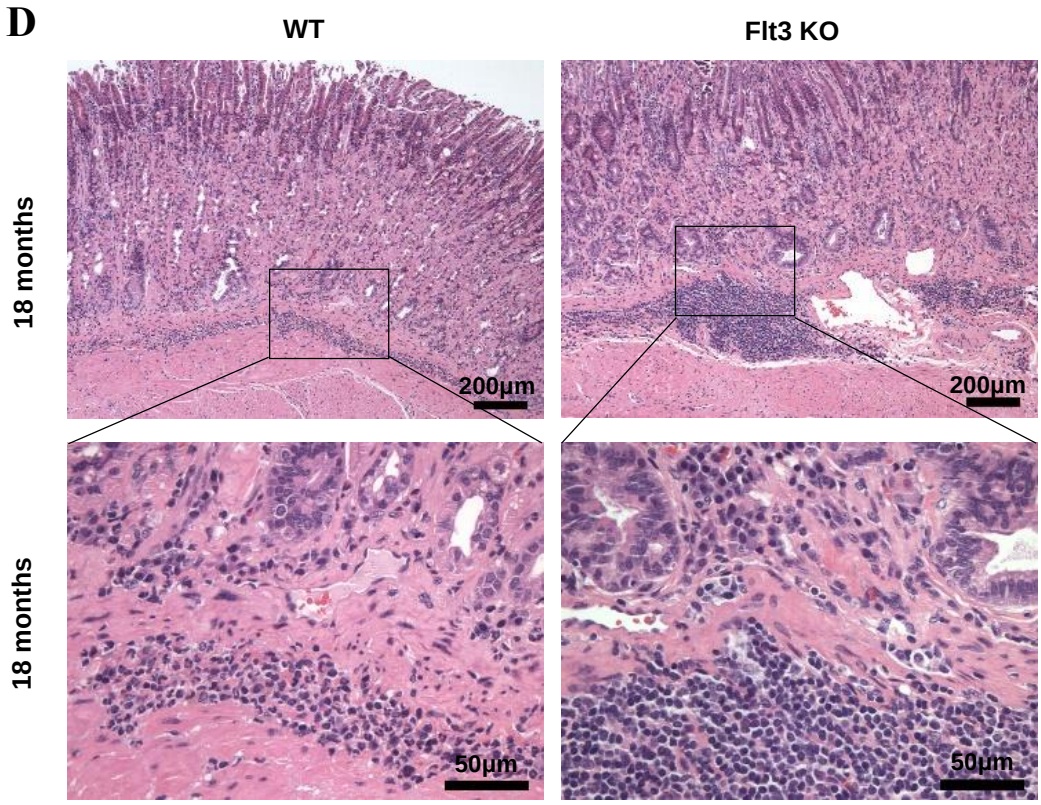
D
WT
Flt3 KO
18 months
18 months
200μm
200μm
50μm
50μm

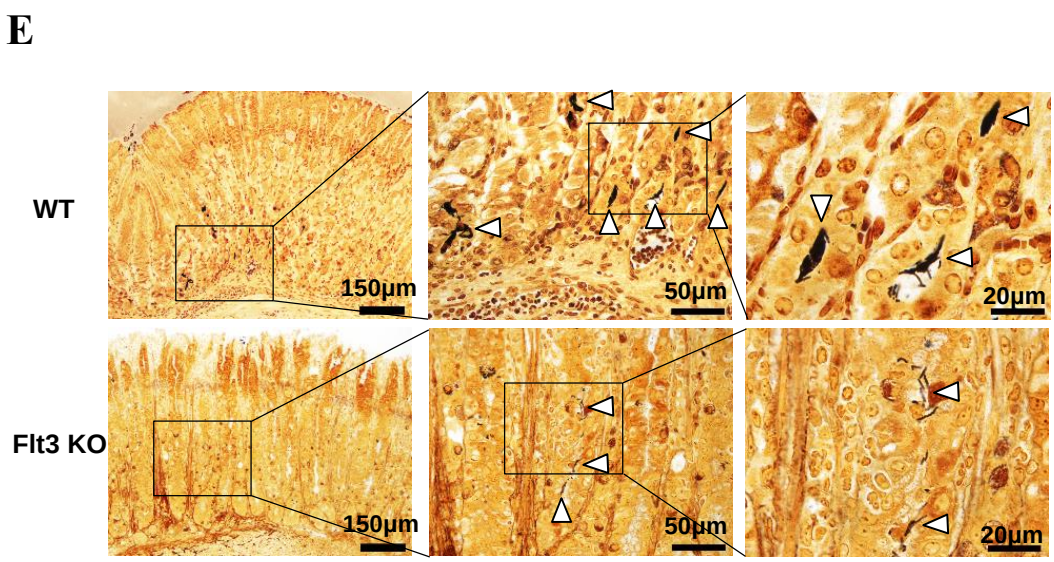
E
WT
Flt3 KO
150μm
50μm
20μm
150μm
50μm
20μm

F

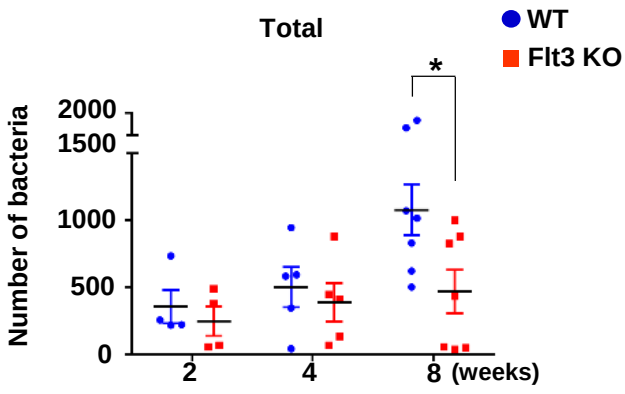
Total
WT
Flt3 KO
Number of bacteria
2000
1500
1000
500
0
*
2
4
8 (weeks)

G

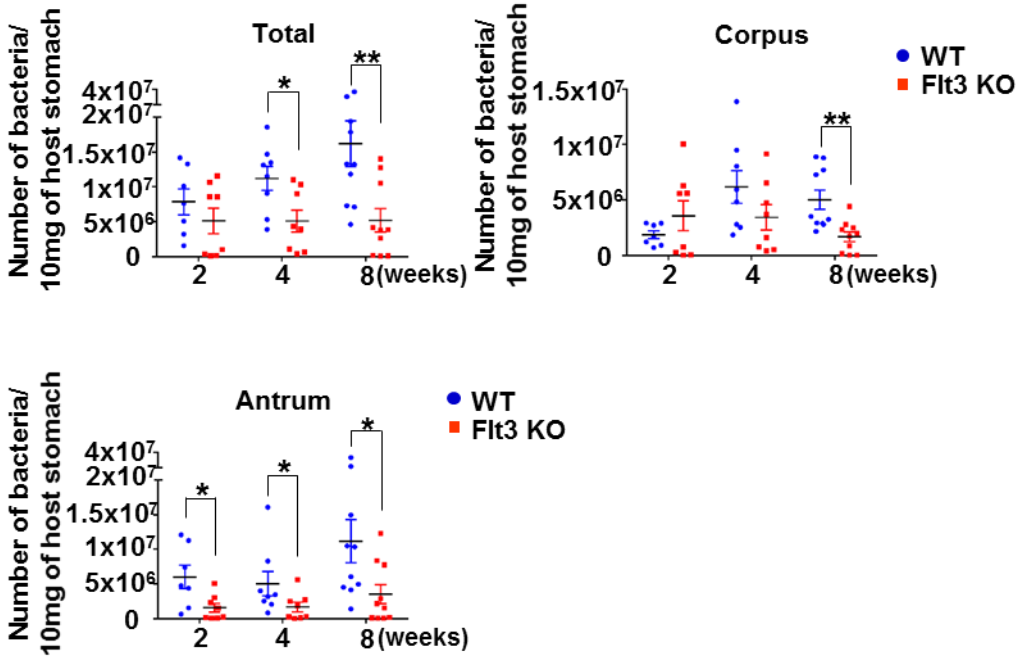
Total
Number of bacteria/ 10mg of host stomach
4x10^7
2x10^7
1.5x10^7
1x10^7
5x10^6
0
*
**
2
4
8(weeks)
Corpus
1.5x10^7
1x10^7
5x10^6
WT
Flt3 KO
Antrum

Fig 3. Deterioration of *Helicobacter*-induced gastric lesions and decrease of bacterial load in Flt3 KO mice (A) Histopathological analysis of *H. felis*-induced gastritis. H&E stained representative images of WT (left panel) and Flt3 KO (right panel) mice were aligned. (B) Histopathological analysis of *H. felis*-induced oxyntic atrophy and mucous metaplasia. Representative serial images of WT (left panel) and Flt3 KO (right panel) mice subjected to Alcian blue staining (top) and H^+/K^+-ATPase IHC (bottom) were aligned. (2, 4, and 8 weeks after *H. felis* infection). (C) Top: Inflammation score. Each mouse was scored (n=13-17 for each group). Middle and Bottom: Mean intensity of mucosal Alcian blue positive and manual cell count number of H^+/K^+-ATPase$^+$ cells (parietal cells), respectively (n=10 for each group). (D) Histopathological analysis of *H. pylori*-induced gastritis. H&E stained representative sections of *H. pylori*-infected WT (left panel) and Flt3 KO (right panel) mice (WT–n=7; Flt3 KO–n=5) (E) Localization of *H. felis* (white arrowheads) in WT and Flt3 KO mouse stomach (Warthin-Starry stain). (F) Manual count number of *H. felis* in 2 paraffin sections (n=4-7 for each group). (G) *H. felis* loads were evaluated using qRT-PCR for *H. felis* Fla-B DNA extracted from the corpus and antrum (n=7-10 for each group). (*$P < 0.05$ and **$P < 0.01$) Weeks: duration of infection

Flt3 KO mice showed more prominent CD8$^+$ T cell accumulation than WT mice during Helicobacter infection

FACS analysis was used to observe the changes in various leukocyte populations that infiltrated into *H. felis*-infected stomach (Fig 4). Among the leukocyte populations, T cell infiltration was the most prominent difference between WT and Flt3 KO mice. In Flt3 KO mice, infiltration of CD8$^+$ T cell was dramatically higher than that in WT mice. In addition, infiltration of CD4$^+$ T cell tended to be greater in Flt3 KO mice than in WT mice when the *H. felis* infection persisted for 8 weeks. However, no difference in the extent of Treg infiltration was noted between the two groups (Fig 5A). These phenotypes were recapitulated in the *H. pylori*-infected Flt3 KO mice (Fig 5B). The T cell infiltration was more prominent in not only submucosa but also mucosal lamina propria in Flt3 KO mice than in WT mice (Fig 5C). Meanwhile, in the gastric lymph node and spleen, the degree of T cell accumulation was not different between the two groups (Fig 5D and 5E). To confirm a clear correlation between infiltrated immune cells and *H. felis* clearance, the degree of infiltration of each leukocyte population and *H. felis* loads were compared in each *H. felis*-infected mouse. As the result, CD8$^+$ and CD4$^+$ T cells seemed to have the major effect on bacterial clearance (Fig 5F). *H. felis* infection increased the mRNA expression of various cytokines related to inflammation. The expression of IFN-γ was significantly higher by approximately 6 fold in Flt3 KO mice than in WT mice. In addition, granzyme A and perforin, which are closely related to CD8$^+$ T cell activity, were approximately 2.9 and 2.2 fold higher in Flt3 KO mice than in WT mice, respectively. On the other hand, no significant difference in IL-10 and TGF-β was observed between the two groups

(Fig 5G). The levels of various chemokines, including CCL2 (MCP-1), CCL3 (MIP-1α), CCL4 (MIP-1β), CCL5 (RANTES), and CCL8 (MCP-2), were higher in the gastric tissue of *H. felis*-infected Flt3 KO mice than in that of WT mice. The difference between the two groups was clearly observed after 8 weeks of *H. felis* infection (Fig 5H). The abovementioned chemokines belong to the C-C chemokine family, which has chemotactic effect mainly on monocytes and lymphocytes (Yamaoka, Kita et al. 1998), and are particularly well known for promoting T cell induction (Roth, Carr et al. 1995). CCL2, CCL3, CCL4, and CCL5 are produced in activated $CD8^+$ T cells, and CCL2 and CCL5 contribute to T cell migration to the peripheral infection site (Kim, Nottingham et al. 1998; Ohtani, Ohtani et al. 2004). These data indicate DC ablation increased pro-inflammatory chemokines which induce further T cell infiltration.

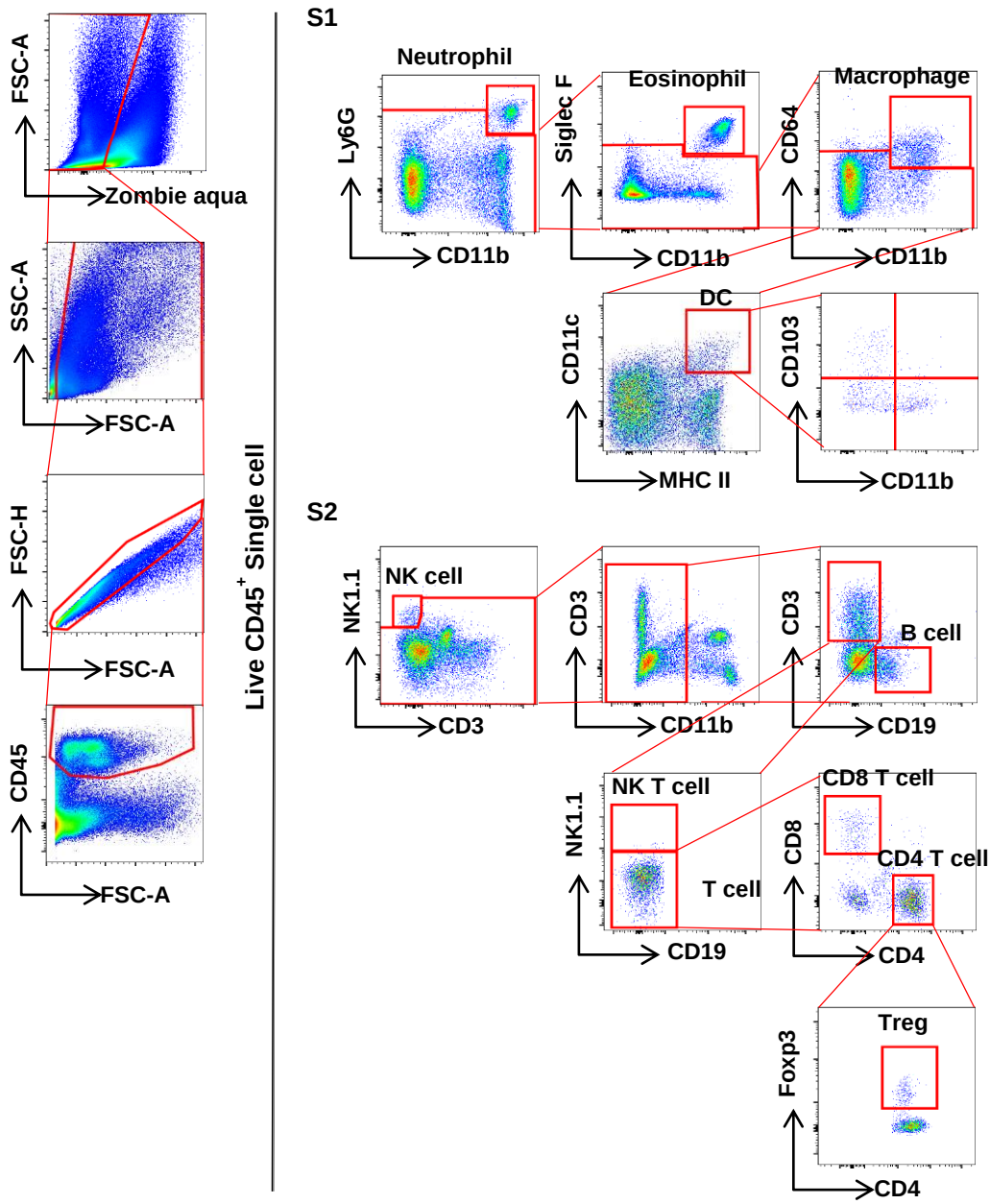

Fig 4. Gating strategy to identify various types of immune cells from isolated cells of the entire glandular stomach upon *H. felis* infection.

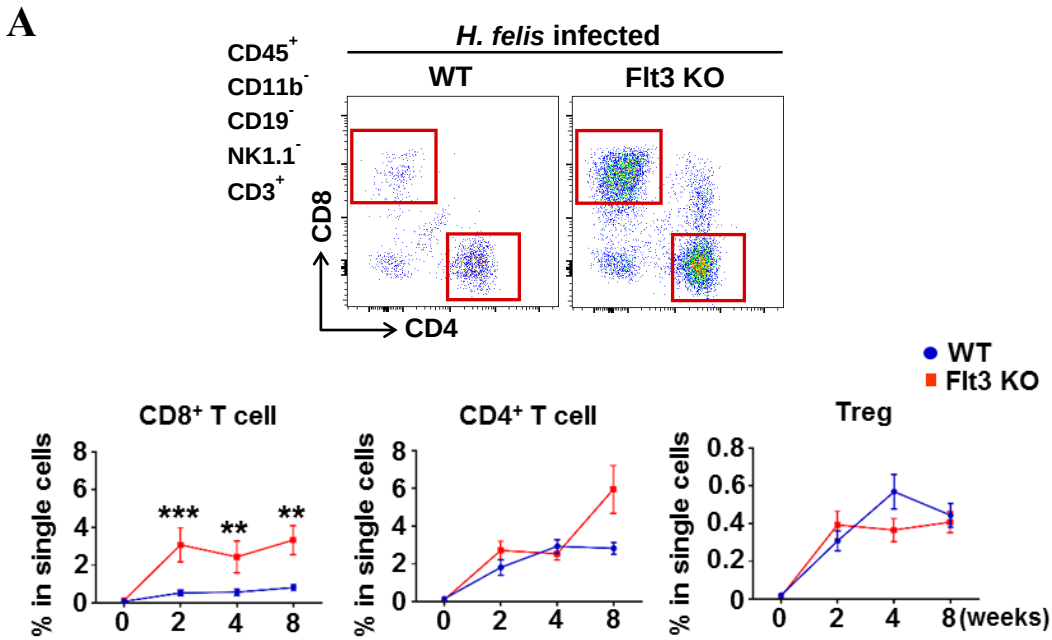
A
H. felis infected
WT
Flt3 KO
CD45+
CD11b-
CD19-
NK1.1-
CD3+
CD8
CD4
WT
Flt3 KO
CD8+ T cell
CD4+ T cell
Treg
% in single cells
***
**
**
0 2 4 8
0 2 4 8
0 2 4 8 (weeks)

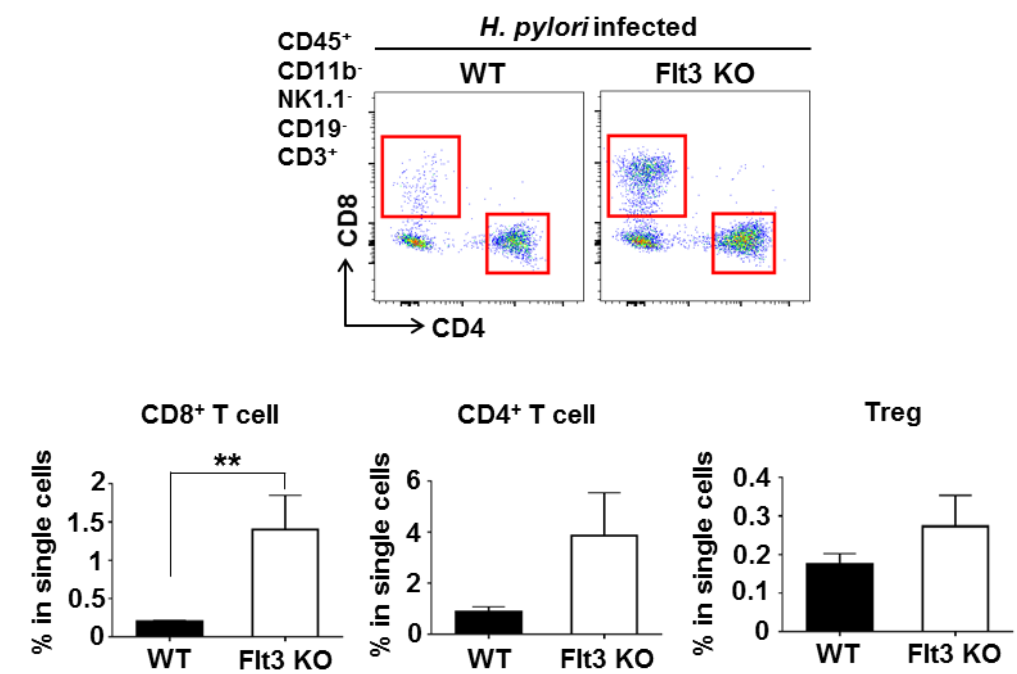
B
H. pylori infected
WT
Flt3 KO
CD45+
CD11b-
NK1.1-
CD19-
CD3+
CD8
CD4
CD8+ T cell
CD4+ T cell
Treg
% in single cells
**
WT
Flt3 KO

C

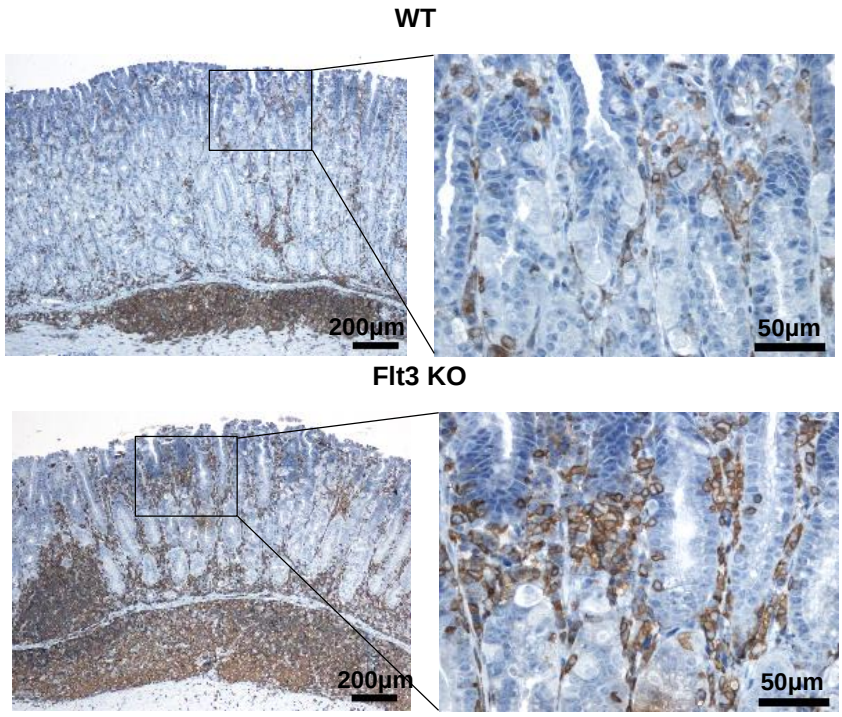
WT
200μm
50μm
Flt3 KO
200μm
50μm

D

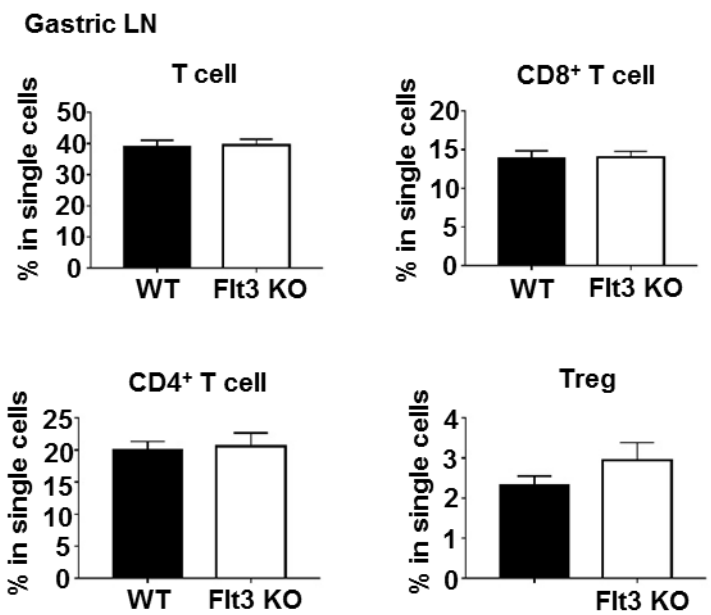
Gastric LN
T cell
% in single cells
50
40
30
20
10
0
WT
Flt3 KO
CD8+ T cell
% in single cells
20
15
10
5
0
WT
Flt3 KO
CD4+ T cell
% in single cells
25
20
15
10
5
0
WT
Flt3 KO
Treg
% in single cells
4
3
2
1
0
Flt3 KO

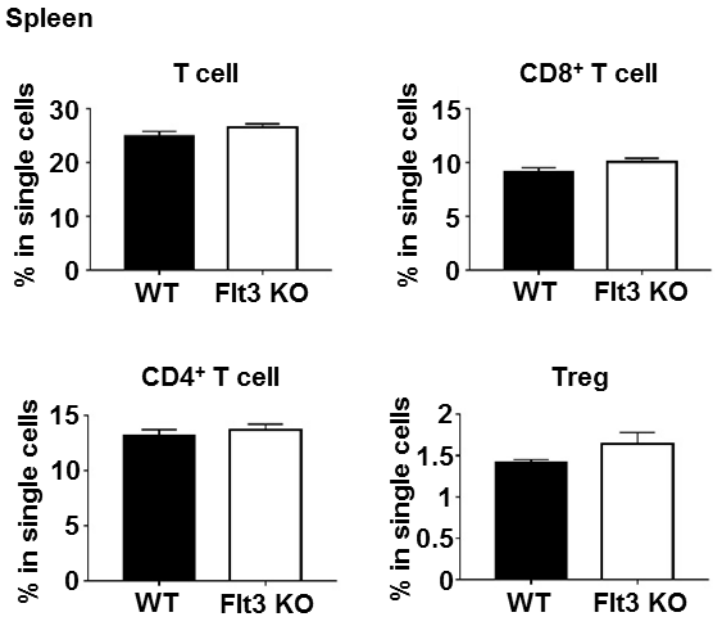
Spleen
T cell
% in single cells
30
20
10
0
WT
Flt3 KO
CD8+ T cell
% in single cells
15
10
5
0
WT
Flt3 KO
CD4+ T cell
% in single cells
15
10
5
0
WT
Flt3 KO
Treg
% in single cells
2
1.5
1
0.5
0
WT
Flt3 KO

E

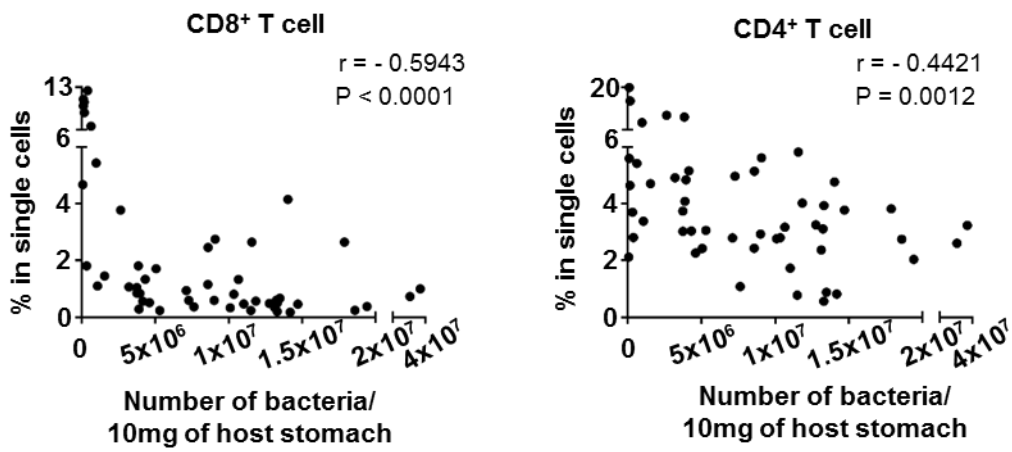
CD8+ T cell
r = - 0.5943
P < 0.0001
% in single cells
13
6
4
2
0
0
5x10^6
1x10^7
1.5x10^7
2x10^7
4x10^7
Number of bacteria/
10mg of host stomach
CD4+ T cell
r = - 0.4421
P = 0.0012
% in single cells
20
6
4
2
0
0
5x10^6
1x10^7
1.5x10^7
2x10^7
4x10^7
Number of bacteria/
10mg of host stomach

F

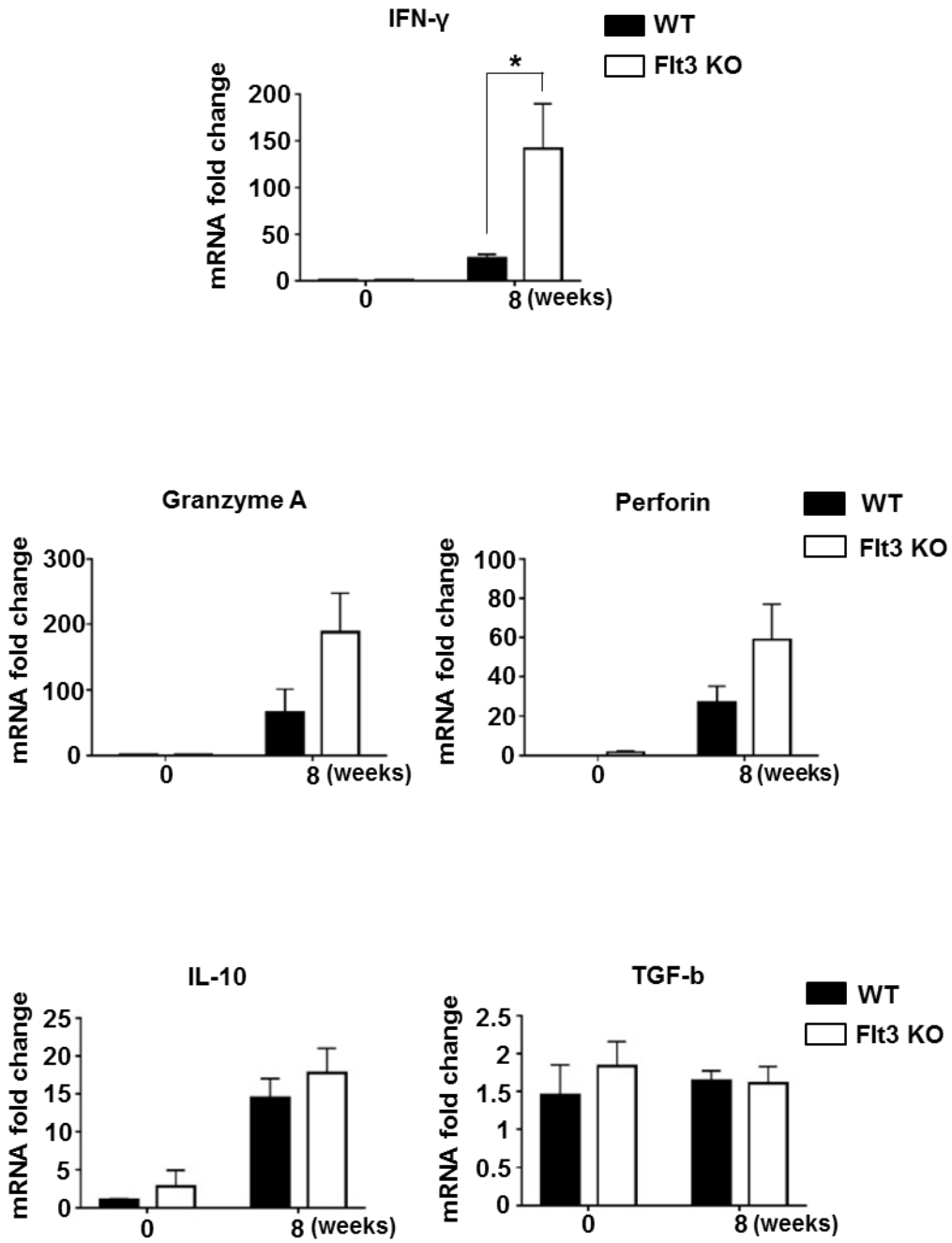
IFN-γ
WT
Flt3 KO
*
mRNA fold change
200
150
100
50
0
0
8 (weeks)
Granzyme A
mRNA fold change
300
200
100
0
0
8 (weeks)
Perforin
WT
Flt3 KO
mRNA fold change
100
80
60
40
20
0
0
8 (weeks)
IL-10
mRNA fold change
25
20
15
10
5
0
0
8 (weeks)
TGF-b
WT
Flt3 KO
mRNA fold change
2.5
2
1.5
1
0.5
0
0
8 (weeks)

G

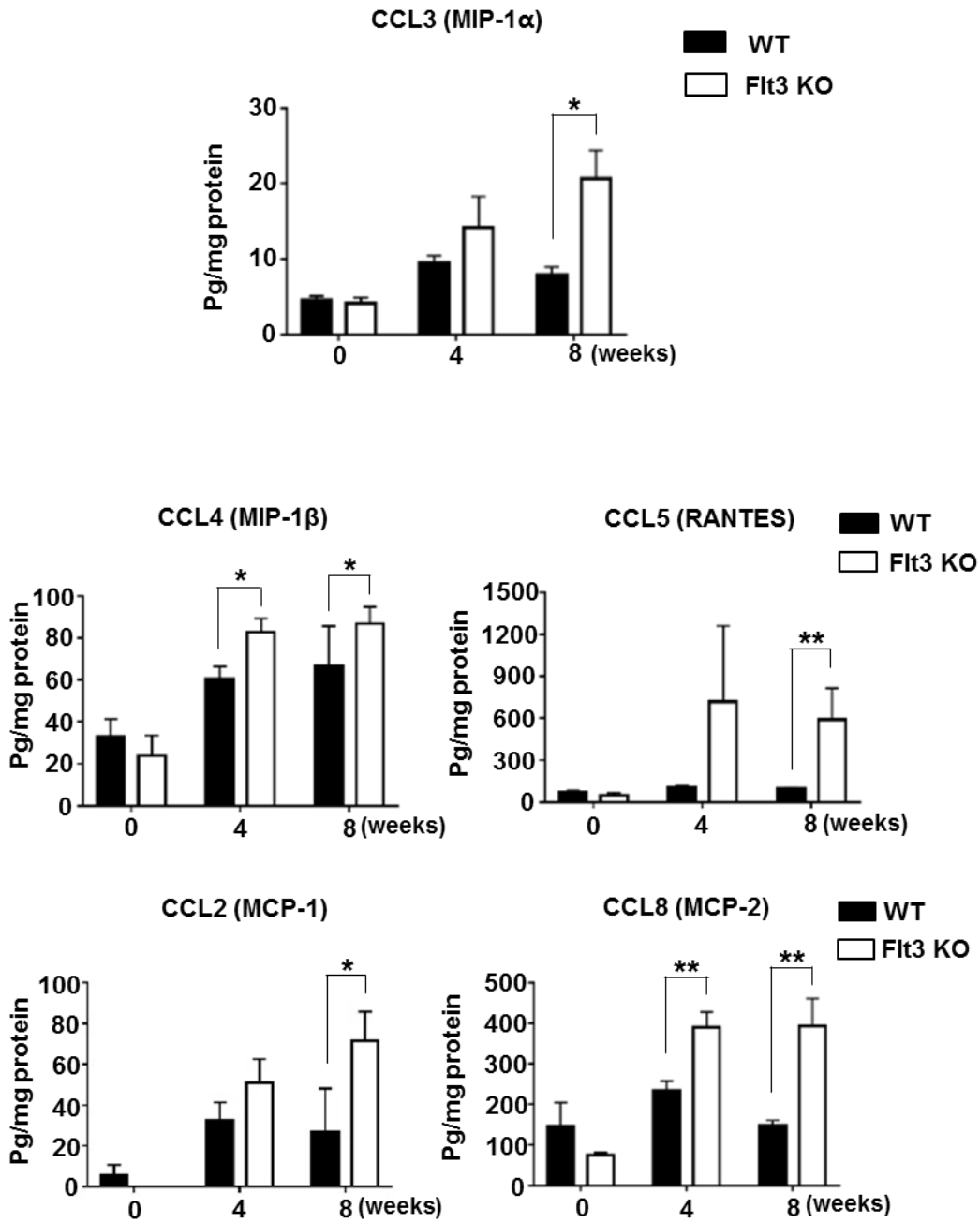
CCL3 (MIP-1α)
WT
Flt3 KO
Pg/mg protein
30
20
10
0
*
0
4
8 (weeks)
CCL4 (MIP-1β)
Pg/mg protein
100
80
60
40
20
0
*
*
0
4
8 (weeks)
CCL5 (RANTES)
WT
Flt3 KO
Pg/mg protein
1500
1200
900
600
300
0
**
0
4
8 (weeks)
CCL2 (MCP-1)
Pg/mg protein
100
80
60
40
20
0
*
0
4
8 (weeks)
CCL8 (MCP-2)
WT
Flt3 KO
Pg/mg protein
500
400
300
200
100
0
**
**
0
4
8 (weeks)

Fig 5. Prominent $CD8^+$ T cell response of *H. felis*-infected Flt3 KO mice. (A) The percentage of $CD8^+$ and $CD4^+$ T cells and Tregs in the live single cells of the stomach in the Flt3 KO and WT mice with *H. felis* infection (n=13-17 for each *H. felis* infection group, n=9-11 for the non-infection group). Representative FACS plots (top panel). (B) As in (A), but with *H. pylori* infection (WT–n=7; Flt3 KO–n=5). Note that $CD8^+$ T cells are higher in Flt3 KO mice. (C) More severe mucosal infiltration of T cells in the stomach of Flt3 KO mice. Representative images of CD3 IHC (DAB). (D) T cell accumulation in the gastric lymph node (LN) and spleen of WT and Flt3 KO mice after *H. felis* infection for 8 weeks. The percentage of total, $CD8^+$, and $CD4^+$ T cells, and Tregs in the live single cells of the gastric LN and spleen. Note that DC depletion did not affect the T cell ratio in single cells in gastric LN and spleen. (gastric LN: WT–n=9; Flt3 KO–n=10, spleen: WT–n=10; Flt3 KO–n=9) (E) Correlation between the severity of T cell infiltration and *H. felis* bacterial clearance in the stomach. A total of 51 WT and Flt3 KO mice infected with *H. felis* for 2 to 8 weeks were plotted against the percentage of $CD8^+$ T cells and $CD4^+$ T cells in the live single cells of the stomach and the number of *H. felis*. Note that *H. felis*-induced $CD8^+$ and $CD4^+$ T cell responses are negatively correlated with *H. felis* bacterial loads ($P < 0.0001$ and $P = 0.0012$) (F) Relative gastric mRNA expression level of inflammatory cytokines. Results are shown as fold change compared with that in the non-infection group. (n=6-7 for *H. felis* infection group, n=2-3 for the non-infection group). (G) Analysis of gastric chemokine levels of *H. felis*-infected Flt3 KO and WT mice by using magnetic luminex immunoassay. The measured protein concentrations (pg/ml) were corrected for the total protein content (mg/ml). (n=7 and 9 for group with 4 and 8 weeks of *H. felis* infection; n=5 for non-infection group) (*$P < 0.05$, **$P < 0.01$, and ***$P < 0.001$) Weeks: duration of infection

Enhanced gastric inflammation of Helicobacter-infected Flt3 KO mice was hematopoietic cell-intrinsic

To determine whether the *H. felis*-induced immune response in Flt3 KO mice was hematopoietic cell-intrinsic, BM chimeras were created by transplantation Flt3 KO or WT BM into irradiated WT mice. The *H. felis*-infected recipient mice were analyzed after 8 weeks. FACS analysis of the gastric tissues showed that all subsets of gastric DCs were significantly decreased in the Flt3 KO BM transplanted mice, compared with WT BM transplanted mice (Fig 6A). The $CD8^+$ and $CD4^+$ T cell response was more prominent in Flt3 KO BM transplanted mice than in WT BM transplanted mice. There was no difference in the degree of infiltration of Tregs between the two groups (Fig 6B). The bacterial load in the stomach was lower in Flt3 KO BM transplanted mice than in WT BM transplanted mice (Fig 6C).

A

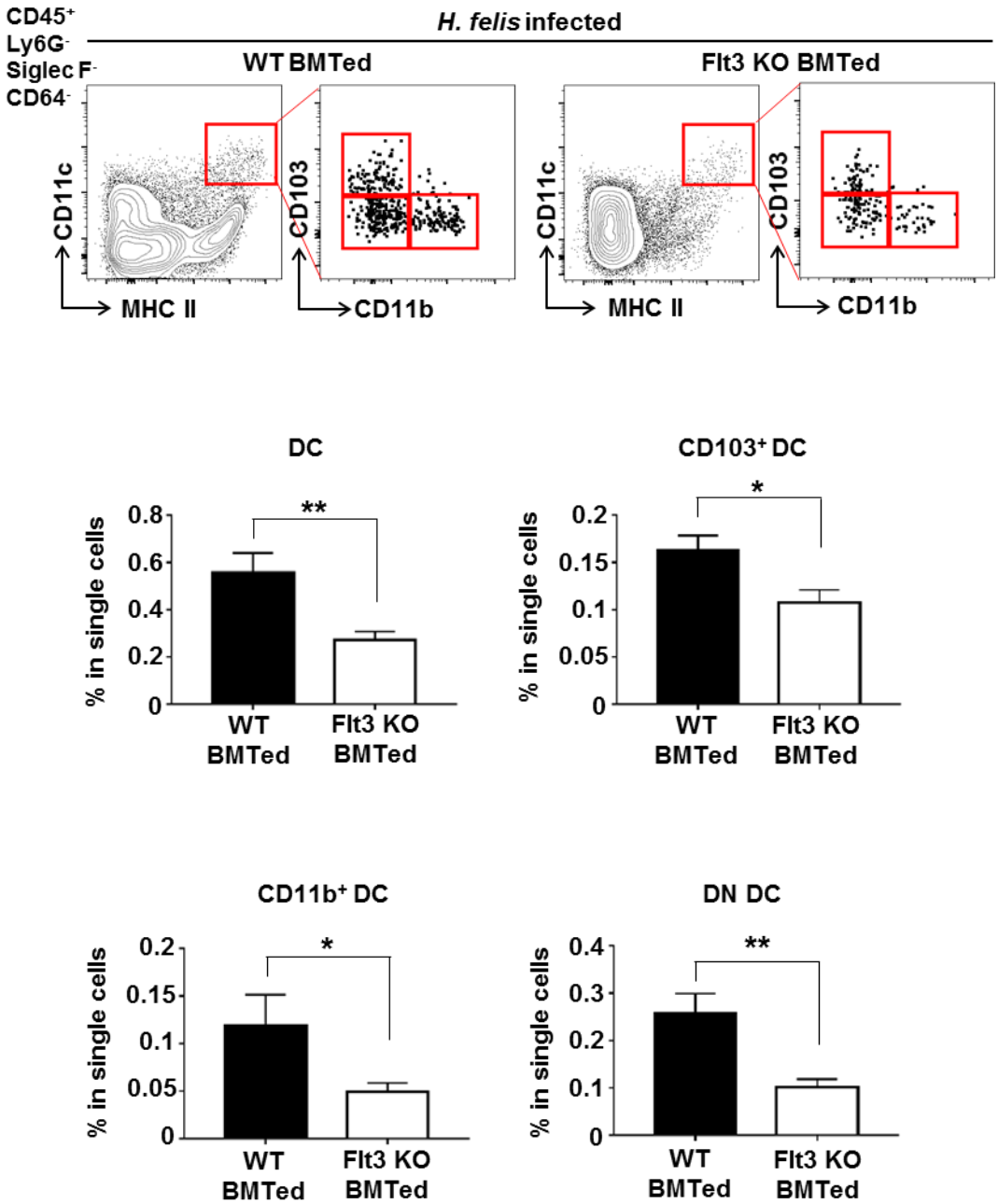
CD45+
Ly6G-
Siglec F-
CD64-
H. felis infected
WT BMTed
Flt3 KO BMTed
CD11c
MHC II
CD103
CD11b
DC
CD103+ DC
CD11b+ DC
DN DC
% in single cells
WT BMTed
Flt3 KO BMTed
**
*
*
**

B

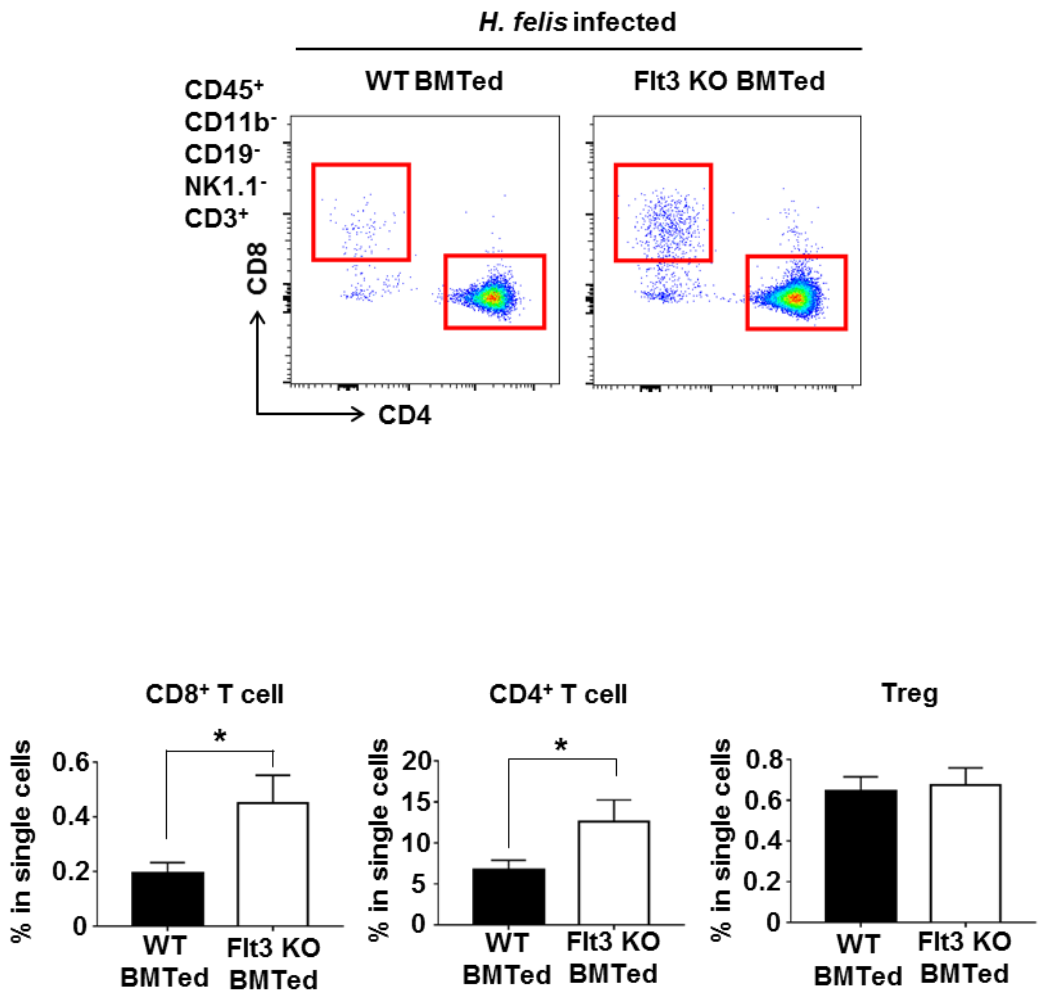
H. felis infected
WT BMTed
Flt3 KO BMTed
CD45+
CD11b-
CD19-
NK1.1-
CD3+
CD8
CD4
CD8+ T cell
CD4+ T cell
Treg
% in single cells
0.6
0.4
0.2
0
20
15
10
5
0.8
*
WT BMTed
Flt3 KO BMTed

C

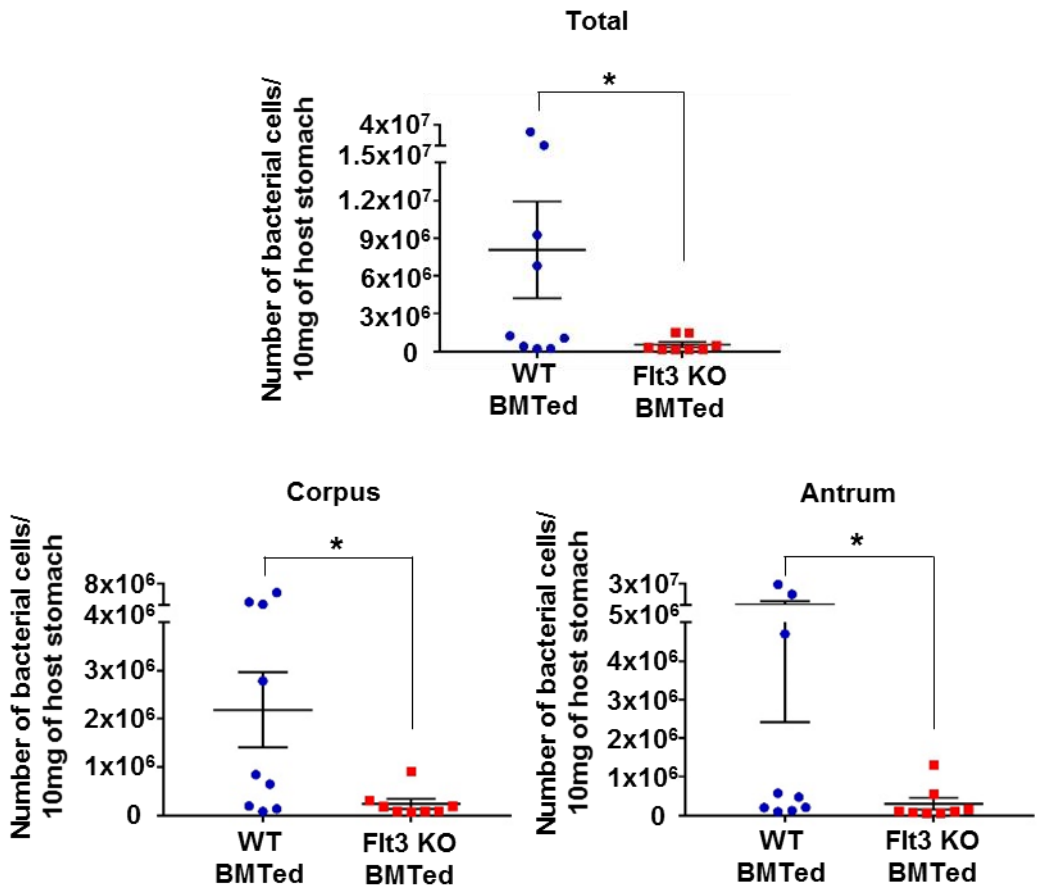

Fig 6. Prominent $CD8^+$ T cell response and decrease of bacterial load in *H. felis*-infected Flt3 KO BMTed mice after *H. felis* infection for 8 weeks. (A) The percentage of DCs and DC subsets in the live single cells of the stomach in the Flt3 KO BMTed (n=8) and WT BMTed (n=9) mice. Representative FACS plots (left panel). (B) The percentage of $CD8^+$ and $CD4^+$ T cells and Tregs in the live single cells of the stomach in the Flt3 KO BMTed (n=8) and WT BMTed (n=9) mice. Representative FACS plots (top panel). (C) *H. felis* loads were evaluated using qRT-PCR for *H. felis* Fla-B DNA extracted from corpus and antrum. (WT BMTed–n=9; Flt3 KO BMTed–n=8) (*$P < 0.05$ and **$P < 0.01$; BMTed: BM transplanted)

Depletion of cDCs enhanced Helicobacter-induced gastric inflammation

Since Flt3 KO mice lack pDCs as well as cDCs, the involvement of pDCs in the suppression of T cell response to *H. felis* could not be ruled out. Therefore, I attempted to elucidate the function of Flt3-dependent cDCs and pDCs on the immune response to *H. felis* infection by using Zbtb46-DTR mice and BDCA2-DTR mice, in which only cDC and pDC ablation is noted, respectively. DT injection has been shown to be lethal to Zbtb46-DTR mice within 1–2 days (Rombouts, Cools et al. 2017). In BDCA2-DTR mice, BM transplantation can lead to long-term depletion of pDCs (Yun, Lee et al. 2016). Thus, BM of Zbtb46-DTR and BDCA2-DTR mice was transplanted into irradiated WT mice. Gastric DCs were effectively ablated by DT injection in Zbtb46-DTR BM transplanted mice (Fig 7A). Among the other leukocyte populations, both $CD4^+$ and $CD8^+$ T cell responses were more prominent in cDC-ablated mice. However, gastric Tregs were not affected by cDC depletion (Fig 7B). Histologically, cDC ablation produced more severe inflammation and pathological mucosal changes (Fig 7C, 7D, and 7E). The expression of IFN-γ mRNA in the gastric tissues was markedly increased in cDC-ablated mice (Fig 7F).

Meanwhile, gastric pDCs were defined as $CD64^-CD11b^-Ly6C^{hi}PDCA1^+B220^+$Siglec H^+ population (Fig 8A). The pDCs were effectively ablated by DT injection in BDCA2-DTR BM transplanted mice (Fig 8B). However, no differences in T cell accumulation in the stomach were noted between pDC-ablated mice and control mice (Fig 8C). Taken together, these results indicate that gastric cDCs, but not pDCs, control gastric T cell populations during *Helicobacter* infection.

A

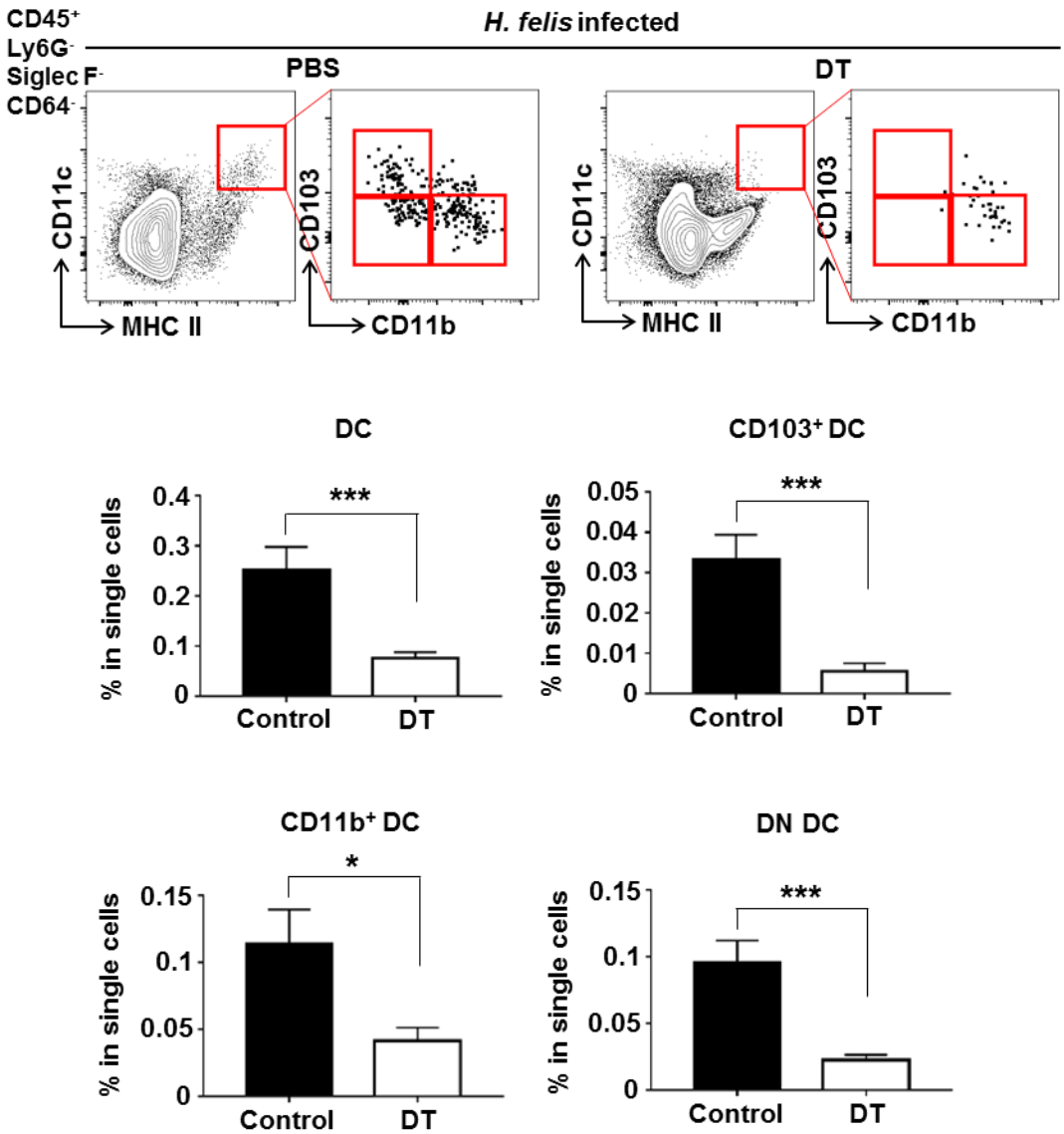
CD45+
Ly6G-
Siglec F-
CD64-
H. felis infected
PBS
DT
CD11c
MHC II
CD103
CD11b
DC
CD103+ DC
CD11b+ DC
DN DC
% in single cells
Control
DT
***
*

B

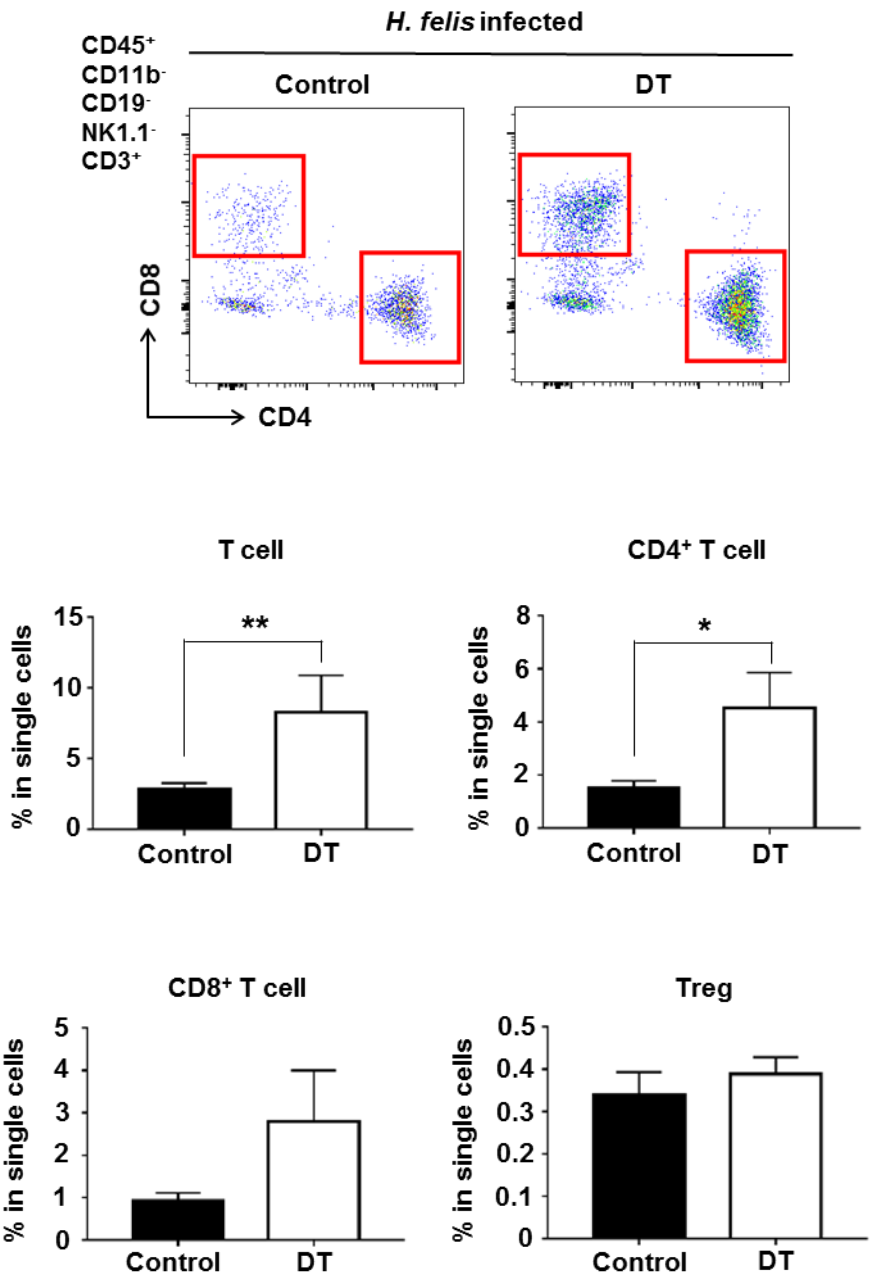
H. felis infected
CD45+
CD11b-
CD19-
NK1.1-
CD3+
Control
DT
CD8
CD4
T cell
CD4+ T cell
CD8+ T cell
Treg
% in single cells
**
*
Control
DT

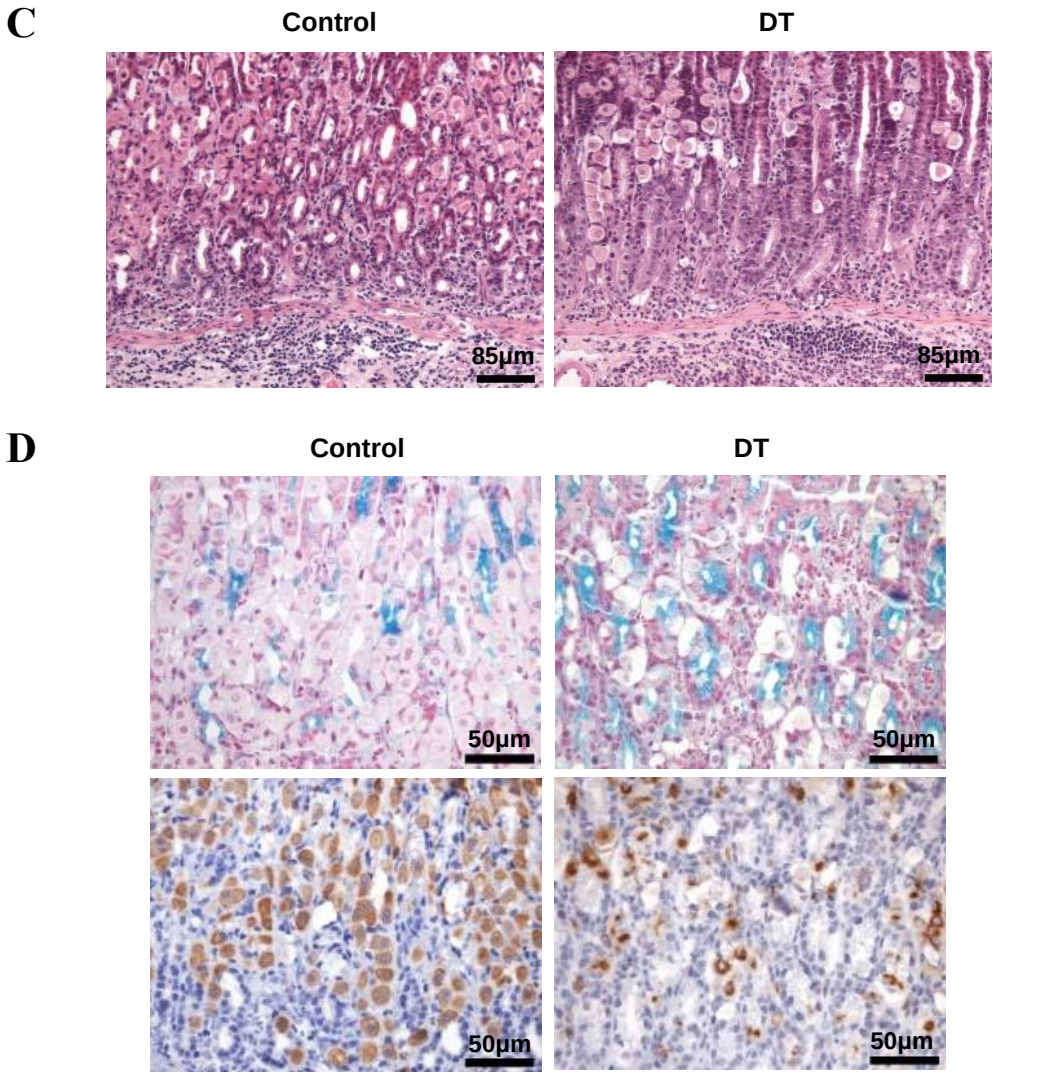
C
Control
DT
85μm
85μm
D
Control
DT
50μm
50μm
50μm
50μm
E
Inflammation score
0
1
2
3
4
5
6
Control
DT
*
Mean intensity in mucosa
0
10
20
30
40
Control
DT
*
Parietal cell number
0
200
400
600
800
1000
Control
DT
*

F

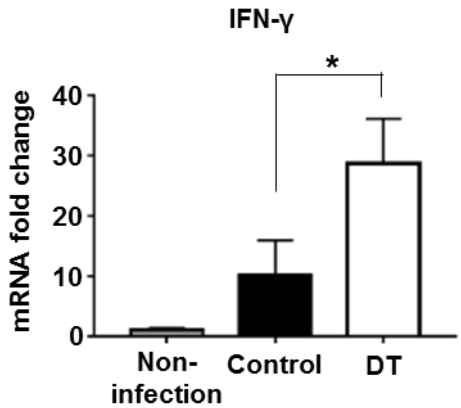

Fig 7. Deterioration of *H. felis*-induced gastric lesions and prominent T cell response in DT-injected Zbtb46-DTR BMTed mice (cDC-ablated mice) after *H. felis* infection for 4 weeks. (A) The percentage of DCs and DC subsets in the live single cells of the stomach in the cDC-ablated mice (n=10) and PBS-injected Zbtb46-DTR BMTed mice (control mice; n=8). Representative FACS plots (left panel). Note that gastric DCs and DC subsets are Zbtb46-dependent cDCs. (B) The percentage of total, $CD8^+$, and $CD4^+$ T cells, and Tregs in the live single cells of the stomach in the cDC-ablated (n=10) and control (n=8) mice. Representative FACS plots (left panel). Note that cDC depletion did not affect the Tregs ratio in single cells. (C) Histopathological analysis of *H. felis*-induced gastritis. H&E stained representative images of control (left panel) and cDC-ablated (right panel) mice. (D) Histopathological analysis of *H. felis*-induced oxyntic atrophy and mucous metaplasia. Representative serial images of control (left panel) and cDC-ablated (right panel) mice subjected to Alcian blue staining (top) and H^+/K^+-ATPase IHC (bottom). (E) Left: Inflammation score, Middle: Mean intensity of mucosal Alcian blue positive, Right: Manual cell count number of H^+/K^+-$ATPase^+$ cells (parietal cells) (control mice–n=8; cDC-ablated mice–n=10) (F) Relative gastric mRNA expression level of IFN-γ. Results are shown as fold change compared with that in the non-infection group. (non-infection group–n=3; control group–n=8; cDC-ablated group–n=10) (*$P < 0.05$, **$P < 0.01$, and ***$P < 0.001$; BMTed: BM transplanted)

A

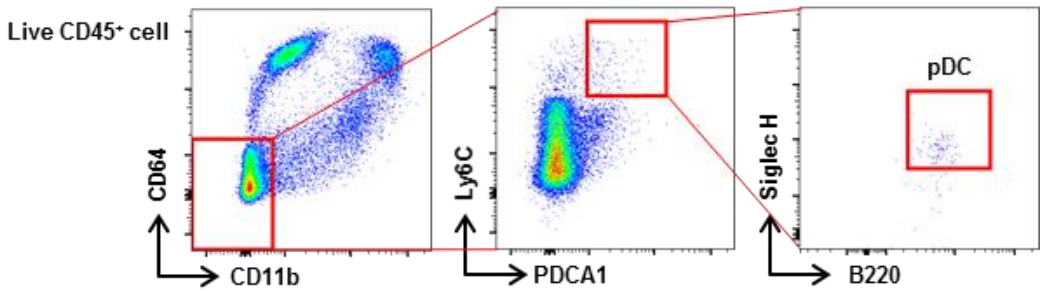
Live CD45+ cell
CD64
CD11b
Ly6C
PDCA1
Siglec H
B220
pDC

B

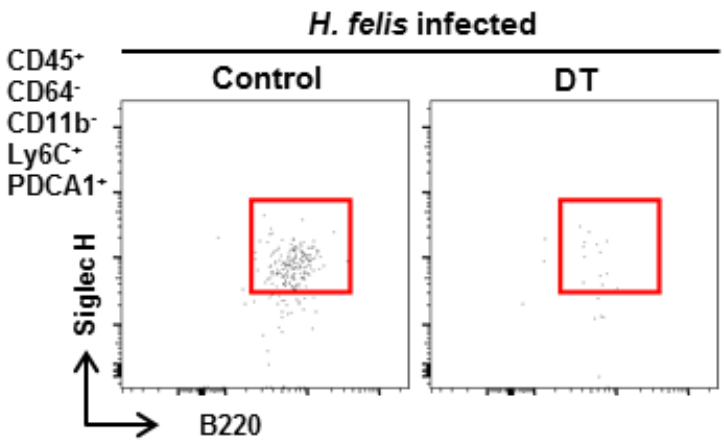
H. felis infected
Control
DT
CD45+
CD64-
CD11b-
Ly6C+
PDCA1+
Siglec H
B220

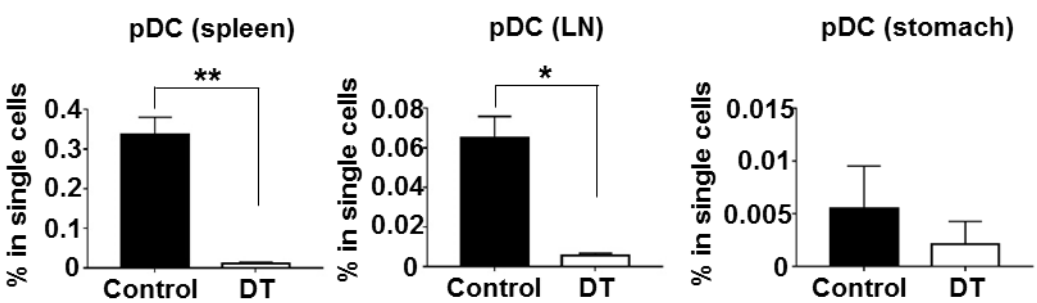
pDC (spleen)
pDC (LN)
pDC (stomach)
% in single cells
**
*
0.4
0.3
0.2
0.1
0
0.08
0.06
0.04
0.02
0.015
0.01
0.005
Control
DT

C

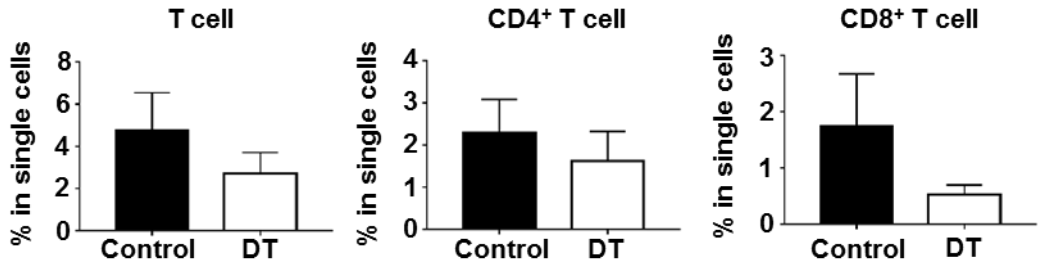

Fig 8. T cell response of DT-injected BDCA2-DTR BMTed mice (pDC-ablated mice) upon *H. felis* infection (A) Gating strategy to identify pDCs from isolated cells of the entire glandular stomach upon *H. felis* infection (B) The percentage of pDCs in the live single cells of the spleen, gastric lymph node (LN), and stomach in the pDC-ablated mice (n=5) and PBS-injected BDCA2-DTR BMTed mice (control mice) (n=6) Representative FACS plot of four pooled stomachs per group (left panel). (C) The percentage of total, $CD8^+$ and $CD4^+$ T cells in the live single cells of the stomach in the pDC-ablated mice (n=5) and control mice (n=6) (*$P <$ 0.001 and **$P < 0.0001$; BMTed: BM transplanted)

Discussion

Despite many previous studies, the role of DCs in *Helicobacter*-infected individuals remains unclear. The mouse models with DC deficiency enabled the identification of the effects of DC deficiency on immune responses to *Helicobacter* and progression of gastric lesions. Interestingly, this study suggested that gastric cDCs attenuate T cell accumulation during *Helicobacter* infection and thus appear to limit immunopathology for the host stomach.

Compared to the DCs present in other organs, relatively little is known about gastric DC; thus, the characterization of gastric DCs was focused first. Gastric DCs were defined as $CD64^{-}CD11c^{+}$MHC II^{hi} population and gastric DCs were composed of $CD103^{+}$, $CD11b^{+}$, and DN subsets. Because macrophages can also express CD11c and MHC II to varying levels and might be contained in the $CD11b^{+}$ subset, macrophages were excluded in advance by using CD64 and CD11b markers (Bain, Scott et al. 2013). The DCs and their subset populations adequately expressed transcription factors Zbtb46, IRF8, and IRF4 as well as the chemokine receptor XCR1 (Satpathy, KC et al. 2012; Mildner and Jung 2014), and were dependent on the Flt3–Flt3L pathway. Moreover, these populations were ablated by DT injection in Zbtb46-DTR mice. From these results, it was confirmed that the gastric $CD64^{-}CD11c^{+}$MHC II^{hi} population and its subsets are cDCs.

Although the expression of the mature DC markers CD103 and CD11b was deficient in the DN subsets, they have been regarded as bona fide DCs, considering their similarity with the characteristics of mature DCs. Recent studies have shown that DN subsets are DC populations in an intermediate maturation stage, and reside in various organs, including the heart, lung, and liver (Clemente-Casares,

Hosseinzadeh et al. 2017). In this study, gastric DN subsets showed a two-peak pattern for the expression of IRF4, IRF8, and XCR1. These results seem to be similar to the findings of another study showing that DN subsets consist of two subtypes with the ability to mature into $CD103^+$ and $CD11b^+$ DCs (Clemente-Casares, Hosseinzadeh et al. 2017). Thus, this study suggests that bona fide DN DCs are also present in the stomach.

Conversely, a few $CD103^+CD11b^+$ cells were found in gastric DCs. One study considered $CD103^+CD11b^+$ cells to be one of the gastric DC subsets (Arnold, Zhang et al. 2017),; however, in this study, $CD103^+CD11b^+$ cells were not significantly depleted in the Flt3 KO and DT-treated Zbtb46-DTR BM transplanted mice. Although the $CD103^+CD11b^+$ DC subset has been identified in the intestine, further studies are needed on this population in the stomach.

In this study, during *Helicobacter* infection, the infiltration of all gastric DC subsets was significantly increased, and T cells were accumulated in the stomach. Gastric lymph node was grossly enlarged in both WT and DC-deficient mice (Van den Broeck, Derore et al. 2006), and populations expressing the same surface markers as gastric DCs were found in the gastric lymph node. Considering that migration from a non-lymphoid organ to lymph node is a special ability of DCs (Worbs, Hammerschmidt et al. 2017), gastric DCs distributed in the superficial layer of the mucosal lamina propria seem to migrate to the gastric lymph node for T cell priming after recognizing and capturing *Helicobacter* antigens. However, these results show that the T cell priming process is sufficient with only a few gastric DCs and highlight that gastric DCs are committed to the role of peripheral T cell tolerance during *Helicobacter* infection.

When DCs are absent, $CD8^+$ T cell infiltration increases extraordinarily in immune response to *Helicobacter* infection. Expression of anti-inflammatory cytokines: IL-10 and TGF-β did not changed, however, pro-inflammatory cytokines or chemokines like CCL2(MCP-1), CCL3(MIP-1α), CCL4(MIP-1β), CCL5(RANTES), and CCL8(MCP-2) were significantly upregulated in the stomach with gastritis. These pro-inflammatory chemokines would recruit CCR5-expressing T cells to the stomach. Also, infiltrated $CD8^+$ T cells appear to produce MIP-1α, MIP-1β, RANTES and MCP-1, which could result in consistent infiltration of T cells (Kim, Nottingham et al. 1998; Ohtani, Ohtani et al. 2004). These indicate gastric DCs suppress $CD8^+$ T cells, which inhibit further T cell infiltration. Secretion of IFN-γ, Granzyme-A, and Perforin may be useful to eliminate *Helicobacter*, but eventually lead to deterioration of immunopathological damage (Sayi, Kohler et al. 2009).

During *Helicobacter* infection, mucosal damage is accompanied by the loss of parietal cells and glandular structures (atrophy), SPEM, and further intestinal metaplasia when the lesion becomes more severe (Petersen, Mills et al. 2016). Mucosal epithelial metaplasia has been regarded as precancerous lesions because it is closely related to gastric cancer incidence in humans (Mera, Bravo et al. 2018). Interestingly, when DCs are absent, worsened oxyntic atrophy and mucous metaplasia were accompanied with an increase in T cell accumulation in the gastric mucosa. The gastric DCs may be involved in defense mechanism against carcinogenesis by slowing the progression of gastritis into gastric cancer.

In conclusion, gastric DCs and DC subsets were finely characterized. It was also confirmed that gastric DCs are dependent on Flt3-Flt3L signaling and Zbtb46

and that gastric DCs are present in specific regions of the stomach, and they increase in number when gastritis is developed due to *Helicobacter* infection. In addition, it was determined that gastric DCs depress the infiltration of T cell into gastric mucosa, which results in protection against precancerous tissue damage. These findings contribute to a better understanding of the pathology of *Helicobacter*-induced gastritis.

CHAPTER II.

Programmed death ligand 1 expressing gastric classical dendritic cells attenuate *Helicobacter*-induced gastric inflammation via controlling local T cell immunity

Abstract

DCs play a crucial role in peripheral T cell tolerance as well as in inducing T cell immunity as immune regulator. Peripheral T cell tolerance by DCs in *Helicobacter* infection has been observed, and my previous *in vivo* studies supported this observation. Tregs induction, the secretion of anti-inflammatory cytokines and the expression of immune checkpoint molecules have been reported as the mechanisms by which DCs maintain peripheral T cell tolerance. In this study, one of the immune checkpoint molecules, PD-L1 was examined. A blockade of PD-L1 enhanced gastritis with severe T cell accumulation during *Helicobacter* infection. In addition, gastric DCs expressed considerably higher level of PD-L1 than other immune cells and co-localized with T cells in the stomachs of mice and humans. These findings suggest that gastric DCs attenuate *Helicobacter*-induced gastritis by regulating T cell recruitment through PD-L1 expression.

Introduction

DCs have been recognized as typical immune cells that play a sentinel role in various organs, recognize invading pathogens, and induce a pathogen-specific acquired immune response. However, DCs are also imperative in inducing and maintaining central and peripheral immune tolerance (Steinman, Hawiger et al. 2003; Thomson 2010), and these tolerogenic DCs are attracting attention as a potential type of immunotherapy to prevent autoimmune diseases and transplant rejection (Funes, Manrique de Lara et al. 2019). In general, tolerogenic DCs are immature or semi-mature, unlike immunogenic DCs that induce T cell activation, and the maturation state is determined by the expression level of MHC II, co-stimulatory molecules CD80 and CD86, and the production of pro-inflammatory cytokines (Steinman, Hawiger et al. 2003; Funes, Manrique de Lara et al. 2019).

DCs can inhibit effector T cells through a variety of pathways, such as the induction of Tregs, the production of anti-inflammatory cytokines, and the expression of immune checkpoint molecules. T cell inhibition by immune checkpoint molecules is mediated by the transfer of inhibitory signaling via inhibitory receptors expressed on T cells and the interruption of stimulatory T cell signaling (Arasanz, Gato-Cañas et al. 2017; Fife, Pauken et al. 2009). PD-1 and CTLA-4 are known to be typical inhibitory receptors of T cells (Cox, Nechanitzky et al. 2017), and DCs can bind to PD-1 and CTLA-4, respectively, by expressing the programmed death-ligands and B7-1 (CD80) and B7-2 (CD86).

PD-1 is a member of the CD28 and CTLA-4 immunoglobulin superfamily and interacts with two B7 family ligands, PD-L1 (CD274) and PD-L2 (CD273) (Fife, Pauken et al. 2009). PD-L1 is known to be expressed in both hematopoietic and

non-hematopoietic cells in various organs, while PD-L2 is known to be expressed only in DCs and monocytes (Ishida, Iwai et al. 2002; Yamazaki, Akiba et al. 2002). PD-1 signaling modulates T cell-mediated immunity by regulating the number of T cells and their activities in multiple ways, such as inducing T cell exhaustion (Blank and Mackensen 2007; Day, Kaufmann et al. 2006; Sakuishi, Apetoh et al. 2010), anergy (Chikuma, Terawaki et al. 2009; Selenko-Gebauer, Majdic et al. 2003; Tsushima, Yao et al. 2007), and apoptosis (Chiu, Tsai et al. 2018; Dong, Strome et al. 2002; Petrovas, Casazza et al. 2006) and inhibiting T cell proliferation (Patsoukis, Sari et al. 2012). These effects of PD-1 signaling have been reported mainly in tumor, autoimmune, or viral infectious diseases, but they have recently been reported in bacterial infectious diseases (Jurado, Alvarez et al. 2008; Fankhauser and Starnbach 2014).

In this study, the mechanism of the Tregs-independent T cell inhibition of gastric DCs in *Helicobacter* infection was examined. It was confirmed that gastric DCs strongly express PD-L1, not PD-L2, more than other immune cells and that the expression intensity increases with *Helicobacter* infection. In addition, PD-L1 expressing gastric DCs were co-localized with T cells in the stomachs of mice and humans. It was also found that *Helicobacter*-induced T cell responses deteriorated when PD-1-PD-L1 signaling was deficient through PD-L1 antibody injection and the PD-L1 KO BM recipient mouse model. These findings indicate that gastric DCs attenuate *Helicobacter*-induced T cell recruitment through PD-L1 expression.

Materials and Methods

Mice

Male C57BL/6J WT mice were purchased from the Japan SLC Inc. (Hamamatsu, Shizuoka, Japan) through the Central Lab. Animal Inc. (Seoul, Korea). All mice experiments were approved by the Animal Care and Use Committees of Seoul National University or Hanyang University (certification number: SNU-140320-2-9, HY-IACUC-18-0048).

Bone marrow transplantation

BM cells from PD-L1 KO mice were injected intravenously into lethally irradiated (500 rad twice, 3 hours interval) WT C57BL/6 mice. BM transplanted mice were fed water containing 7.6% Baytril (Bayer Korea, Seoul, Korea) for 2 weeks and monitored about, 6 weeks, until the transplanted BM is effectively reconstructed.

PD-L1 in vivo blockade

Anti-mouse PD-L1 (B7-H1) antibody (10F.9G2; Bio X Cell, West Lebanon, NH, USA) was intraperitoneally administered to *H. felis*-infected mice to block the PD-L1–PD-1 pathway during *H. felis* infection. 300 μg PD-L1 antibody diluted in *InVivo*Pure pH 6.5 Dilution Buffer (Bio X Cell) was administered 6 times, once every 3 days, before necropsy. The rat IgG2b isotype control antibody (Bio X Cell) diluted in *InVivo*Pure pH 7.0 Dilution Buffer (Bio X Cell) was used as control.

Helicobacter culture and Infection

H. felis (ATCC 49179) was cultured in sterile-filtered brucella broth (Becton Dickinson, Sparks, MD, USA) containing 10% FBS. Mouse-adapted *H. pylori* SS1 was cultured on brain heart infusion agar plates (Becton Dickinson) containing 10% sheep blood and *H. pylori* Selective Supplement (Thermo Fisher Scientific, Rockford, IL, USA). The brucella broth and brain heart infusion agar plates were maintained under microaerobic conditions produced using the GasPak^{TM} EZ Campy Container System (Becton Dickinson) at 37°C. The brucella broth was maintained at 150 rpm shaking. After 24 hour fasting, 8-week-old mice were orally administered 0.2 ml suspension containing 2×10^8 *H. felis* or 1×10^9 colony-forming unit/ml *H. pylori* 4 times every other day.

Necropsy and Tissue preparation

At 4 weeks after *H. felis* infection, each group of mice was sacrificed together with the non-infected control group, and stomach, gastric lymph node, and spleen were removed. The stomach was incised along the greater curvature and spread on a filter paper. After cutting the lesser curvature, half of the stomach was used for FACS and *H. felis* quantification. The lesser curvature portion of the other half was fixed in 10% neutral buffered formalin for histopathologic examinations, and the remaining was stored in a -70°C deep freezer for subsequent analysis. At 18 months after *H. pylori* infection, the *H. pylori*-infected groups were treated in the same manner as above.

Histopathologic Examinations

Gastric tissues fixed in 10% neutral buffered formalin were cut into two strips. After standard tissue processing, gastric tissues were embedded in paraffin wax. Paraffin sections were stained with H&E and Alcian Blue (pH 2.5) stain kit (Vector Laboratories, Burlingame, CA, USA) and performed IHC for H^+/K^+-ATPase to assess histopathological changes. The degree of gastritis and pathological mucosal changes were assessed on the basis of previously established updated Sydney classification (Chen, van der Hulst et al. 1999; Sayi, Kohler et al. 2009). In the sections stained with Alcian blue, the amount of mucin in the gastric mucosa was measured using mean intensity in Image J software (National Institutes of Health, Bethesda, MD, USA). In the sections with IHC for H^+/K^+-ATPase, the number of positive cells was manually counted. The mucosa of two different areas was examined per slide at ×100 magnification, and the same anatomic areas were selected for each sample.

Single-Cell Preparations and Flow Cytometric Analysis

Gastric single cells were prepared to investigate the type of inflammatory cells that infiltrate into the stomach during *Helicobacter* infection. The gastric tissues were incubated in HBSS containing 2 mM EDTA (Cosmo Genetech, Seoul, Korea), 2% FBS, and 1 mM DL-Dithiothreitol (Sigma-Aldrich, St. Louis, MO, USA) for 15 min at 37°C with shaking. Then, the gastric tissue was finely trimmed and grinded using gentleMACS^{TM} Dissociator (Miltenyi Biotec, Bergisch Gladbach, Germany) and incubated in HBSS containing 100 U/ml collagenase D (Roche, Mannheim, Germany), 10% FBS, and 10 mM HEPES for 30 min at 37°C with

shaking. After incubation, the gastric tissue was grinded once more using the gentleMACS^{TM} Dissociator, filtered through a 70 μm cell strainer, and centrifuged to collect the separated single cells. Finally, the single cells were prepared by combining the cells collected from the suspension and from the gastric tissue. The gastric lymph node and spleen were incubated with 400 U/ml collagenase D at 37°C for 20 min to obtain separated single cells. The prepared single cells were primarily stained with Zombie Aqua (BioLegend, San Diego, CA, USA) to discriminate dead cells as per manufacturer's protocol. Zombie aqua stained cells were then processed for Fc receptor block by using TruStain FcX antibody (anti-CD16/32, clone 93, BioLegend), to avoid non-specific binding. After the Fc receptors block, cells were incubated with a mixture of fluorochrome-labelled antibodies at 4°C for 30 min. To stain transcription factors (Foxp3), cells were fixed and permeabilized with Foxp3/Transcription Factor Staining Buffer Set (Thermo Fisher Scientific), as per manufacturer's protocol, and then stained with antibody against each transcription factor. After washing briefly with RPMI 1640 medium with 10% FBS, cells were analyzed using BD LSRFortessa (BD Biosciences, San Jose, CA, USA) and FlowJo software (version 9.9 and 10.4; developed by FlowJo, LLC).

Antibodies for flow cytometry

The antibodies used for FACS are listed in Table 1.

Table 1. List of antibodies

Antibody	Clone	Catalog No.	Source
CD103	2E7	11-1031-81	eBioscience

Foxp3	FJK-16s	17-5773-82	eBioscience
CD40	1C10	17-0401-81	eBioscience
CD4	GK1.5	553730	BD Bioscience
PD-L2	TY25	564245	BD Bioscience
Siglec-F	E50-2440	562681	BD Bioscience
CD11b	M1/70	101206, 101216, 101212, 101226	BioLegend
CD64	X54-5/7.1	139304, 149320	BioLegend
MHC II	M5/114.15.2	107621, 107628	BioLegend
Ly6C	HK1.4	128006	BioLegend
CD45	30-F11	103130	BioLegend
CD11c	N418	117318	BioLegend
NK1.1	PK136	108714	BioLegend
CD8α	53-6.7	100762	BioLegend
F4/80	BM8	123146	BioLegend
PD-L1	10F.9G2	124315	BioLegend
CD86	GL-1	105012	BioLegend
CD19	6D5	115527	BioLegend
B220	RA3-6B2	103223	BioLegend
CD3	17A2	100228	BioLegend
Ly6G	1A8	127641	BioLegend
CD80	16-10A1	104725	BioLegend
Rat IgG2α, κ Isotype	RTK2758	400507, 400511, 400526, 400542, 400549	BioLegend

Immunohistochemistry and Immunofluorescence

After paraffin-embedded sections were dewaxed and hydrated, antigen retrieval was performed using citrate buffer (pH 6.0; Sigma-Aldrich). Next, the sections were incubated with 0.3% hydrogen peroxide solution for 30 min to block endogenous peroxidase activity. The ImmPRESS Peroxidase Polymer kit (Vector Laboratories) was used according to manufacturer's protocol. Briefly, paraffin-embedded sections were blocked with 2.5% normal horse serum or 2.5% normal goat serum for 1 hour and then incubated with the following primary antibodies at 4°C overnight or at 20°C for 2 hours: rabbit anti-CD3 (1:200; Dako, Glostrup, Denmark), mouse anti-ATPase (1:4000; MBL, Woburn, MA, USA), rat anti-CD8α (1:200; Novus, Centennial, CO, USA), and rabbit anti-PD-1 (1:100; Cell Signaling Technology). The paraffin-embedded sections were washed with PBS and then incubated with appropriate horseradish peroxidase-conjugated secondary antibody (Vector Laboratories) for 1 hour. ImmPACT DAB substrate (Vector Laboratories) was used for chromogenic detection. The sections were counterstained with hematoxylin. The immunofluorescence was detected using Alexa594-conjugated goat anti-rat IgG (Jackson ImmunoResearch, West Grove, PA, USA) and Alexa488-conjugated goat anti-rabbit IgG (Invitrogen, Carlsbad, CA, USA) at 1:400. The sections were counterstained with DAPI (Thermo Fisher Scientific) and mounted using mounting medium (Vector Laboratories). In anti-ATPase IHC, Mouse on Mouse ImmPRESS Peroxidase Polymer Kit (Vector Laboratories) was used to block endogenous mouse immunoglobulin.

For frozen sections, after blocking with 2.5% normal goat serum (Vector Laboratories) for 1 hour and following primary antibodies were used for overnight

incubation at 4°C: rat anti-CD45 (1:100; Abcam, Cambridge, UK), rabbit anti-PD-L1 (1:100; Invitrogen), Armenian hamster anti-CD11c (1:100; BD Biosciences), and rat anti-CD8α (1:100; Novus, Centennial, CO, USA). Immunofluorescence was detected using Alexa594-conjugated goat anti-rat IgG (Jackson ImmunoResearch), Alexa594-conjugated goat anti-rabbit IgG (Invitrogen), Alexa488-conjugated goat anti-rabbit IgG (Invitrogen) and Alexa488-conjugated goat anti-Armenian hamster IgG (Jackson ImmunoResearch) at 1:400. The sections were counterstained with DAPI and mounted using mounting medium (Vector Laboratories). The images were obtained using confocal fluorescence microscope (Eclipse TE200; Nikon, Japan).

H. felis Quantification

Total DNA was extracted from the gastric tissues (corpus and antrum) by using QIAamp DNA mini kit (Qiagen, Hilden, Germany) and used to identify *H. felis* DNA. qRT-PCR was performed using specific primers for *H. felis* flagellar filament B (Fla-B), Rotor-Gene SYBR Green PCR kit, and Rotor-Gene Q (Qiagen). The amplified target DNA was analyzed using Rotor-Gene Q series software. The *H. felis* Fla-B primer–F: 5′-TTC GAT TGG TCC TAC AGG CTC AGA-3′ and R: 5′-TTC TTG TTG ATG ACA TTG ACC AAC GCA-3′– was used (El-Zaatari M, Kao et al. 2013).

Quatitative Reverse Transcription-PCR

Total RNA from gastric tissues was extracted using Hybrid-R RNA purification kit (GeneAll, Seoul, Korea). The cDNA was synthesized from 0.1 μg

of RNA by using QuantiTect Reverse Transcription kit (Qiagen). qRT-PCR was performed using specific primers, Rotor-Gene SYBR Green PCR kit, and Rotor-Gene Q (Qiagen). The amplified target cDNA was analyzed using Rotor-Gene Q series software against the housekeeping gene GAPDH. The specific primer pairs were F: 5′-TGC ACC ACC AAC TGC TTA G-3′ and R: 5′-GGA TGC AGG GAT GAT GTT C-3′ for mouse GAPDH; F: 5′-AGC GGC TGA CTG AAC TCA GAT TGT AG-3′ and R: 5′-GTC ACA GTT TTC AGC TGT ATA GGG-3′ for mouse IFN-γ; and F: 5′-TGG ACA AAC AGT GAC CAC CAA-3′ and R: 5′-CCC CTC TGT CCG GGA AGT-3′ for mouse PD-L1.

Tissue-microarrayed human gastric tissue and multiplexed immunohistochemistry

Formalin-fixed paraffin-embedded tissue samples of surgically resected human gastric tissue were retrieved from the archives of Department of Pathology, Seoul National University Bundang Hospital. The collected tissue samples were remaining samples after proper histologic diagnosis and relevant molecular study. Representative tissue area were reviewed and selected for the construction of tissue microarray.

In this study, formalin-fixed paraffin-embedded gastric tissue samples of 20 *H. pylori*-negative patients, 31 *H. pylori*-positive patients, and 46 patients with mucosal dysplasia were analyzed. Each tissue sample was 1–2 mm in diameter. Multiplexed IHC was performed sequentially on each single slide in the order of PD-L1, CD11c, and CD3 by using Autostainer Link48 (Dako) as previously described (Koh, Kwak et al. 2019). The primary antibodies used were as follows:

rabbit anti-PD-L1 (1:30; Cell Signaling Technology), rabbit anti-CD11c (1:100; Abcam), and rabbit anti-CD3 (1:300; Dako). After the immunostained sections were scanned using the Aperio AT2 (Leica Biosystems, Newcastle, UK), the slides were incubated in pre-mixed stripping buffer for antibody stripping. The slides were microwaved at low power to obtain more effective stripping, followed by immunostaining for next primary antibody.

The study was approved by the Institutional Review Board (IRB) of Seoul National University Bundang Hospital (IRB number: B-1606/349-308) and Seoul National University Hospital (IRB number: 1706-105-860) and performed in accordance with the principles of the Declaration of Helsinki. The informed consent was waived.

Statistical Analysis

All data are shown as means ± standard errors. Statistical analysis was performed using GraphPad Prism 7.00 (GraphPad Software, San Diego, CA, USA). Two groups were compared using Mann-Whitney *U* test or unpaired *t*-test with two-tailed distributions. When three or more groups were included, the results were analyzed using Kruskal-Wallis test or ordinary one-way ANOVA followed by Mann-Whitney *U* test or unpaired *t*-test with two-tailed distributions. Two-tailed *P* values less than 0.05 were considered significant.

Results

Gastric cDCs expressed high level of PD-L1 and co-localized with T cells in Helicobacter-infected gastric mucosa and submucosa

To elucidate the cause of severe T cell accumulation in DC-deficient mice during *Helicobacter* infection, the mechanisms of T cell inhibition of DCs were examined. DCs can inhibit T cells via immune tolerance mechanisms such as induction of Tregs, production of anti-inflammatory cytokines, and expression of immune checkpoint molecules (Sharpe, Wherry et al. 2007; Darrasse-Jèze, Deroubaix et al. 2009; Schülke 2018). In my previous study, cDC depletion did not affect Treg infiltration and IL-10 and TGF-β mRNA expression. Therefore, in this study, the expression of immune checkpoint molecules on gastric DCs was focused and the expression level of PD-L1, PD-L2, and T cell co-stimulatory molecules, including CD80, CD86, and CD40 were examined. Regardless of *H. felis* infection, all gastric DC subsets expressed higher level of PD-L1 than other gastric immune cells, including macrophages and neutrophils. PD-L1 expression of DCs was increased by *H. felis* infection, whereas that of macrophages and neutrophils remained similar regardless of *H. felis* infection (Fig 1A). The gastric DCs also expressed higher level of PD-L1 than splenic DCs (Fig 1B). *H. pylori* infection increased PD-L1 expression on gastric DCs, which was also significantly higher than that of other immune cells. In particular, PD-L1 expression on $CD11b^{+}$ DC subset was markedly increased by *H. pylori* infection (Fig 1C). *Helicobacter* infection did not affect the expression of PD-L2, CD80, and CD40, but increased

the expression of CD86 on cDCs (Fig 1D and 1E). Furthermore, PD-L1 mRNA expression was decreased in Flt3 KO mice during *H. felis* infection (Fig 1F).

Immunofluorescence staining for PD-L1, CD45, CD11c, CD8α, and PD-1 in the gastric tissue revealed that PD-L1$^+$ cells were mainly located in the submucosa and mucosal laminar propria right above the muscularis mucosa. However, the mucosal epithelial cells showed scant PD-L1 expression (Fig 2A and 2B). The majority of PD-L1$^+$ cells were co-stained with CD45 antibody (Fig 2A), and these CD45$^+$PD-L1$^+$ cells were in contact with CD8α$^+$ cells (Fig 2B). In addition, CD11c$^+$ cells expressed PD-L1, and the majority of CD8α$^+$ cells co-expressed PD-1 (Fig 2C). These results indicate that PD-L1-expressing gastric DCs interacted with PD-1$^+$CD8$^+$ T cells in the *H. felis*-infected stomach.

A

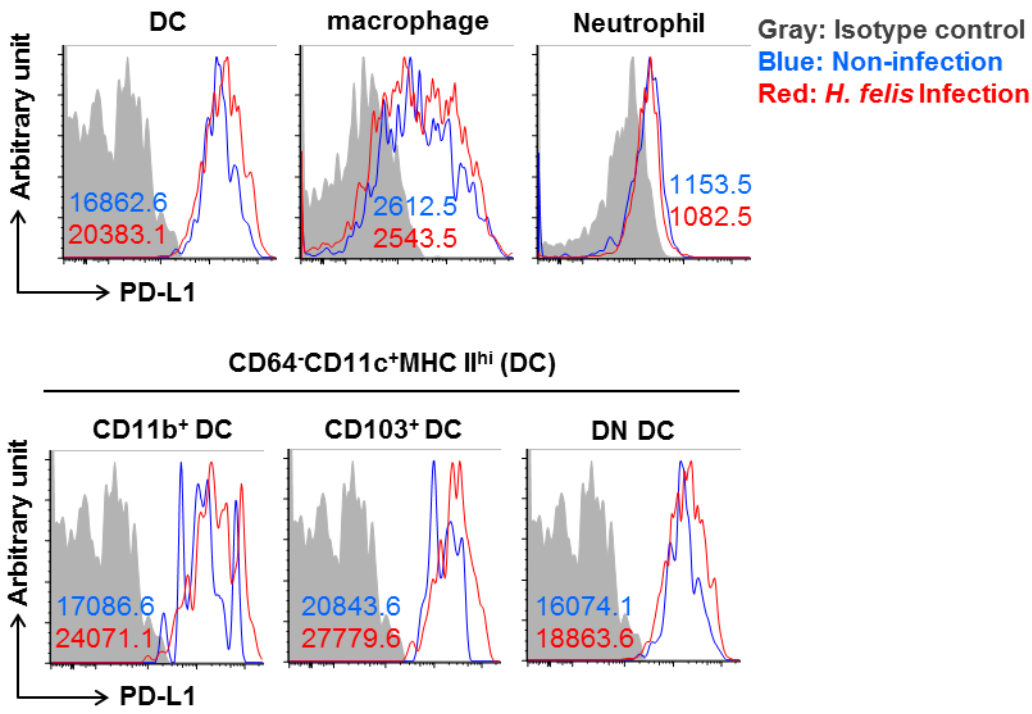
DC
macrophage
Neutrophil
Gray: Isotype control
Blue: Non-infection
Red: H. felis Infection
Arbitrary unit
16862.6
20383.1
2612.5
2543.5
1153.5
1082.5
PD-L1
CD64-CD11c+MHC IIhi (DC)
CD11b+ DC
CD103+ DC
DN DC
Arbitrary unit
17086.6
24071.1
20843.6
27779.6
16074.1
18863.6
PD-L1

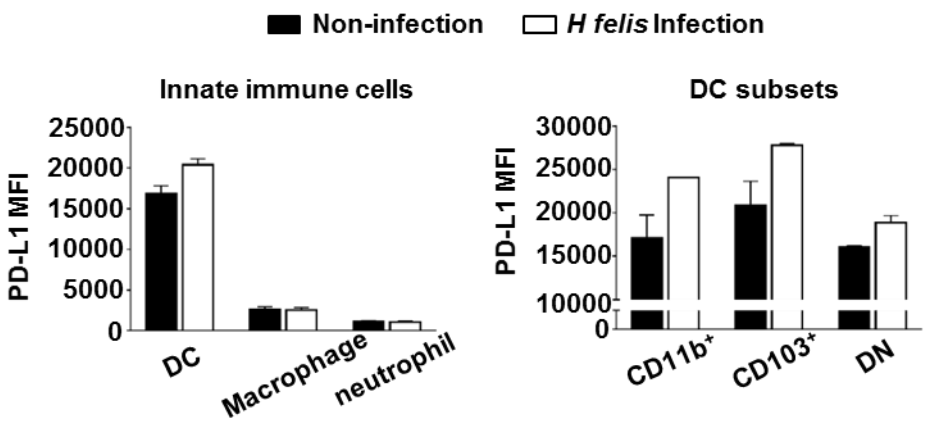
Non-infection
H felis Infection
Innate immune cells
PD-L1 MFI
25000
20000
15000
10000
5000
0
DC
Macrophage
neutrophil
DC subsets
PD-L1 MFI
30000
25000
20000
15000
10000
0
CD11b+
CD103+
DN

B

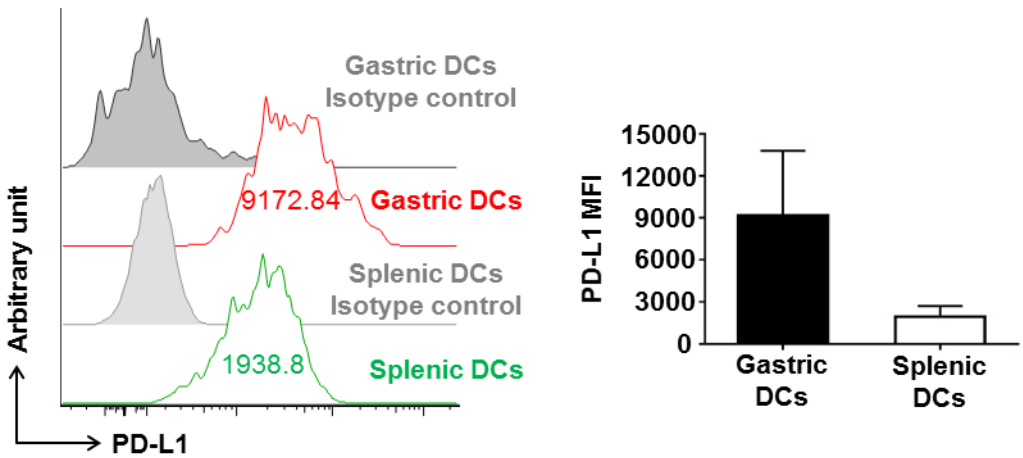
Gastric DCs
Isotype control
9172.84
Gastric DCs
Splenic DCs
Isotype control
1938.8
Splenic DCs
Arbitrary unit
PD-L1
PD-L1 MFI
15000
12000
9000
6000
3000
0
Gastric DCs
Splenic DCs

C

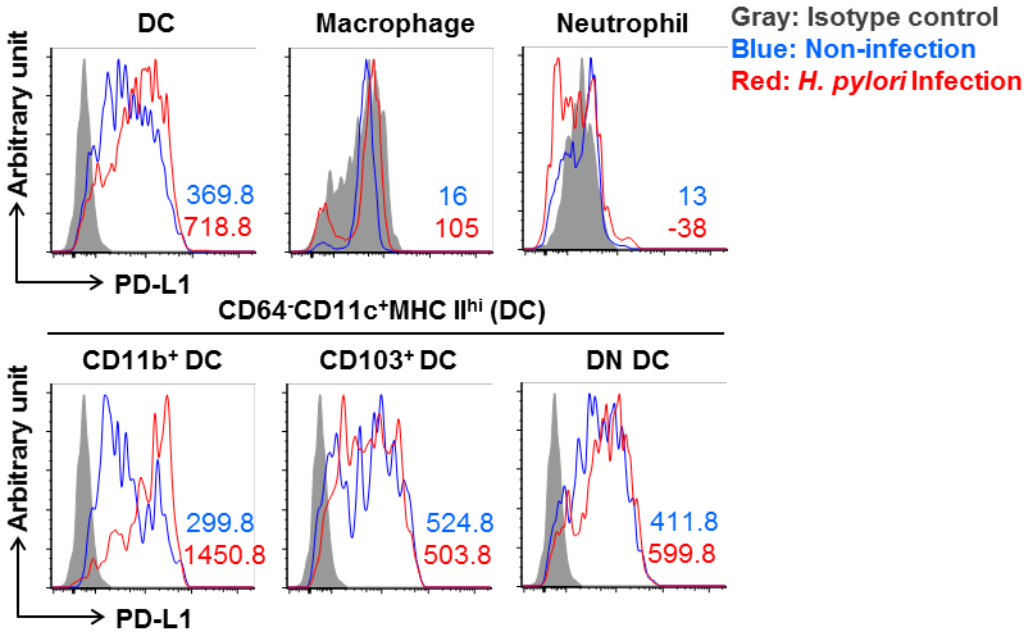
DC
Macrophage
Neutrophil
Gray: Isotype control
Blue: Non-infection
Red: H. pylori Infection
Arbitrary unit
369.8
718.8
16
105
13
-38
PD-L1
CD64-CD11c+MHC IIhi (DC)
CD11b+ DC
CD103+ DC
DN DC
299.8
1450.8
524.8
503.8
411.8
599.8
Arbitrary unit
PD-L1

D

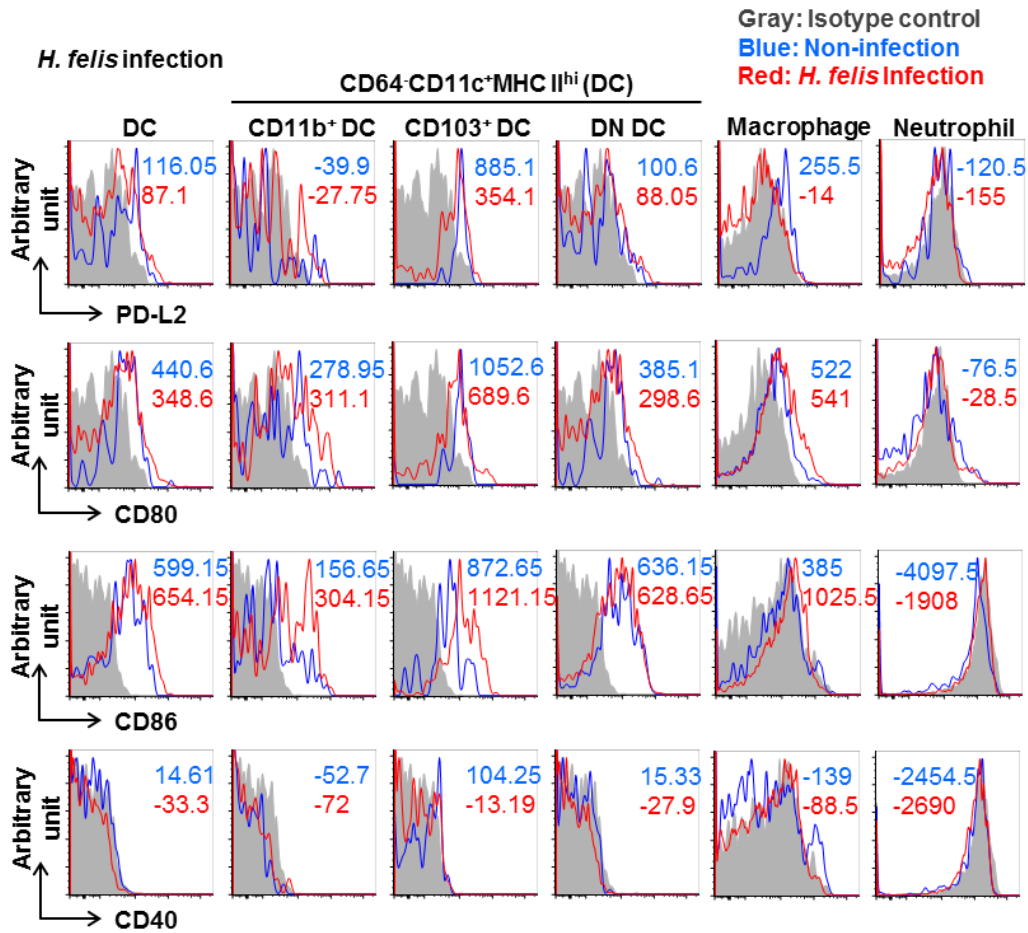
Gray: Isotype control
Blue: Non-infection
Red: H. felis Infection
H. felis infection
CD64-CD11c+MHC IIhi (DC)
DC
CD11b+ DC
CD103+ DC
DN DC
Macrophage
Neutrophil
Arbitrary unit
PD-L2
116.05
87.1
-39.9
-27.75
885.1
354.1
100.6
88.05
255.5
-14
-120.5
-155
CD80
440.6
348.6
278.95
311.1
1052.6
689.6
385.1
298.6
522
541
-76.5
-28.5
CD86
599.15
654.15
156.65
304.15
872.65
1121.15
636.15
628.65
385
1025.5
-4097.5
-1908
CD40
14.61
-33.3
-52.7
-72
104.25
-13.19
15.33
-27.9
-139
-88.5
-2454.5
-2690

E

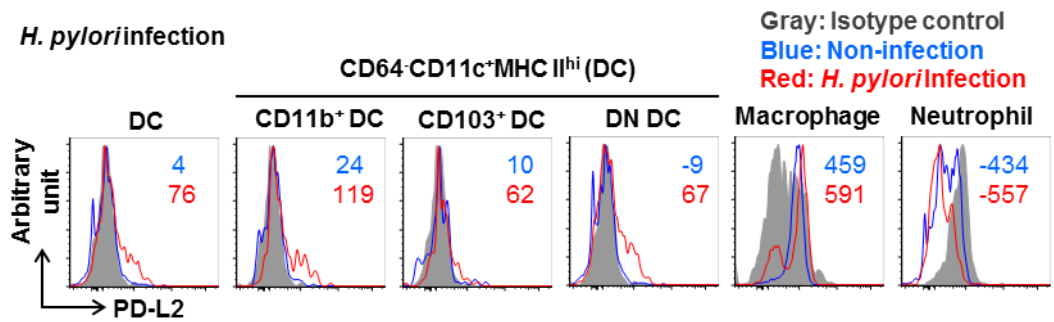
H. pylori infection
Gray: Isotype control
Blue: Non-infection
Red: H. pylori Infection
CD64-CD11c+MHC IIhi (DC)
DC
CD11b+ DC
CD103+ DC
DN DC
Macrophage
Neutrophil
Arbitrary unit
PD-L2
4
76
24
119
10
62
-9
67
459
591
-434
-557

F

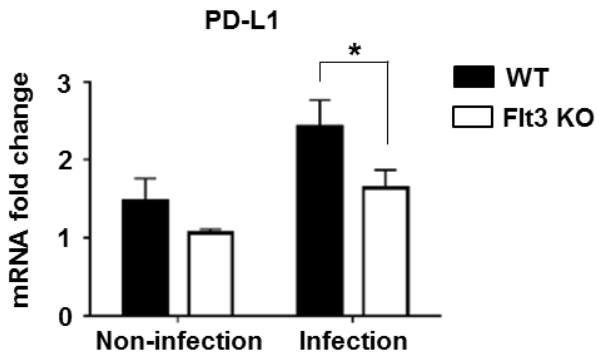

Fig 1. High level of PD-L1 expression of gastric DCs and location of PD-L1 expressing gastric DCs in the stomach during *Helicobacter* infection (A) PD-L1 expression on innate immune cells against *H. felis* infection. Note that DCs and DC subsets express considerably higher level of PD-L1 than other cell types. Each figure is representative of two experiments. Three mice per group were pooled for each experiment. (B) Comparison of PD-L1 expression level in gastric DCs and splenic DCs during *H. felis* infection. Left figure is representative of at least three experiments. Three mice per group were pooled for each experiment. The stomach and spleen were collected from the same individuals. (C) As in (A), but with *H. pylori* infection. Note that DCs and DC subsets express considerably higher level of PD-L1 than other cell types. (D) Expression level of PD-L2, CD80, CD86, and CD40 on innate immune cells against *H. felis* infection. Each figure is representative of two experiments. Three mice per group were pooled for each experiment. (E) Expression level of PD-L2 on innate immune cells against *H. pylori* infection. Three mice per group were pooled for the experiment. The number in the histogram means the median fluorescence intensity (MFI) value. The MFI value was calculated by subtracting the MFI value of the isotype control corresponding to each population. (F) Relative PD-L1 mRNA expression level of Flt3 KO and WT mice after *H. felis* infection for 8 weeks. Results are shown as fold change compared with non-infection group (non-infection group–n=2; *H. felis* infection group–n=7) (*$P < 0.05$)

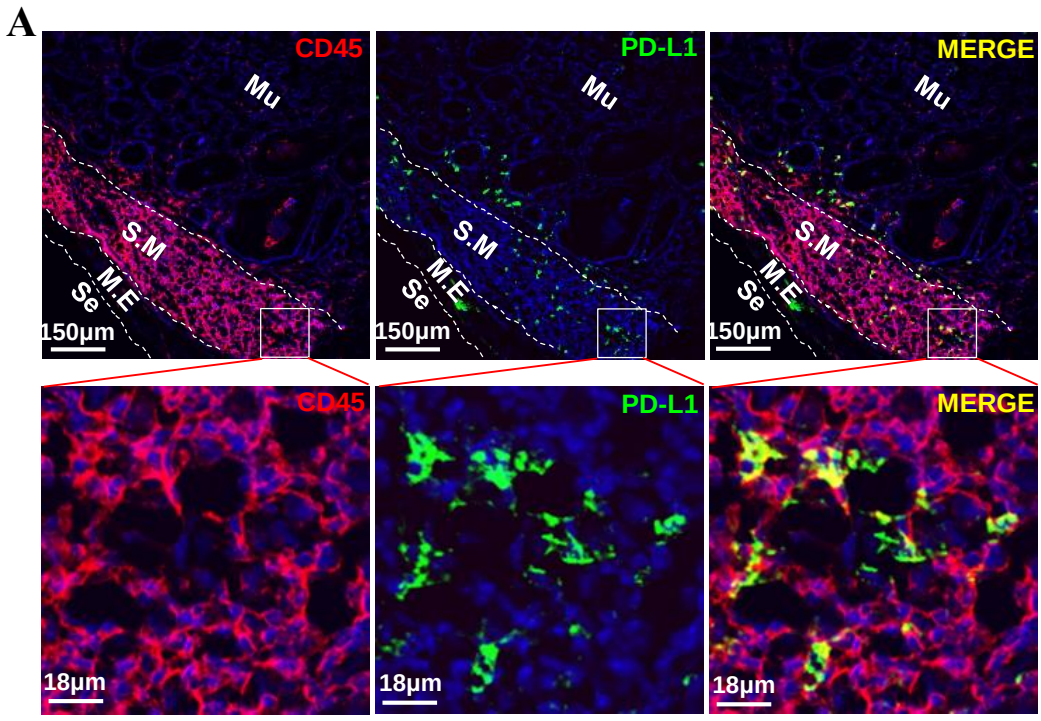
A
CD45
PD-L1
MERGE
Mu
S.M
M.E
Se
150μm
18μm

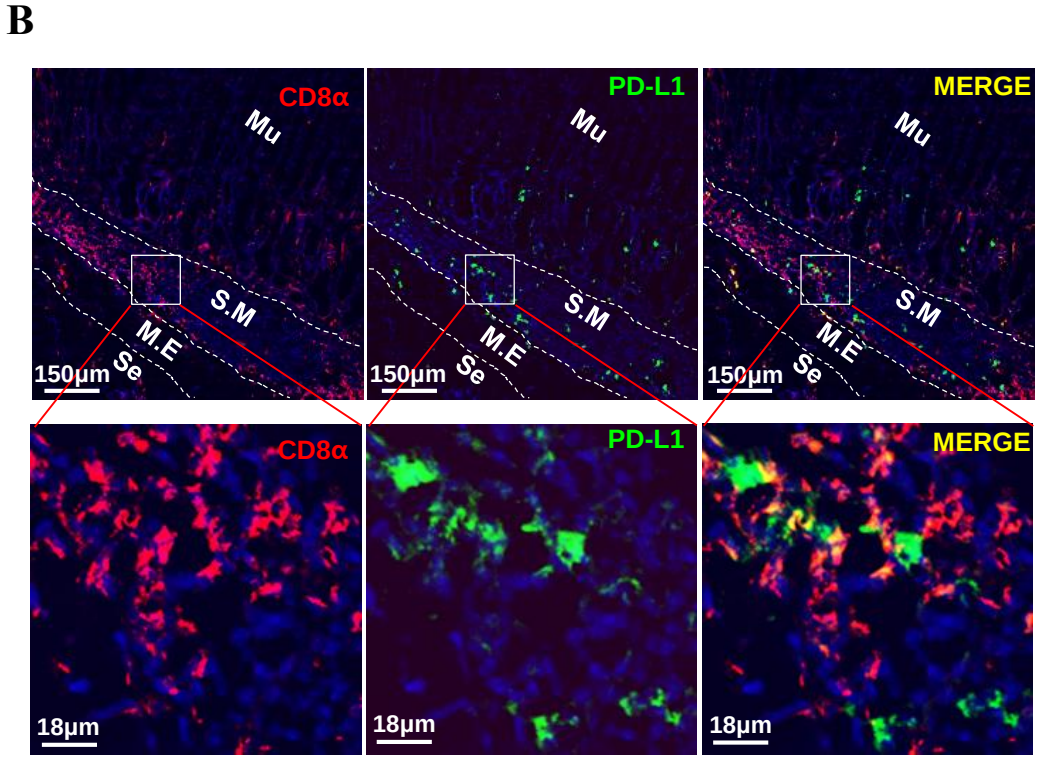
B
CD8α
PD-L1
MERGE
Mu
S.M
M.E
Se
150μm
18μm

C

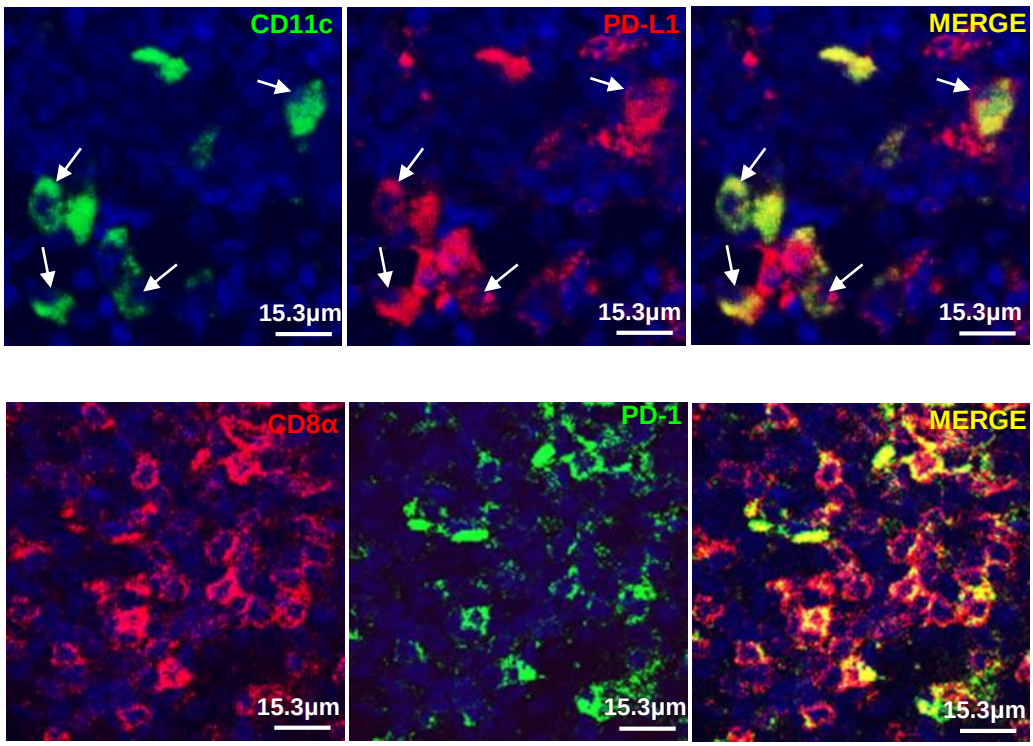

Fig 2. (A and B) Immunofluorescence for PD-L1, CD45, and CD8α on *H. felis*-infected WT mice stomach. Note the localization of PD-L1$^+$ cells (submucosa and mucosal laminar propria right above the muscularis mucosa). PD-L1$^+$ cells are co-stained with CD45 and co-localize with CD8$^+$ T cells. (Mu: mucosa, S.M: submucosa, M.E: muscularis externa, and Se: serosa) (C) PD-L1$^+$CD11c$^+$ DCs (arrows) and PD-1$^+$CD8$^+$ T cells in the submucosa

Blockade of PD-L1 enhanced the gastric inflammation with severe T cell accumulation upon Helicobacter infection

To confirm the role of PD-L1 in the host immune response to *Helicobacter* infection, PD-L1 antibodies (Ab) were injected into *H. felis*-infected WT mice to block PD-L1 signals. Next, gastric lesions were analyzed at 4 weeks after infection. Histologically, lymphocyte infiltration into the gastric submucosa and mucosal lamina propria and pathological mucosal changes were markedly more severe in the PD-L1 Ab injection group than in the isotype Ab injection group (Fig 3A). Furthermore, T cell infiltration into the mucosal lamina propria was prominent in the PD-L1 Ab injection group (Fig 3B). The infiltration of $CD8^+$ and $CD4^+$ T cells was more prominent in the PD-L1 Ab injection group than in the isotype Ab injection group, but the infiltration of Tregs was not affected by antibody injection (Fig 3C).

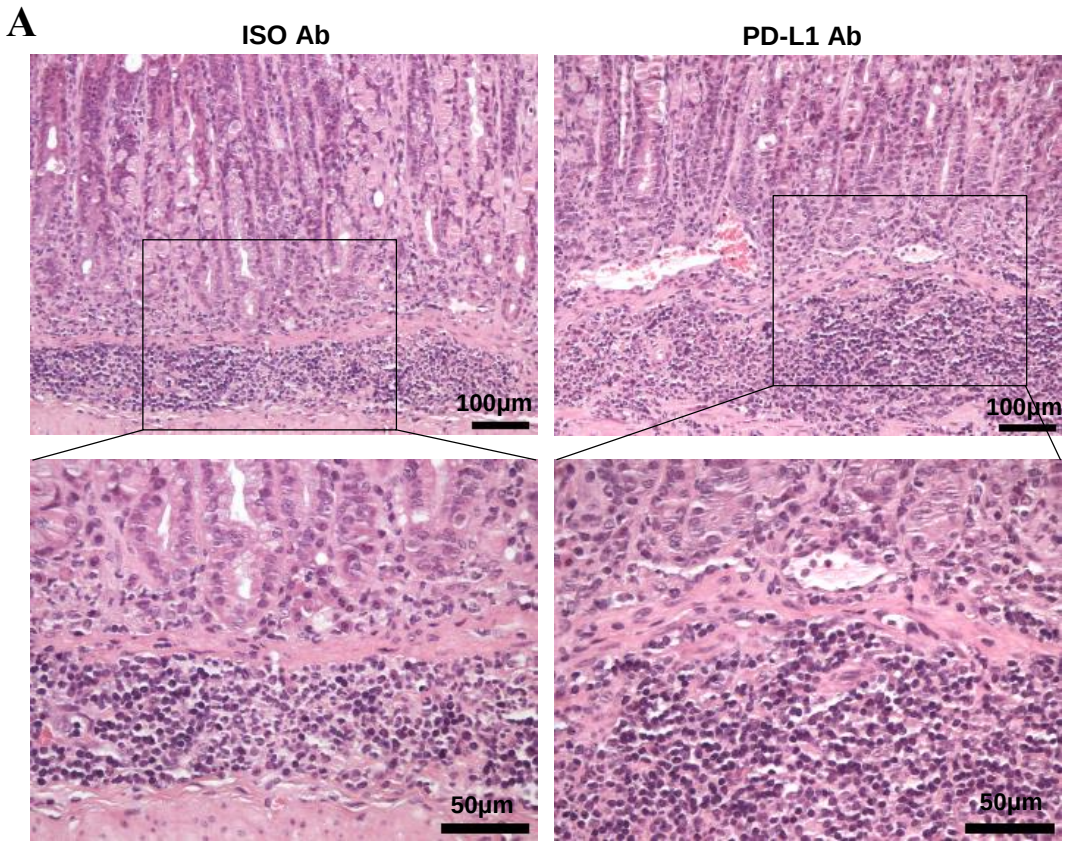
A
ISO Ab
PD-L1 Ab
100μm
100μm
50μm
50μm

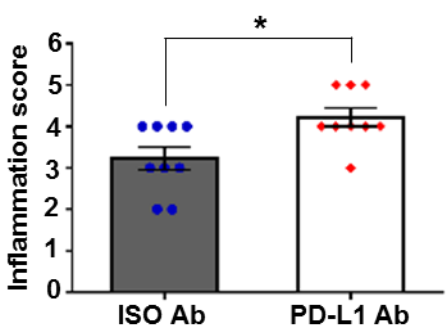
Inflammation score
*
0
1
2
3
4
5
6
ISO Ab
PD-L1 Ab

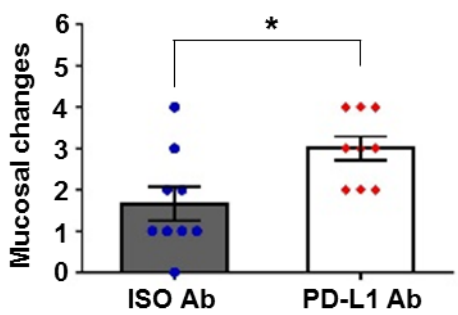
Mucosal changes
*
0
1
2
3
4
5
6
ISO Ab
PD-L1 Ab

B

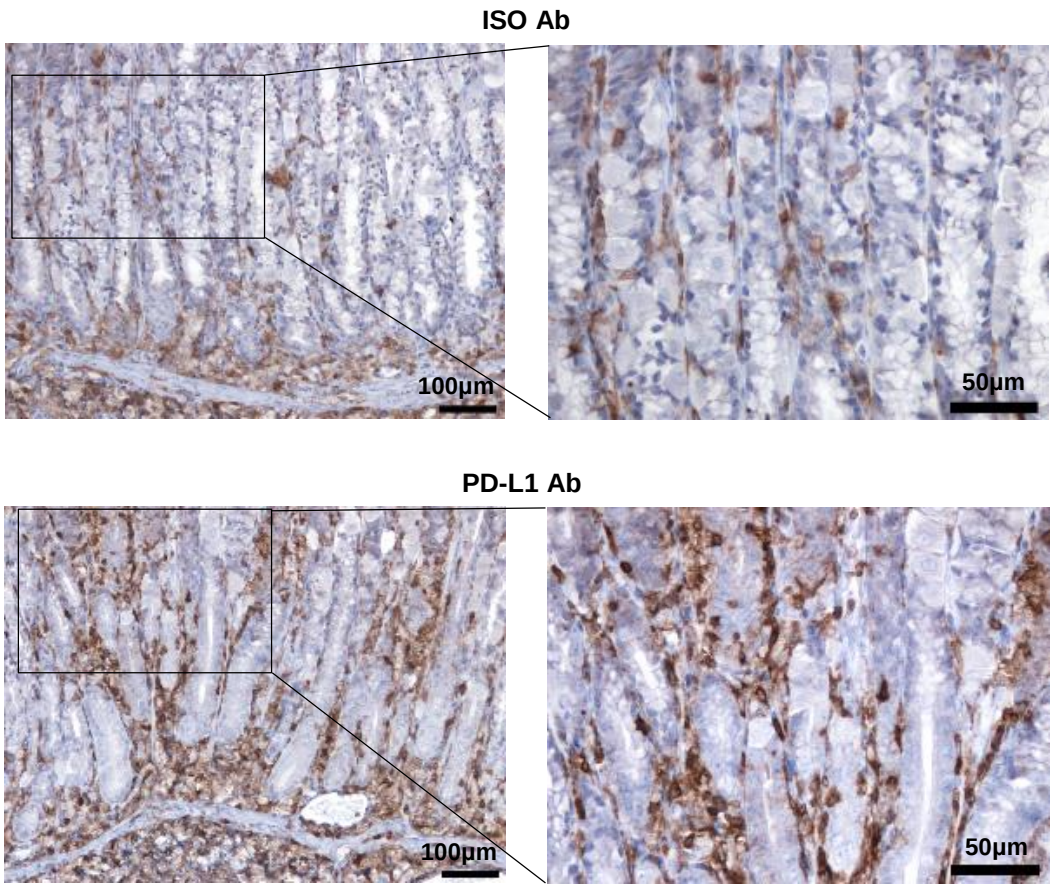

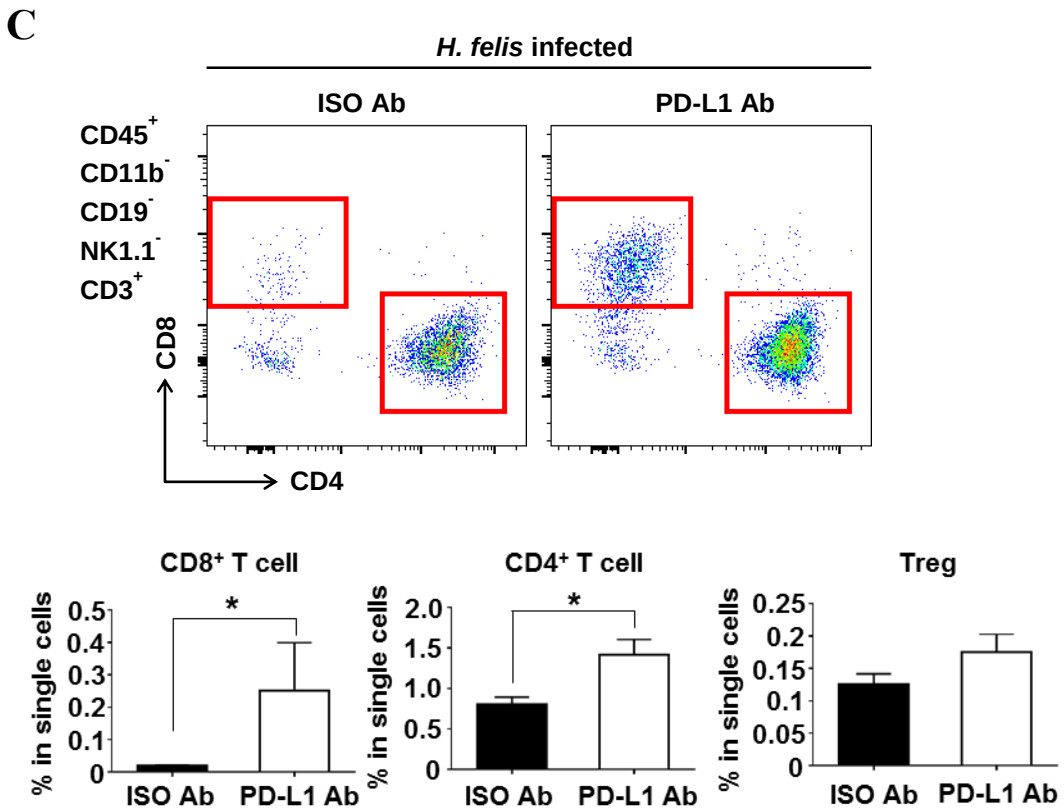

Fig 3. Deterioration of *H. felis*-induced gastric lesions and prominent T cell response in mice with PD-L1 blockade by using PD-L1 antibody injection after *H. felis* infection for 4 weeks. (A) Histopathological analysis of *H. felis*-induced gastritis, oxyntic atrophy, and mucous metaplasia according to grading standards on H&E stain. H&E stained representative images of isotype control mice (left panel) and mice with PD-L1 blockade (right panel). Bottom left: Inflammation score, Bottom right: Mucosal change score (isotype control mice–n=9; PD-L1 blockade mice–n=9) (B) More severe mucosal infiltration of T cells in the stomach of mice with PD-L1 blockade. Representative images of CD3 IHC (DAB). (C) The percentage of $CD8^+$ and $CD4^+$ T cells and Tregs in the live single cells of the stomach in the mice with PD-L1 blockade (n=9) and isotype control mice (n=9). Representative FACS plots (top panel) (*$P < 0.05$)

PD-L1 deficiency in BM-derived cells enhanced gastric inflammation upon Helicobacter infection

PD-L1 has been known to be expressed in not only various hematopoietic cells but also non-hematopoietic cells such as muscle cells, mucosal epithelial cells, and vascular endothelial cells (Sharpe, Wherry et al. 2007). Several studies have shown that PD-L1 expressed on the mucosal epithelial cells was increased in response to *H. pylori* infection, which plays an important role in suppressing T cell responses in the stomach (Das, Suarez et al. 2006; Holokai, Chakrabarti et al. 2019). To analyze the influence of PD-L1 on BM-derived cells in *Helicobacter* infection, BM chimeras were created by transplantation of PD-L1 KO or WT BM into irradiated WT mice. The *H. felis*-infected recipient mice were analyzed after 4 weeks. Histologically, the inflammatory lesions and pathological mucosal changes were more prominent in the PD-L1 KO BM transplanted mice than in the WT BM transplanted mice (Fig 4A, 4B, and 4C). FACS analysis of gastric tissues showed that both $CD8^+$ and $CD4^+$ T cell responses were markedly prominent in PD-L1 KO BM transplanted mice than in WT BM transplanted mice, and Treg infiltration was further increased in the PD-L1 KO BM transplanted mice (Fig 4D). The bacterial load in the stomach was lower in PD-L1 KO BM transplanted mice than in WT BM transplanted mice (Fig 4E).

A

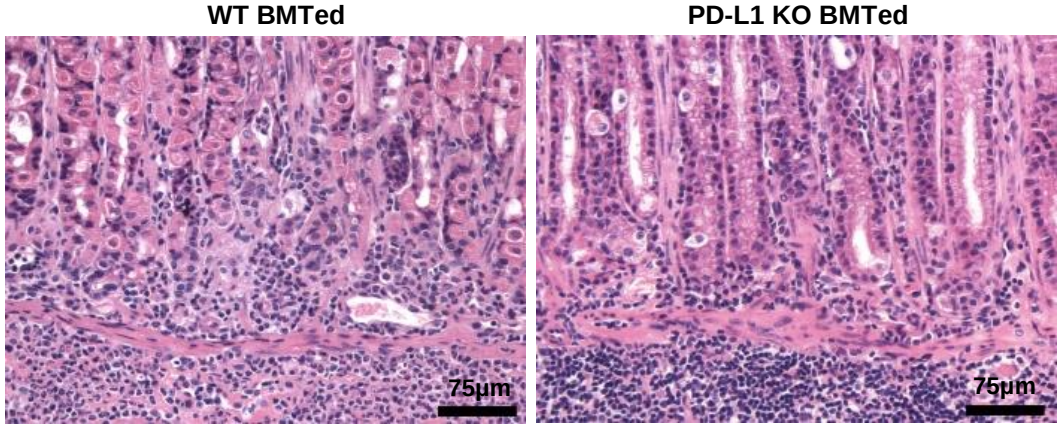
WT BMTed
PD-L1 KO BMTed
75μm
75μm

B

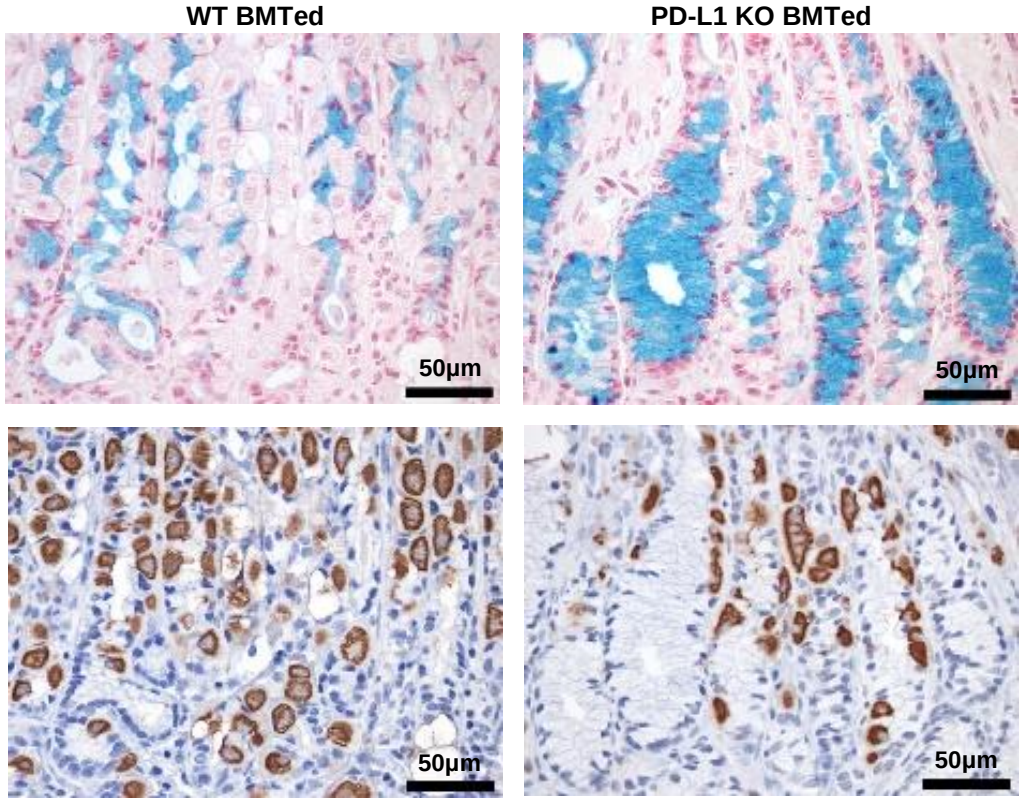
WT BMTed
PD-L1 KO BMTed
50μm
50μm
50μm
50μm

C

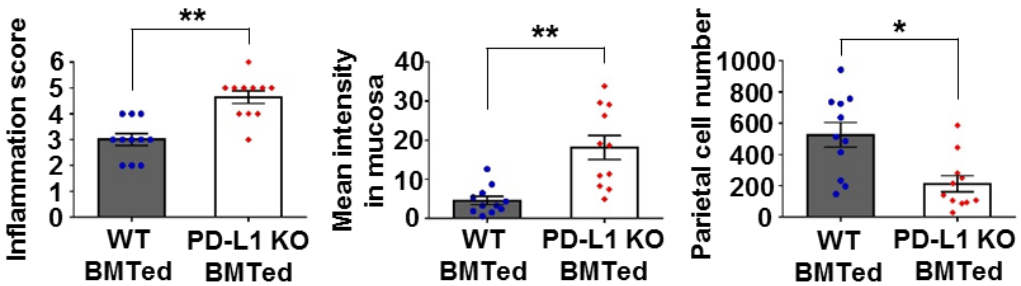
Inflammation score
**
WT BMTed
PD-L1 KO BMTed
Mean intensity in mucosa
**
WT BMTed
PD-L1 KO BMTed
Parietal cell number
*
WT BMTed
PD-L1 KO BMTed

D

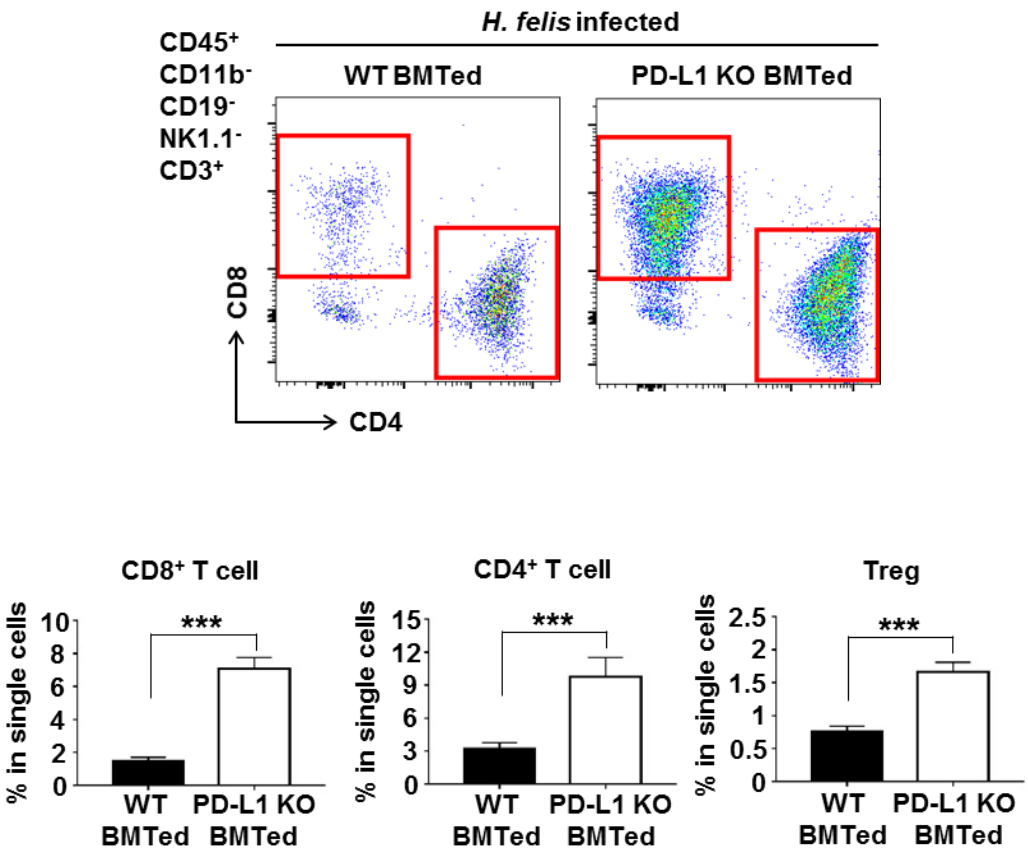
H. felis infected
CD45+
CD11b-
CD19-
NK1.1-
CD3+
WT BMTed
PD-L1 KO BMTed
CD8
CD4
CD8+ T cell
% in single cells
***
WT BMTed
PD-L1 KO BMTed
CD4+ T cell
% in single cells
***
WT BMTed
PD-L1 KO BMTed
Treg
% in single cells
***
WT BMTed
PD-L1 KO BMTed

E

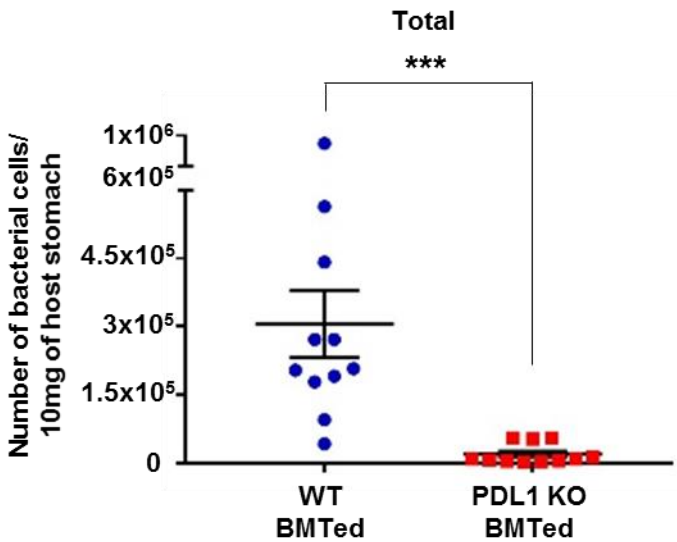

Fig 4. Deterioration of *H. felis*-induced gastric lesions and prominent T cell response in PD-L1 KO BMTed mice after *H. felis* infection for 4 weeks (A) Histopathological analysis of *H. felis*-induced gastritis. H&E stained representative images of WT BMTed (left panel) and PD-L1 KO BMTed (right panel) mice. (B) Histopathological analysis of *H. felis*-induced oxyntic atrophy and mucous metaplasia. Representative serial images of WT BMTed (left panel) and PD-L1 KO BMTed (right panel) mice subjected to Alcian blue staining (top) and H^+/K^+-ATPase IHC (bottom). (C) Left: Inflammation score, Middle: Mean intensity of mucosal Alcian blue positive, Right: Manual cell count number of H^+/K^+-ATPase$^+$ cells (parietal cells) (WT BMTed–n=11; PD-L1 KO BMTed–n=11) (D) The percentage of $CD8^+$ and $CD4^+$ T cells and Tregs in the live single cells of the stomach in the WT BMTed (n=11) and PD-L1 KO BMTed (n=11) mice. Representative FACS plots (top panel) (E) *H. felis* loads were evaluated using qRT-PCR for *H. felis* Fla-B DNA extracted from gastric tissues (WT BMTed–n=11, PD-L1 KO BMTed–n=11) (*$P < 0.01$, **$P < 0.001$, and ***$P < 0.0001$; BMTed: BM transplanted)

PD-L1 expressing DCs co-localized with T cells in human Helicobacter-positive gastritis

To determine whether PD-L1-expressing DCs co-localize with T cells in the gastric mucosa of *H. pylori*-infected patients, multiplexed IHC for CD11c, PD-L1, and CD3 was performed. $CD11c^+$ cells were distributed in the mucosal lamina propria and submucosa, and their numbers were significantly higher in the stomach of *H. pylori*-positive patients and patients with mucosal dysplasia than in *H. pylori*-negative patients. PD-L1 expression was mostly found in infiltrated cells not in epithelial cells. Importantly, the $CD11c^+PDL1^+$ cells were in contact with $CD3^+$ cells in the gastric mucosa (Fig 5A and 5B). The $CD11c^+PDL1^+$ cells were higher in the gastric mucosa of *H. pylori*-positive patients than in *H. pylori*-negative controls. The patients with mucosal dysplasia had more $CD11c^+PDL1^+$ cells (Fig 5C).

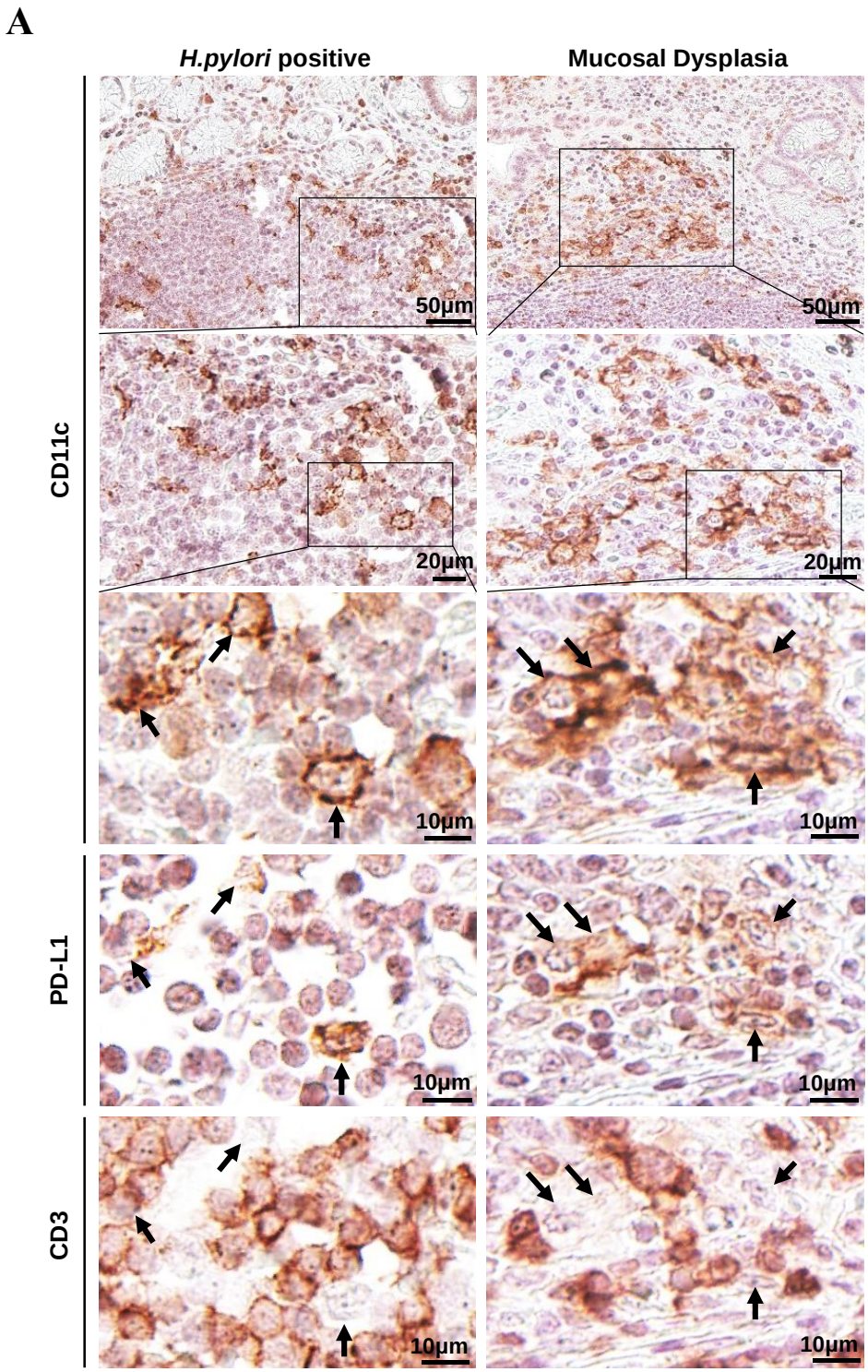
A
H.pylori positive
Mucosal Dysplasia
CD11c
PD-L1
CD3
50μm
20μm
10μm

B

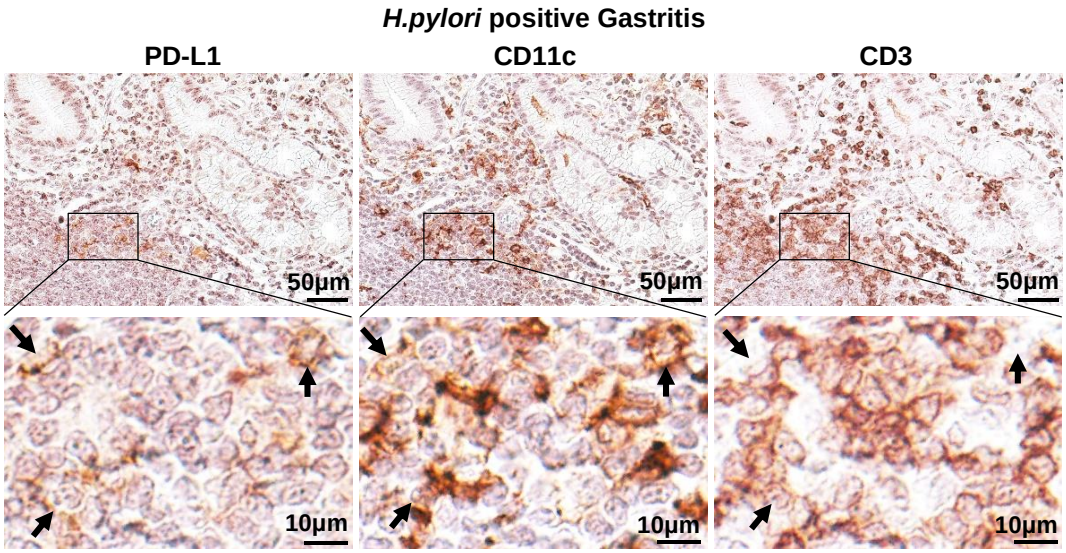
H.pylori positive Gastritis
PD-L1
CD11c
CD3
50μm
50μm
50μm
10μm
10μm
10μm

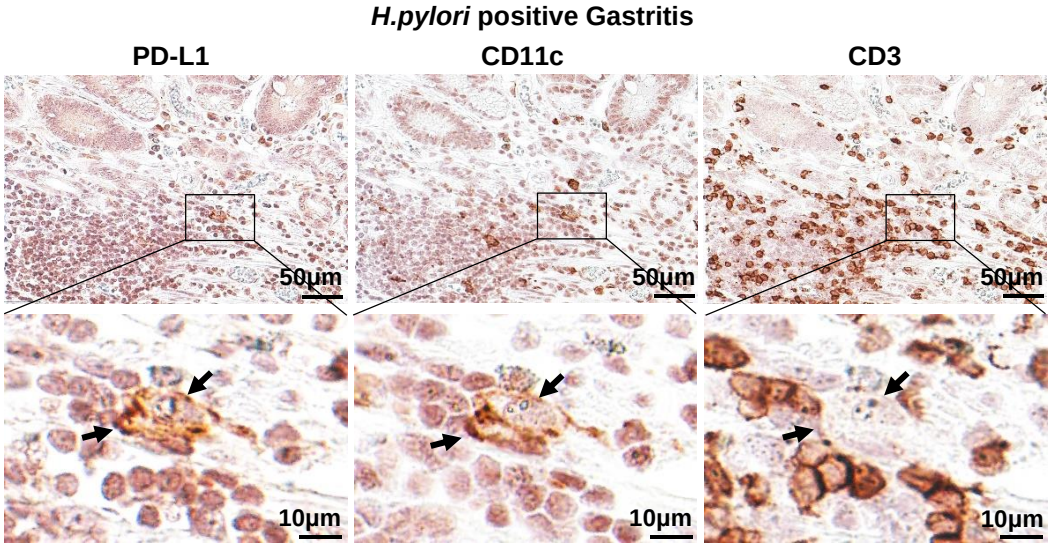
H.pylori positive Gastritis
PD-L1
CD11c
CD3
50μm
50μm
50μm
10μm
10μm
10μm

C

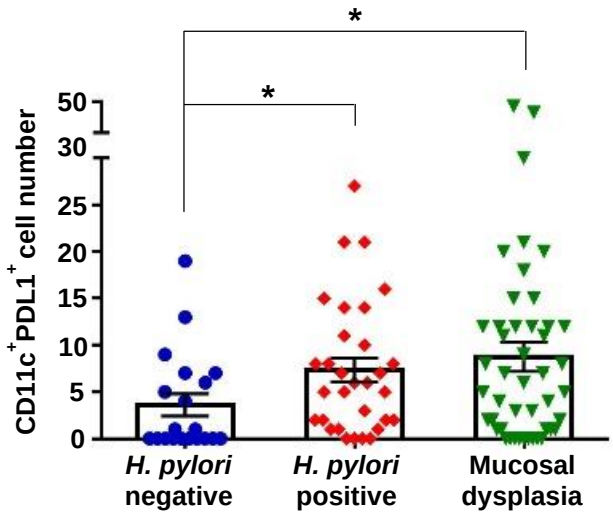

Fig 5. Co-localization of PD-L1$^+$CD11c$^+$ DCs and CD3$^+$ T cells in the human stomach. (A) Multiplexed IHC-stained representative images of the stomach of *H. pylori*-positive patients (left panel) and patients with mucosal dysplasia (right panel). All images immunostained on the gastric tissue from each patient came from the same paraffin section. Note that PD-L1$^+$CD11c$^+$ cells (arrows) co-localize with CD3$^+$ cells. (B) Multiplexed IHC stained representative images of the stomach of other *H. pylori*-positive patients. Note that the positions of PD-L1$^+$ and CD11c$^+$ cells are similar (low-power fields) and PD-L1$^+$CD11c$^+$ cells (arrows) co-localize with CD3$^+$ cells (high-power fields) (B) Manual cell count number of PD-L1$^+$CD11c$^+$ cells in a section of a biopsy sample (*H. pylori*-negative sample–n=21; *H. pylori*-positive sample–n=31; mucosal dysplasia sample–n=46) (*$P < 0.05$)

Discussion

Despite many previous studies, the role of DCs in *Helicobacter*-infected individuals remains unclear. In my previous study, it was found that gastric DCs attenuated *Helicobacter*-induced gastric lesions by inhibiting T cells. Considering that no significant changes in the Tregs response were observed in DCs deficient mice, immune checkpoint molecules were noted as the mechanism of the T cell suppression of gastric DCs. Interestingly, gastric DCs expressed PD-L1 much more strongly than other immune cells, and the location of PD-L1$^+$ cells in the stomach was similar to that of gastric DCs. PD-L1$^+$CD11c$^+$ cells, which are presumed to be PD-L1 expressing gastric DCs, co-localized with T cells. In addition, the *Helicobacter*-induced immune responses of mouse model with the PD-L1 signal blocked were similar to those of DC-deficient mice. Given these results, gastric DCs appear to suppress *Helicobacter*-induced T cells and to attenuate the pathological progression of gastric lesions by expressing PD-L1.

In general, the mechanisms of immune modulation by DCs are thought to be based on the interaction between DCs and Tregs, in other word, Treg-mediated (Kornete and Piccirillo 2012). Nonetheless, in this study, neither Treg number and percentage nor TGF-β expression was different between WT and the DC-ablated group. This indicates that gastric DCs perform immune modulatory functions via a Treg-independent mechanism.

One of the Treg-bypassing immune modulatory mechanisms of DCs is activating the immune checkpoint pathway of T cells. Immune checkpoint molecules, also known as co-inhibitory molecules, include PD-1 and cytotoxic T lymphocyte-associated antigen 4, which are expressed on T cells; they are known

to offset against T cell co-stimulation by B7 molecules–CD28 interaction. PD-1 has two ligands: PD-L1 and PD-L2, which are expressed on antigen-presenting cells such as macrophages and DCs. Thus, the expression of PD-1 ligands on DCs can regulate T-cell mediated immune responses through a non-Treg-associated manner. These results suggest that the modulation of T cell-mediated immune response via PD-L1–PD-1 signaling by DCs indeed occurs during gastritis *in situ*.

PD-L1–PD-1 signaling modulates T cell-mediated immunity by regulating the number of T cells and their activity, through multiple ways, for instance, by inducing T cell exhaustion (Wherry 2011), anergy (Chikuma, Terawaki et al. 2009), and apoptosis (Dong, Strome et al. 2002) and by inhibiting T cell proliferation (Patsoukis, Sari et al. 2012). These effects of PD-L1–PD-1 signaling have been reported mainly in tumors and autoimmune or viral infectious diseases, but have also been reported in bacterial infectious diseases (Jurado, Alvarez et al. 2008). Inhibition of the host immune response by PD-L1–PD-1 signaling is vulnerable to the control of infectious agents and leads to chronic infection while reducing host tissue damage due to aggressive T cell responses (Sharpe, Wherry et al. 2007). Similarly, in *Helicobacter* infection, when PD-L1 was blocked or depleted on leukocytes, the phenotype similar to that noted in the absence of DCs was observed: worsened gastritis and pathological mucosal changes as well as increment in the number of T cells. These findings indicate that the impairment of DCs is related with a shortage of PD-L1 level in the stomach, which causes the loss of T cell regulation.

Some studies showed that the gastric epithelium expresses PD-L1. These studies were performed using gastric epithelial cell lines (Das, Suarez et al. 2006)

or gastric organoid culture differentiated from human-induced pluripotent stem cells (Holokai, Chakrabarti et al. 2019); thus, they might have not focused on whether PD-L1 is expressed on leukocytes. In this study, PD-L1 expression on DCs was observed by FACS of isolated single cells from the whole stomach and by IHC on tissue sections completely representing the histological structure of the stomach. Therefore, the difference in PD-L1 expression between leukocytes and non-leukocytes, including gastric epithelial cells, could be identified. And it was found that gastric DCs express considerably higher PD-L1 than gastric epithelial cells.

As mentioned above, PD-L1^{+} gastric DCs were located primarily in the submucosa and mucosal laminar propria right above the muscularis mucosa with T cells. These DCs are considered as a cellular barrier, protecting the gastric mucosa from the infiltration of T cells. Without these barrier-functioning DCs, T cells may remarkably infiltrate into the gastric mucosa to kill *Helicobacter*, but inadvertently cause severe damage to the mucosa. During *Helicobacter* infection, mucosal damage is accompanied by the loss of parietal cells and glandular structures (atrophy), SPEM, and further intestinal metaplasia when the lesion becomes more severe (Petersen, Mills et al. 2016). Mucosal epithelial metaplasia has been regarded as precancerous lesions because it is closely related to gastric cancer incidence in humans (Mera, Bravo et al. 2018). Interestingly, when DCs are absent, worsened oxyntic atrophy and mucous metaplasia were accompanied with an increase in T cell accumulation in the gastric mucosa. The gastric DCs may be involved in defense mechanism against carcinogenesis by slowing the progression of gastritis into gastric cancer. However, considering that a recent study showed that immune stromal PD-L1 expression is associated with poor prognosis in patients

with gastric adenocarcinoma (Thompson, Zahurak et al. 2017), and the result of this study that PD-L1^{+} gastric DCs still co-localize with T cells in some patients with mucosal dysplasia, the suppression of T cells by gastric DCs through PD-L1 expression might have a deleterious or beneficial effect on the host depending on the pathological progression of gastric lesions.

Along with other immune checkpoint inhibitors, PD-1 and PD-L1 inhibitors are recently highlighted as novel concepts of anti-cancer therapy. Some of them have received Food and Drug Administration approval and have shown effectiveness, thereby increasing expectations. However, these inhibitors are reported to have inflammatory side-effects called immune-related adverse events (IRAEs), and stomach is a one of the most IRAE-prone organs (Lu, Firpi-Morell et al. 2018; Postow, Sidlow et al. 2018; Samaan, Pavlidis et al. 2018). Thus, considering the possibility of IRAE occurrence in the stomach would be important when treating cancer patients with checkpoint inhibitors. The inflammatory events revealed in this study might provide a basis to elucidate the mechanism of IRAE occurrence in the stomach.

In conclusion, it was found that gastric DCs perform immune modulatory functions in a Treg-independent manner via the PD-L1–PD-1 pathway, which protects against precancerous mucosal damage. This study shows that DCs are important in preventing the progression of gastritis into a more severe form and provide a new concept to understand the pathology of *Helicobacter*-induced gastritis.

OVERALL CONCLUSION

DCs have been reported to play an important role in controlling the immune response to *Helicobacter* infection, which is highly correlated with chronic gastritis and gastric cancer in humans. To determine the role of DCs in *Helicobacter* infection, many previous studies have focused on the response of human moDCs or mouse BM-derived DCs to *Helicobacter in vitro*. However, *in vivo* experiments and characterization of gastric DCs are essential to clarify the role of DCs in *Helicobacter*-infected gastric tissues, but little is known about them. This study was carried out in order to contribute to the knowledge of these deficiencies.

In this study, the DC-deficient mouse models and the PD-L1-deficient mouse models have enabled the identification of the role of gastric cDCs on immune responses to *Helicobacter* and progression of gastric lesions. Gastric cDCs was defined as $CD64^{-}CD11c^{+}$MHC II^{hi} population and identified that gastric DCs are composed of $CD103^{+}$, $CD11b^{+}$, and DN subsets. In normal stomach, gastric cDCs were located mainly in the superficial mucosal lamina propria. However, when gastritis was induced by *Helicobacter* infection, the number of gastric cDCs rapidly increased, and gastric cDCs migrated around muscularis mucosa and submucosa where numerous T cells were present. These gastric cDCs deficiency worsened gastritis with significant T cell infiltration and pathological mucosal changes considered a precancerous lesion during *Helicobacter* infection. Gastric cDCs expressed considerably higher level of PD-L1 than other immune cells and co-localized with T cells in mouse and human stomach. In addition, blockade of PD-

L1 exacerbated gastritis with severe T cell accumulation during *Helicobacter* infection.

In conclusion, gastric cDCs are considered as a cellular barrier, protecting the gastric mucosa from the infiltration of T cells by expressing PD-L1. Without these barrier-functioning gastric cDCs, T cells may remarkably infiltrate into the gastric mucosa to kill *Helicobacter*, but inadvertently cause severe damage to the mucosa.

This study is the first report that gastric cDCs perform immune modulatory functions in the stomach via the PD-L1-PD-1 pathway. In addition, this study shows the possibility of this phenomenon occurring in human gastric tissues and contributes to a better understanding of the pathology of *Helicobacter*-induced gastritis. Furthermore, this study suggests the mechanism of IRAEs occurring in the stomach by the use of PD-1 and PD-L1 inhibitors, which have recently been highlighted as anti-cancer theraphy.

I believe that this study will be of great help in future researches of gastric DCs and immunity in stomach.

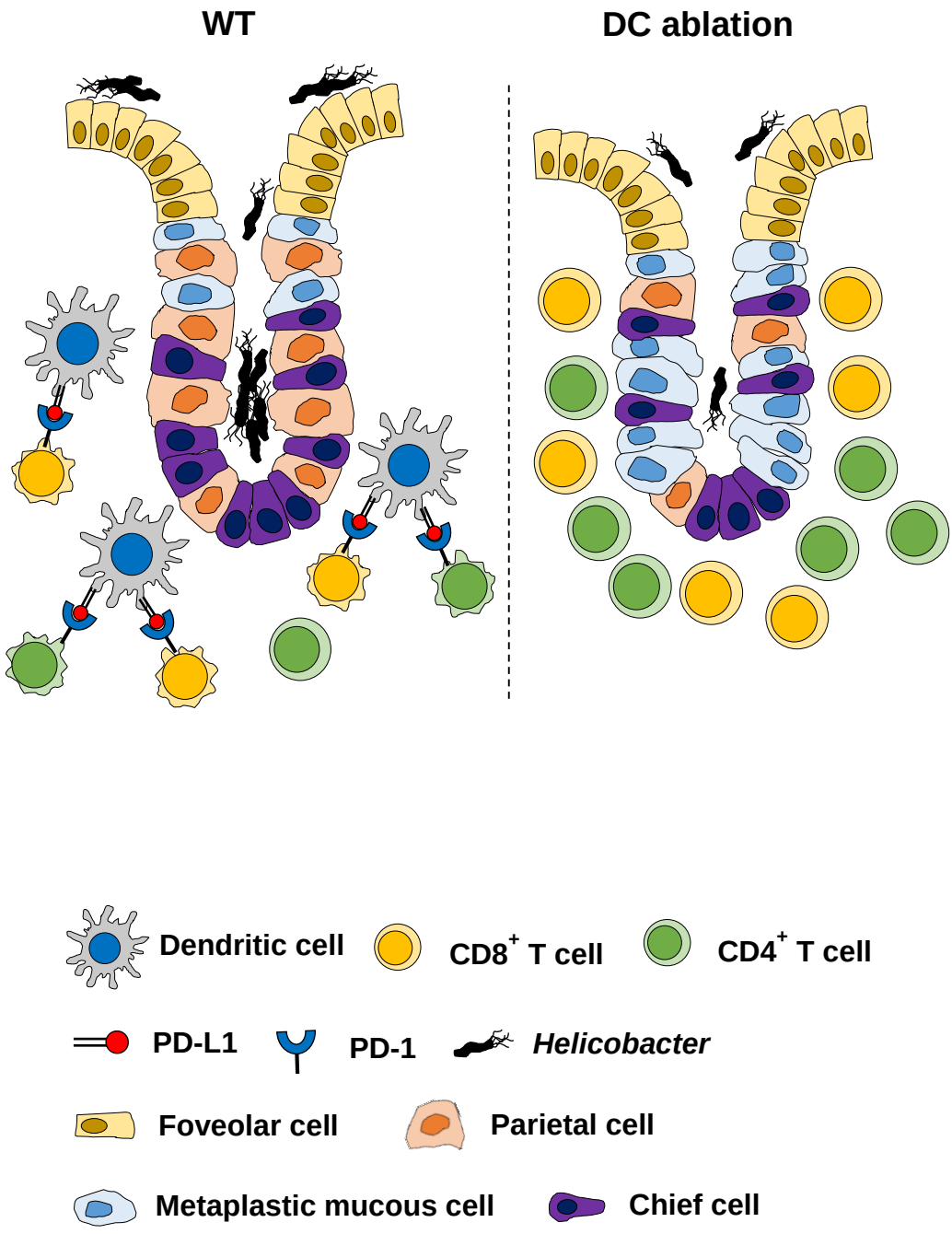
WT
DC ablation
Dendritic cell
CD8+ T cell
CD4+ T cell
PD-L1
PD-1
Helicobacter
Foveolar cell
Parietal cell
Metaplastic mucous cell
Chief cell

국문초록

Helicobacter 감염에 의한 위염에서 위 점막 수지상세포의 역할

고 두 민

지도 교수: 김 대 용

서울대학교 대학원 수의학과 수의병리학 전공

수지상세포는 여러 장기에 존재하는 중요한 면역조절세포로 알려져 있지만, 위 조직 내에 존재하는 수지상세포에 대해서는 알려진 바가 거의 없다. 또한 수지상세포는 *Helicobacter* 감염에서 숙주의 면역 반응을 조절하는데 중요한 역할을 하는 것으로 보고되어왔으나 위 조직 내에서의 역할은 아직 명확하지 않다. 본 연구는 위 조직 내 수지상세포의 표현형을 조사하고 *Helicobacter* 에 의해 유발된 위염에서 이들의 역할을 규명하기 위하여 수행되었다.

본 연구는, *Helicobacter* 에 감염된 수지상세포 결핍 마우스 모델과 각 대조군 마우스의 위 조직을 병리조직학적 분석, 유세포 분석, 면역 조직 화학 염색 및 면역 형광 염색, 실시간 중합효소연쇄반응 및 Luminex 면역 분석법으로 비교 분석하였다. 또한, PD-L1 결핍 마우스 모델을 이용하여 수지상세포의 T 세포 조절 기전을 확인하였고, 다중면역조직화학 염색을

이용하여 사람의 위 조직내에서 PD-L1 을 발현하는 수지상세포와 T 세포의 위치적인 연관성을 확인하였다.

위 점막 수지상세포는 $CD103^{+}CD11b^{-}$, $CD103^{-}CD11b^{+}$ 및 $CD103^{-}CD11b^{-}$ 의 표현형을 발현하는 아형들로 구성되어있었으며 정상 위 조직에서는 점막층에 소수 존재하고 있었다. *Helicobacter* 감염 시, 모든 수지상세포 아형들은 수적으로 증가하였고, 이러한 위 수지상세포들은 염증세포 침윤이 현저한 점막하조직 주변에서 주로 관찰되었다. 수지상세포 결핍 마우스에서는 대조군 마우스에 비하여 현저한 T 세포 침윤을 동반한 심한 위염과 위 점막의 병리학적 변화가 관찰되었다. 수지상세포 결핍 시 관찰된 위 병변의 악화는 *Helicobacter* 감염에서 수지상세포의 염증 억제 역할을 시사한다.

Helicobacter 감염 시, 수지상세포의 결핍은 regulatory T 세포의 침윤 정도에 영향을 주지 않았다. 위 점막 수지상세포는 다른 면역 세포들보다 상당히 높은 수준의 PD-L1 을 발현하고 있었으며, 마우스와 사람의 위 조직 내에서 T 세포와 위치적으로 공존하고 있었다. 또한, *Helicobacter* 에 감염된 PD-L1 결핍 마우스와 수지상세포 결핍 마우스의 위 조직 병변의 양상은 매우 유사하였다.

위의 결과들을 종합해 볼 때, 수지상세포들은 위 조직 내에서 PD-L1 발현을 통해 T 세포 침윤을 직접적으로 억제함으로써 *Helicobacter* 감염에 의하여 유발되는 위염을 약화시키는 것으로 보인다. 본 연구는 위 점막 수지상세포의 역할과 *Helicobacter* 감염에 의하여 위 조직 내에서 일어나는 면역반응에 대한 새로운 지견을 제공함과 더불어 임상적으로 위 조직 내에서 PD-L1 억제제에 의하여 유발되는 염증성 부작용의 기전을 시사한다.

핵심어: 수지상세포, 위염, *Helicobacter*, programmed death ligand 1 (PD-L1), programmed death 1 (PD-1), T 세포

학 번: 2012-21535

REFERENCES

Arasanz H., Gato-Cañas M., Zuazo M., Ibañez-Vea M., Breckpot K., Kochan G. and Escors D. (2017) PD1 signal transduction pathways in T cells. Oncotarget 8(31):51936-51945.

Ardouin L., Luche H., Chelbi R., Carpentier S., Shawket A., Montanana Sanchis F., Santa Maria C., Grenot P., Alexandre Y., Grégoire C., Fries A., Vu Manh T. P., Tamoutounour S., Crozat K., Tomasello E., Jorquera A., Fossum E., Bogen B., Azukizawa H., Bajenoff M., Henri S., Dalod M. and Malissen B. (2016) Broad and largely concordant molecular changes characterize tolerogenic and immunogenic dendritic cell maturation in thymus and periphery. Immunity 45(2):305-318.

Arnold I. C., Zhang X., Urban S., Artola-Borán M., Manz M. G., Ottemann K. M. and Müller A. (2017) NLRP3 controls the development of gastrointestinal CD11b+ dendritic cells in the steady state and during chronic bacterial infection. Cell Rep 21(13):3860-3872.

Audiger C., Rahman M. J., Yun T. J., Tarbell K. V. and Lesage S. (2017) The importance of dendritic cells in maintaining immune tolerance. J Immunol 198(6):2223-2231.

Bachem A., Güttler S., Hartung E., Ebstein F., Schaefer M., Tannert A., Salama A., Movassaghi K., Opitz C., Mages H. W., Henn V., Kloetzel P. M., Gurka S. and Kroczek R. A. (2010) Superior antigen cross-presentation and XCR1 expression define human CD11c+CD141+ cells as homologues of mouse CD8+ dendritic cells. J Exp Med 207(6):1273-1281.

Bain C. C., Scott C. L., Uronen-Hansson H., Gudjonsson S., Jansson O., Grip O., Guilliams M., Malissen B., Agace W. W. and Mowat A. M. (2013) Resident and pro-inflammatory macrophages in the colon represent alternative context-dependent fates of the same Ly6Chi monocyte precursors. Mucosal Immunol 6(3):498-510.

Bamford K. B., Fan X., Crowe S. E., Leary J. F., Gourley W. K., Luthra G. K., Brooks E. G., Graham D. Y., Reyes V. E. and Ernst P. B. (1998) Lymphocytes in the human gastric mucosa during *Helicobacter pylori* have a T helper cell 1 phenotype. Gastroenterology 114(3):482-492.

Banchereau J. and Steinman R. M. (1998) Dendritic cells and the control of immunity. Nature 392(6673):245-252.

Bedoui S., Whitney P. G., Waithman J., Eidsmo L., Wakim L., Caminschi I., Allan R. S., Wojtasiak M., Shortman K., Carbone F. R., Brooks A. G. and Heath W. R. (2009) Cross-presentation of viral and self antigens by skin-derived CD103+ dendritic cells. Nat Immunol 10(5):488-495.

Bennett C. L. and Clausen B. E. (2007) DC ablation in mice: promises, pitfalls, and challenges. Trends Immunol 28(12):525-531.

Bimczok D., Clements R. H., Waites K. B., Novak L., Eckhoff D. E., Mannon P. J., Smith P. D. and Smythies L. E. (2010) Human primary gastric dendritic cells induce a Th1 response to *H. pylori*. Mucosal Immunol 3(3):260-269.

Blank C. and Mackensen A. (2007) Contribution of the PD-L1/PD-1 pathway to T-cell exhaustion: an update on implications for chronic infections and tumor evasion. Cancer Immunol Immunother 56(5):739-745.

Cantorna M. T. and Balish E. (1990) Inability of human clinical strains of *Helicobacter pylori* to colonize the alimentary tract of germfree rodents. Can J Microbiol 36(4):237-241.

Chen X. Y., van der Hulst R. W., Bruno M. J., van der Ende A., Xiao S. D., Tytgat G. N. and Ten Kate F. J. (1999) Interobserver variation in the histopathological scoring of *Helicobacter pylori* related gastritis. J Clin Pathol 52(8):612-615.

Chikuma S., Terawaki S., Hayashi T., Nabeshima R., Yoshida T., Shibayama S., Okazaki T. and Honjo T. (2009) PD-1-mediated suppression of IL-2 production induces CD8+ T cell anergy in vivo. J Immunol 182(11):6682-6689.

Chiu Y. M., Tsai C. L., Kao J. T., Hsieh C. T., Shieh D. C., Lee Y. J., Tsay G. J., Cheng K. S. and Wu Y. Y. (2018) PD-1 and PD-L1 up-regulation promotes T-cell apoptosis in gastric adenocarcinoma. Anticancer Res 38(4):2069-2078.

Choi J. H., Cheong C., Dandamudi D. B., Park C. G., Rodriguez A., Mehandru S., Velinzon K., Jung I. H., Yoo J. Y., Oh G. T. and Steinman R. M. (2011)

Flt3 signaling-dependent dendritic cells protect against atherosclerosis. Immunity 35(5):819-831.

Chow K. V., Sutherland R. M., Zhan Y. and Lew A. M. (2017) Heterogeneity, functional specialization and differentiation of monocyte-derived dendritic cells. Immunol Cell Biol 95(3):244-251.

Clemente-Casares X., Hosseinzadeh S., Barbu I., Dick S. A., Macklin J. A., Wang Y., Momen A., Kantores C., Aronoff L., Farno M., Lucas T. M., Avery J., Zarrin-Khat D., Elsaesser H. J., Razani B., Lavine K. J., Husain M., Brooks D. G., Robbins C. S., Cybulsky M. and Epelman S. (2017) A CD103+ conventional dendritic cell surveillance system prevents development of overt heart failure during subclinical viral myocarditis. Immunity 47(5):974-989.

Colonna M., Trinchieri G. and Liu Y. J. (2004) Plasmacytoid dendritic cells in immunity. Nat Immunol 5(12):1219-1226.

Correa P. (1983) The gastric precancerous process. Cancer Surv 2:437-450.

Correa P. (1984) Chronic gastritis as a cancer precursor. Scand J Gastroenterol Suppl 104:131-136.

Cox M. A., Nechanitzky R. and Mak T. W. (2017) Check point inhibitors as therapies for infectious diseases. Curr Opin Immunol 48:61-67.

Darrasse-Jèze G., Deroubaix S., Mouquet H., Victora G. D., Eisenreich T., Yao K. H., Masilamani R. F., Dustin M. L., Rudensky A., Liu K. and Nussenzweig M. C. (2009) Feedback control of regulatory T cell homeostasis by dendritic cells in vivo. J Exp Med 206(9):1853-1862.

Das S., Suarez G., Beswick E. J., Sierra J. C., Graham D. Y. and Reyes V. E. (2006) Expression of B7-H1 on gastric epithelial cells: its potential role in regulating T cells during *Helicobacter pylori* infection. J Immunol 176(5):3000-3009.

Day C. L., Kaufmann D. E., Kiepiela P., Brown J. A., Moodley E. S., Reddy S., Mackey E. W., Miller J. D., Leslie A. J., DePierres C., Mncube Z., Duraiswamy J., Zhu B., Eichbaum Q., Altfeld M., Wherry E. J., Coovadia H. M., Goulder P. J., Klenerman P., Ahmed R., Freeman G. J. and Walker

B. D. (2006) PD-1 expression on HIV-specific T cells is associated with T-cell exhaustion and disease progression. Nature 443(7109):350-354.

del Rio M. L., Rodriguez-Barbosa J. I., Kremmer E. and Förster R. (2007) CD103- and CD103+ bronchial lymph node dendritic cells are specialized in presenting and cross-presenting innocuous antigen to CD4+ and CD8+ T cells. J Immunol 178(11):6861-6866.

den Haan J. M., Lehar S. M. and Bevan M. J. (2000) CD8+ but not CD8− dendritic cells cross-prime cytotoxic T cells in vivo. J Exp Med 192(12):1685-1696.

Dong H., Strome S. E., Salomao D. R., Tamura H., Hirano F., Flies D. B., Roche P. C., Lu J., Zhu G., Tamada K., Lennon V. A., Celis E. and Chen L. (2002) Tumor-associated B7-H1 promotes T-cell apoptosis: a potential mechanism of immune evasion. Nat Med 8(8):793-800.

Duckworth C. A., Burkitt M. D., Williams J. M., Parsons B. N., Tang J. M. and Pritchard D. M. (2015). Murine models of *Helicobacter* (*pylori* or *felis*)-associated gastric cancer. Curr Protoc Pharmacol 69:14.34.1-35.

Edelson B. T., KC W., Juang R., Kohyama M., Benoit L. A., Klekotka P. A., Moon C., Albring J. C., Ise W., Michael D. G., Bhattacharya D., Stappenbeck T. S., Holtzman M. J., Sung S. S., Murphy T. L., Hildner K. and Murphy K. M. (2010) Peripheral CD103+ dendritic cells form a unified subset developmentally related to CD8alpha+ conventional dendritic cells. J Exp Med 207(4):823-836.

Ehlers S., Warrelmann M. and Hahn H. (1988) In search of an animal model for experimental *Campylobacter pylori* infection: administration of *Campylobacter pylori* to rodents. Zentralbl Bakteriol Mikrobiol Hyg A 268(3):341-346.

El-Zaatari M., Kao J. Y., Tessier A., Bai L., Hayes M. M., Fontaine C., Eaton K. A. and Merchant J. L. (2013) Gli1 deletion prevents *Helicobacter*-induced gastric metaplasia and expansion of myeloid cell subsets. PLoS One 8(3):e58935.

Fankhauser S. C. and Starnbach M. N. (2014) PD-L1 limits the mucosal CD8+ T cell response to *Chlamydia trachomatis*. J Immunol 192(3):1079-1090.

Fife B. T., Pauken K. E., Eagar T. N., Obu T., Wu J., Tang Q., Azuma M., Krummel M. F. and Bluestone J. A. (2009) Interactions between PD-1 and PD-L1 promote tolerance by blocking the TCR-induced stop signal. Nat Immunol 10(11):1185-1192.

Fox J. G., Sheppard B. J., Dangler C. A., Whary M. T., Ihrig M. and Wang T. C. (2002) Germ-line p53-targeted disruption inhibits *helicobacter*-induced premalignant lesions and invasive gastric carcinoma through down-regulation of Th1 proinflammatory responses. Cancer Res 62(3):696-702.

Funes S. C., Manrique de Lara A., Altamirano-Lagos M. J., Mackern-Oberti J. P., Escobar-Vera J. and Kalergis A. M. (2019) Immune checkpoints and the regulation of tolerogenicity in dendritic cells: Implications for autoimmunity and immunotherapy. Autoimmun Rev 18(4):359-368.

Goudot C., Coillard A., Villani A. C., Gueguen P., Cros A., Sarkizova S., Tang-Huau T. L., Bohec M., Baulande S., Hacohen N., Amigorena S. and Segura E. (2017) Aryl hydrocarbon receptor controls monocyte differentiation into dendritic cells versus macrophages. Immunity 47(3):582-596.

Guilliams M., Dutertre C. A., Scott C. L., McGovern N., Sichien D., Chakarov S., Van Gassen S., Chen J., Poidinger M., De Prijck S., Tavernier S. J., Low I., Irac S. E., Mattar C. N., Sumatoh H. R., Low G. H. L., Chung T. J. K., Chan D. K. H., Tan K. K., Hon T. L. K., Fossum E., Bogen B., Choolani M., Chan J. K. Y., Larbi A., Luche H., Henri S., Saeys Y., Newell E. W., Lambrecht B. N., Malissen B. and Ginhoux F. (2016) Unsupervised high-dimensional analysis aligns dendritic cells across tissues and species. Immunity 45(3):669-684.

Hafsi N., Voland P., Schwendy S., Rad R., Reindl W., Gerhard M. and Prinz C. (2004) Human dendritic cells respond to *Helicobacter pylori*, promoting NK cell and Th1-effector responses in vitro. J Immunol 173(2):1249-1257.

Hitzler I., Oertli M., Becher B., Agger E. M. and Müller A. (2011) Dendritic cells prevent rather than promote immunity conferred by a *helicobacter* vaccine using a mycobacterial adjuvant. Gastroenterology 141(1):186-196.

Holokai L., Chakrabarti J., Broda T., Chang J., Hawkins J. A., Sundaram N., Wroblewski L. E., Peek R. M. Jr., Wang J., Helmrath M., Wells J. M. and

Zavros Y. (2019) Increased programmed death-ligand 1 is an early epithelial cell response to *Helicobacter pylori* infection. PLoS Pathog 15(1):e1007468.

Ishida M., Iwai Y., Tanaka Y., Okazaki T., Freeman G. J., Minato N. and Honjo T. (2002) Differential expression of PD-L1 and PD-L2, ligands for an inhibitory receptor PD-1, in the cells of lymphohematopoietic tissues. Immunol Lett 84(1):57-62.

Jurado J. O., Alvarez I. B., Pasquinelli V., Martínez G. J., Quiroga M. F., Abbate E., Musella R. M., Chuluyan H. E. and García V. E. (2008) Programmed death (PD)-1:PD-ligand 1/PD-ligand 2 pathway inhibits T cell effector functions during human tuberculosis. J Immunol 181(1):116-125.

Khamri W., Walker M. M., Clark P., Atherton J. C., Thursz M. R., Bamford K. B., Lechler R. I. and Lombardi G. (2010) *Helicobacter pylori* stimulates dendritic cells to induce interleukin-17 expression from CD4+ T lymphocytes. Infect Immun 78(2):845-853.

Kim J. J., Nottingham L. K., Sin J. I., Tsai A., Morrison L., Oh J., Dang K., Hu Y., Kazahaya K., Bennett M., Dentchev T., Wilson D. M.., Chalian A A., Boyer J. D., Agadjanyan M. G. and Weiner D. B. (1998) CD8 positive T cells influence antigen-specific immune responses through the expression of chemokines. J Clin Invest 102(6):1112-1124.

Kingston D., Schmid M. A., Onai N., Obata-Onai A., Baumjohann D. and Manz M. G. (2009) The concerted action of GM-CSF and Flt3-ligand on in vivo dendritic cell homeostasis. Blood 114(4):835-843.

Koh J., Kwak Y., Kim J. and Kim W. H. (2019) High-throughput multiplex immunohistochemical imaging of the tumor and its microenvironment. Cancer Res Treat doi: 10.4143/crt.2019.195.

Kornete M. and Piccirillo C. A. (2012) Functional crosstalk between dendritic cells and Foxp3(+) regulatory T cells in the maintenance of immune tolerance. Front Immunol 3:165.

Kronsteiner B., Bassaganya-Riera J., Philipson N. and Hontecillas R. (2014) Novel insights on the role of CD8+ T cells and cytotoxic responses during *Helicobacter pylori* infection. Gut Microbes 5(3):357-362.

Kusters J. G., van Vliet A. H. and Kuipers E. J. (2006) Pathogenesis of *Helicobacter pylori* infection. Clin Microbiol Rev 19(3):449-490.

Lee A., Fox J. G., Otto G. and Murphy J. (1990) A small animal model of human *Helicobacter pylori* active chronic gastritis. Gastroenterology 99(5):1315-1323.

Lee A., O'Rourke J., De Ungria M. C., Robertson B., Daskalopoulos G. and Dixon M. F. (1997) A standardized mouse model of *Helicobacter pylori* infection: introducing the Sydney strain. Gastroenterology 112(4):1386-1397.

Lewis K. L., Caton M. L., Bogunovic M., Greter M., Grajkowska L. T., Ng D., Klinakis A., Charo I. F., Jung S., Gommerman J. L., Ivanov I. I., Liu K., Merad M. and Reizis B. (2011) Notch2 receptor signaling controls functional differentiation of dendritic cells in the spleen and intestine. Immunity 35(5):780-791.

Liu K. and Nussenzweig M. C. (2010) Origin and development of dendritic cells. Immunol Rev 234(1):45-54.

Lu J., Firpi-Morell R. J., Dang L. H., Lai J. and Liu X.(2018) An unusual case of gastritis in one patient receiving PD-1 blocking therapy: coexisting immune-related gastritis and cytomegaloviral infection. Gastroenterology Res 11(5):383-387.

Mera R. M., Bravo L. E., Camargo M. C., Bravo J. C., Delgado A. G., Romero-Gallo J., Yepez M. C., Realpe J. L., Schneider B. G., Morgan D. R., Peek R. M. Jr., Correa P., Wilson K. T. and Piazuelo M. B. (2018) Dynamics of *Helicobacter pylori* infection as a determinant of progression of gastric precancerous lesions: 16-year follow-up of an eradication trial. Gut 67(7):1239-1246.

Mildner A. and Jung S. (2014) Development and function of dendritic cell subsets. Immunity 40(5):642-656.

Mildner A., Yona S. and Jung S. (2013) A close encounter of the third kind: monocyte-derived cells. Adv Immunol 120:69-103.

Nussenzweig M. C., Steinman R. M., Gutchinov B. and Cohn Z. A. (1980) Dendritic cells are accessory cells for the development of anti-trinitrophenyl cytotoxic T lymphocytes. J Exp Med 152(4):1070-1084.

Oertli M., Sundquist M., Hitzler I., Engler D. B., Arnold I. C., Reuter S., Maxeiner J., Hansson M., Taube C., Quiding-Järbrink M. and Müller A. (2012) DC-derived IL-18 drives Treg differentiation, murine *Helicobacter pylori*-specific immune tolerance, and asthma protection. J Clin Invest 122(3):1082-1096.

Ohtani N., Ohtani H., Nakayama T., Naganuma H., Sato E., Imai T., Nagura H. and Yoshie O. (2004) Infiltration of CD8+ T cells containing RANTES/CCL5+ cytoplasmic granules in actively inflammatory lesions of human chronic gastritis. Lab Invest 84(3):368-375.

Patsoukis N., Sari D. and Boussiotis V. A. (2012) PD-1 inhibits T cell proliferation by upregulating p27 and p15 and suppressing Cdc25A. Cell Cycle 11(23):4305-4309.

Peek R. M. Jr., Fiske C. and Wilson K. T. (2010) Role of innate immunity in *Helicobacter pylori*-induced gastric malignancy. Physiol Rev 90(3):831-858.

Petersen C. P., Mills J. C and Goldenring J. R. (2016) Murine models of gastric corpus preneoplasia. Cell Mol Gastroenterol Hepatol 3(1):11-26.

Petrovas C., Casazza J. P., Brenchley J. M., Price D. A., Gostick E., Adams W. C., Precopio M. L., Schacker T., Roederer M., Douek D. C. and Koup R. A. (2006) PD-1 is a regulator of virus-specific CD8+ T cell survival in HIV infection. J Exp Med 203(10):2281-2292.

Popov A., Driesen J., Abdullah Z., Wickenhauser C., Beyer M., Debey-Pascher S., Saric T., Kummer S., Takikawa O., Domann E., Chakraborty T., Krönke M., Utermöhlen O. and Schultze J. L. (2008) Infection of myeloid dendritic cells with Listeria monocytogenes leads to the suppression of T cell function by multiple inhibitory mechanisms. J Immunol 181(7):4976-4988.

Postow M. A., Sidlow R. and Hellmann M. D. (2018) Immune-related adverse events associated with immune checkpoint blockade. N Engl J Med 378(2):158-168.

Probst H. C., McCoy K., Okazaki T., Honjo T. and van den Broek M. (2005) Resting dendritic cells induce peripheral CD8+ T cell tolerance through PD-1 and CTLA-4. Nat Immunol 6(3):280-286.

Probst H. C., Tschannen K., Odermatt B., Schwendener R., Zinkernagel R. M. and Van Den Broek M. (2005) Histological analysis of CD11c-DTR/GFP mice after in vivo depletion of dendritic cells. Clin Exp Immunol 141(3):398-404.

Quiding-Järbrink M., Lundin B. S., Lönroth H. and Svennerholm A. M. (2001) CD4+ and CD8+ T cell responses in *Helicobacter pylori*-infected individuals. Clin Exp Immunol 123(1):81-87.

Rad R., Ballhorn W., Voland P., Eisenächer K., Mages J., Rad L., Ferstl R., Lang R., Wagner H., Schmid R. M., Bauer S., Prinz C., Kirschning C. J. and Krug A. (2009) Extracellular and intracellular pattern recognition receptors cooperate in the recognition of *Helicobacter pylori*. Gastroenterology 136(7):2247-2257.

Reizis B. (2012) Classical dendritic cells as a unique immune cell lineage. J Exp Med 209(6):1053-1056.

Rizzuti D., Ang M., Sokollik C., Wu T., Abdullah M., Greenfield L., Fattouh R., Reardon C., Tang M., Diao J., Schindler C., Cattral M. and Jones N. L. (2015) *Helicobacter pylori* inhibits dendritic cell maturation via interleukin-10-mediated activation of the signal transducer and activator of transcription 3 pathway. J Innate Immun 7(2):199-211.

Robbins S. H., Walzer T., Dembélé D., Thibault C., Defays A., Bessou G., Xu H., Vivier E., Sellars M., Pierre P., Sharp F. R., Chan S., Kastner P. and Dalod M. (2008) Novel insights into the relationships between dendritic cell subsets in human and mouse revealed by genome-wide expression profiling. Genome Biol 9(1):R17.

Rock K. L. (2003) The ins and outs of cross-presentation. Nat Immunol 4(10):941-943.

Rombouts M., Cools N., Grootaert M. O., de Bakker F., Van Brussel I., Wouters A., De Meyer G. R., De Winter B. Y. and Schrijvers D. M. (2017) Long-term depletion of conventional dendritic cells cannot be maintained in an atherosclerotic Zbtb46-DTR mouse model. PLoS One 12(1):e0169608.

Roth S. J., Carr M. W. and Springer T. A. (1995) C-C chemokines, but not the C-X-C chemokines interleukin-8 and interferon-gamma inducible protein-10, stimulate transendothelial chemotaxis of T lymphocytes. Eur J Immunol 25(12):3482-3488.

Sakagami T., Dixon M., O'Rourke J., Howlett R., Alderuccio F., Vella J., Shimoyama T. and Lee A. (1996) Atrophic gastric changes in both *Helicobacter felis* and *Helicobacter pylori* infected mice are host dependent and separate from antral gastritis. Gut 39(5):639-648.

Sakuishi K., Apetoh L., Sullivan J. M., Blazar B. R., Kuchroo V. K. and Anderson A. C. (2010) Targeting Tim-3 and PD-1 pathways to reverse T cell exhaustion and restore anti-tumor immunity. J Exp Med 207(10):2187-2194.

Salomon B., Lenschow D. J., Rhee L., Ashourian N., Singh B., Sharpe A. and Bluestone J. A. (2000) B7/CD28 costimulation is essential for the homeostasis of the CD4+CD25+ immunoregulatory T cells that control autoimmune diabetes. Immunity 12(4):431-440.

Samaan M. A., Pavlidis P., Papa S., Powell N. and Irving P. M. (2018) Gastrointestinal toxicity of immune checkpoint inhibitors: from mechanisms to management. Nat Rev Gastroenterol Hepatol 15(4):222-234.

Sapoznikov A., Fischer J. A., Zaft T., Krauthgamer R., Dzionek A. and Jung S. (2007) Organ-dependent in vivo priming of naive CD4+, but not CD8+, T cells by plasmacytoid dendritic cells. J Exp Med 204(8):1923-1933.

Satpathy A. T., KC W., Albring J. C., Edelson B. T., Kretzer N. M., Bhattacharya D., Murphy T. L. and Murphy K. M. (2012) Zbtb46 expression distinguishes classical dendritic cells and their committed progenitors from other immune lineages. J Exp Med 209(6):1135-1152.

Sayi A., Kohler E., Hitzler I., Arnold I., Schwendener R., Rehrauer H. and Müller A. (2009) The CD4+ T cell-mediated IFN-gamma response to *Helicobacter infection* is essential for clearance and determines gastric cancer risk. J Immunol 182(11):7085-7101.

Schülke S. (2018) Induction of interleukin-10 producing dendritic cells as a tool to suppress allergen-specific T helper 2 responses. Front Immunol 9:455.

Segura E. and Amigorena S. (2013) Inflammatory dendritic cells in mice and humans. Trends Immunol 34(9):440-445.

Seillet C., Jackson J. T., Markey K. A., Brady H. J., Hill G. R., Macdonald K. P., Nutt S. L. and Belz G. T. (2013) CD8α+ DCs can be induced in the absence of transcription factors Id2, Nfil3, and Batf3. Blood 121(9):1574-1583.

Selenko-Gebauer N, Majdic O, Szekeres A, Höfler G, Guthann E, Korthäuer U, Zlabinger G., Steinberger P., Pickl W. F., Stockinger H., Knapp W. and Stöckl J. (2003) B7-H1 (programmed death-1 ligand) on dendritic cells is involved in the induction and maintenance of T cell anergy. J Immunol 170(7):3637-3644.

Sharpe A. H., Wherry E. J., Ahmed R. and Freeman G. J. (2007) The function of programmed cell death 1 and its ligands in regulating autoimmunity and infection. Nat Immunol 8(3):239-245.

Shiu J. and Blanchard T. G. (2013) Dendritic cell function in the host response to *Helicobacter pylori* infection of the gastric mucosa. Pathog Dis 67(1):46-53.

Sivakumaran S., Henderson S., Ward S., Sousa P. S., Manzo T., Zhang L., Conlan T., Means T. K., D'Aveni M., Hermine O., Rubio M. T., Chakraverty R. and Bennett C. L. (2016) Depletion of CD11c+ cells in the CD11c-DTR model drives expansion of unique CD64+ Ly6C+ monocytes that are poised to release TNF-α. Eur J Immunol 46(1):192-203.

Steinman R. M. (2012) Decisions about dendritic cells: past, present, and future. Annu Rev Immunol 30:1-22.

Steinman R. M. and Cohn Z. A. (1973) Identification of a novel cell type in peripheral lymphoid organs of mice. J Exp Med 137(5):1142-1162.

Steinman R. M. and Cohn Z. A. (1974) Identification of a novel cell type in peripheral lymphoid organs of mice. J Exp Med 139(2):380-397.

Steinman R. M., Hawiger D. and Nussenzweig M. C. (2003) Tolerogenic dendritic cells. Annu Rev Immunol 21:685-711.

Thompson E. D., Zahurak M., Murphy A., Cornish T., Cuka N., Abdelfatah E., Yang S., Duncan M., Ahuja N., Taube J. M.., Anders R A. and Kelly R. J. (2017) Patterns of PD-L1 expression and CD8 T cell infiltration in gastric adenocarcinomas and associated immune stroma. Gut 66(5):794-801.

Thomson A. W. (2010) Tolerogenic dendritic cells: all present and correct? Am J Transplant 10(2):214-219.

Tsushima F., Yao S., Shin T., Flies A., Flies S., Xu H., Tamada K., Pardoll D. M. and Chen L. (2007) Interaction between B7-H1 and PD-1 determines initiation and reversal of T-cell anergy. Blood 110(1):180-185.

Van den Broeck W., Derore A. and Simoens P. (2006) Anatomy and nomenclature of murine lymph nodes: Descriptive study and nomenclatory standardization in BALB/cAnNCrl mice. J Immunol Methods 312(1-2):12-19.

Waskow C., Liu K., Darrasse-Jèze G., Guermonprez P., Ginhoux F., Merad M., Shengelia T., Yao K. and Nussenzweig M. (2008) The receptor tyrosine kinase Flt3 is required for dendritic cell development in peripheral lymphoid tissues. Nat Immunol 9(6):676-683.

Weis V. G., Sousa J. F., LaFleur B. J., Nam K. T., Weis J. A., Finke P. E., Ameen N. A., Fox J. G. and Goldenring J. R. (2013) Heterogeneity in mouse spasmolytic polypeptide-expressing metaplasia lineages identifies markers of metaplastic progression. Gut 62(9):1270-1279.

Wherry E. J. (2011) T cell exhaustion. Nat Immunol 12(6):492-499.

Worbs T., Hammerschmidt S. I. and Förster R. (2017) Dendritic cell migration in health and disease. Nat Rev Immunol 17(1):30-48.

Yamaoka Y., Kita M., Kodama T., Sawai N., Tanahashi T., Kashima K. and Imanishi J. (1998) Chemokines in the gastric mucosa in *Helicobacter pylori* infection. Gut 42(5):609-617.

Yamazaki S., Iyoda T., Tarbell K., Olson K., Velinzon K., Inaba K. and Steinman R. M. (2003) Direct expansion of functional CD25+ CD4+ regulatory T cells by antigen-processing dendritic cells. J Exp Med 198(2):235-247.

Yamazaki T., Akiba H., Iwai H., Matsuda H., Aoki M., Tanno Y., Shin T., Tsuchiya H., Pardoll D. M., Okumura K., Azuma M. and Yagita H. (2002) Expression of programmed death 1 ligands by murine T cells and APC. J Immunol 169(10):5538-5545.

Yun T. J., Lee J. S., Machmach K., Shim D., Choi J., Wi Y. J., Jang H. S., Jung I. H., Kim K., Yoon W. K., Miah M. A., Li B., Chang J., Bego M. G., Pham T. N., Loschko J., Fritz J. H., Krug A. B., Lee S. P., Keler T., Guimond J. V., Haddad E.., Cohen E A., Sirois M. G., El-Hamamsy I., Colonna M., Oh G. T., Choi J. H. and Cheong C. (2016) Indoleamine 2,3-dioxygenase-expressing aortic plasmacytoid dendritic cells protect against atherosclerosis by induction of regulatory T cells. Cell Metab 23(5):852-866.

Zhang M., Liu M., Luther J. and Kao J. Y. (2010) *Helicobacter pylori* directs tolerogenic programming of dendritic cells. Gut Microbes 1(5):325-329.